STUDIES IN EPIDEMIOLOGY AND SOCIAL DYNAMICS

A Dissertation

Presented to the Faculty of the Graduate School

of Cornell University

in Partial Fulfillment of the Requirements for the Degree of

Doctor of Philosophy

by

Fabio Sánchez

January 2007

STUDIES IN EPIDEMIOLOGY AND SOCIAL DYNAMICS

Fabio Sánchez, Ph.D.

Cornell University 2007

Part I:

We illustrate different modeling approaches to describe the dynamics of dengue fever (a vector-borne disease). According to the Center for Disease Control and Prevention (CDC), there are an estimated 50 to 100 million cases of dengue fever (the symptoms associated with dengue infection) every year around the world (mostly in the tropics) [1]. We demonstrate that "effective" mosquito control strategies are not sufficient in controlling dengue outbreaks. It is possible for low mosquito densities to cause large outbreaks. Furthermore, mosquito eradication is likely the most effective way to eliminate dengue fever but it is unpractical and nearly impossible to achieve. Based on the epidemiological threshold, $\mathcal{R}_0$, we were able to determine the most sensitive parameters that can lead to enhance the implementation of public health policies and control strategies under different modeling scenarios.

[1] CDC: Fact Sheet: Dengue and Dengue Hemorrhagic Fever. June 19, 2001. World Wide Web. http://www.cdc.gov/ncidod/dvbid/dengue/facts.htm

Part II:

Alcohol abuse has been a problem for a long time in the United States. Drinking behavior patterns have changed over the years and it affects all races, age classes and social status. We used epidemiological approaches and constructed mathematical models to study drinking behavior. We find that *peer pressure* from *moderate* drinkers have the biggest impact on the population of *low-risk* drinkers. Threshold quantities that establish the prevalence of the *drinking communities* are studied and thoroughly analyzed to determine possible prevention strategies. We also explored the effect of the SDR (susceptible ('at-risk'), drinkers, temporarily recovered) model on a 'small-world' structure and a continuous time Markov chain model. We found that network structure does not play a role on drinking behavior dynamics. We conclude that the SDR model is robust. For the stochastic simulations we computed final size drinker distributions. We also explored a more detailed model that includes four drinker classes (abstainers-occasional drinkers-moderate drinkers-heavy drinkers) and n neighborhoods. We computed threshold conditions and conducted an uncertainty analysis. We determine that the key transition to have an endemic drinking culture is from occasional drinker to moderate drinker.

BIOGRAPHICAL SKETCH

Fabio Ariel Sánchez-Peña was born in Santo Domingo, Republica Dominicana on October 19, 1976. His parents are María del Carmen Peña Liranzo and Felix Ruíz Durán. He is the oldest of three siblings. He has a sister and a brother, Yussetti Sánchez and Richard Ruíz. He recently became an uncle when his sister gave birth to baby *Leyra*. Fabio moved to Puerto Rico at age five. During his childhood he has memories of his passion for horse racing and dreaming of being a professional jockey.

In the fall of 1992 Fabio's mother made the bold move of sending her son to New Jersey to live with his Aunt and Uncle (Tía Sonia y Tío Plinio) along with three of his cousins. Fabio went to Harrison High School where his teachers always encouraged him to seek what seems impossible. Fabio's mother was looking for a better future for her son.

After high school Fabio moved back to Puerto Rico with his parents and finished his undergraduate studies at Universidad Metropolitana (UMET) in Cupey, Puerto Rico in June, 2001. At UMET there were many people that positively influenced his life but, in particular, Dr. Juan Arratia and Prof. Martin Engman stand out as the most important people in his undergraduate career.

In the fall of 2001, Fabio joined the Ph.D. program at Cornell University in the BSCB department under the supervision of Prof. Carlos Castillo-Chávez. Fabio followed his advisor to Los Alamos, New Mexico where he spent a year and later on moved to Arizona (ASU) where his advisor is now a professor in the Department of Mathematics and Statistics.

In October 2006, Fabio joined American Express as a Manager in the Credit Strategy Team.

To Mami (María del Carmen Peña), Papi (Felix Ruíz), Ercilia Liranzo, Don Paco, Richard, Yussetti, baby Leyra and Gya.

ACKNOWLEDGEMENTS

I would like to thank my Ph.D. adviser Prof. Carlos Castillo-Chávez for his invaluable advice throughout my graduate school career and life. Members of my Ph.D. committee Prof. Laura C. Harrington and Prof. Martin T. Wells. Also, Prof. Martin Engman, Prof. Karl Hadeler, Dr. Mac Hyman, Prof. Maia Martcheiva, Dr. Gerardo Chowell-Puente, Dr. Ariel Cintrón-Arias, Prof. Horst Thieme, Prof. Hal Smith, Prof. Steven Strogatz for their advice and support during the preparation of this thesis and my graduate school career. The author acknowledges the support of the *Alfred P. Sloan Foundation*, Cornell University, LANL (CNLS) and Arizona State University.

Friends: Thank you.

Dr. Juan F. Arratia, Barbara Deuink (NSA), Dr. Lloyd Douglas (NSF), Dr. Daniel Wiley, Nestor López, David Murillo, Dr. Steve Tennenbaum, Jacqueline Guzmán, Angel (Chimbo) De Los Reyes, Daniel (El Goldo) Meléndez, José (Santito) Ramírez, Manuel Rivera, Dr. Miriam Nuno, Terannie Vázquez, Angela Ortiz and Jayson Vázquez.

TABLE OF CONTENTS

1 Part I: Introduction **1**

2 Epidemiology of dengue **5**
2.1 Ecology of *Aedes aegypti* and *Aedes albopictus* 5
2.2 Transmission cycle 6
2.3 Treatment and control 6
2.4 Seasonal trends and the effects on dengue transmission 7

3 Review of dengue models and results **8**

4 A case study: a single-outbreak model for dengue outbreaks in Singapore **12**
4.1 Single-outbreak model 15
4.2 Results 17
4.3 Conclusions 22

5 Single strain model with vector-life history* **23**
5.1 Disease dynamics and control 27
5.2 Effects of seasonal variations 31
5.3 Conclusions 36

6 Two-strain dengue model with collective host behavior change **38**
6.1 The model 38
6.2 Disease invasion and persistence 41
6.3 Numerical simulations 43
6.4 Conclusions 50

Appendices **52**

A Jacobians and Characteristic Equations for the single strain model **53**

B Jacobian and proofs of two strain model of dengue **62**

Bibliography **67**

7 Part II: Introduction **72**

8 Drinking as an epidemic–a simple mathematical model with recovery and relapse* **75**
8.1 Simple SDR drinking model 77
8.2 Population dynamics of drinking under high relapse rates 81
8.3 Uncertainty and sensitivity analysis 83
8.4 Numerical simulations 88

8.5 Conclusions 92

9 Drinking model in a small-world network and a Markov chain model 93
9.1 Small-world networks 93
9.2 Drinking behavior on small-world networks 94
9.3 Conclusions 96
9.4 Drinking behavior: a continuous Markov chain approach 99
9.5 Methods 100
9.6 Numerical simulations 102
9.7 Conclusions 106

10 Effects of local and global alcohol consumption networks on drinking dynamics 107
10.1 Mean field example 107
10.2 Threshold quantities and simulations 114
10.3 Conclusions 123

Bibliography 124

LIST OF TABLES

4.1 Parameter List 19
4.2 $\mathcal{R}_0$ estimates for dengue outbreaks in Singapore from $2001 - 2005$. 19

5.1 Parameter List 26

8.1 Description of parameters and parameter distribution functions. All rates are *per-capita*. 80
8.2 Description of threshold conditions. 82
8.3 Partial Rank Correlation Coefficient of $\mathcal{R}_\phi$, $\mathcal{R}_\rho$ and $\mathcal{R}_c/\mathcal{R}_\phi$ with their respective p-values. 85
8.4 Estimates of $\mathcal{R}_\phi$, $\frac{\mathcal{R}_c}{\mathcal{R}_\phi}$ and $\mathcal{R}_\rho$ from 10 Monte Carlo simulations. . . 87

9.1 SDR drinking network model. $\mathcal{D}_i$ denotes the number of *"problem" drinker* neighbors of node i. 102

10.1 Sub population and classes. i is the neighborhood index. 110
10.2 Parameters. i is referred to the index of a neighborhood. 111
10.3 Estimates of $\mathcal{R}_0^1$ from 10 Monte Carlo simulations. 118
10.4 Estimates of $\mathcal{R}_0^2$ from 10 Monte Carlo simulations. 119
10.5 Parameter distributions. 121

LIST OF FIGURES

1.1 World distribution of dengue epidemic [10]. 2

2.1 Manifestations of the dengue syndrome [42]. 6
2.2 Transmission cycle [11]. 7

4.1 Confirmed DF/DHF weekly cases from $2001-2006$ in Singapore [13]. 13
4.2 Confirmed DF/DHF cases [13]. 14
4.3 Map of Singapore. 15
4.4 Geographical distribution of DF/DHF in Singapore from $2001-$ 2004 [13]. 16
4.5 Distribution of *Ae. aegpyti* by top five breeding habitats, 2004 [13]. 17
4.6 Age-specific incidence (per/100,000) rates of DF/DHF cases [13]. . 18
4.7 Singapore data from the 2001 dengue outbreak. Estimates of the parameters: $\beta = 0.73$, $\alpha = 0.75$, $\gamma = 4.2$, $\rho = 2.3$, $\phi = 0.5$ and $\mu = 0.1$. The estimated basic reproductive number for this outbreak is $\mathcal{R}_0 = 1.1$. 20
4.8 Data from the 2004 dengue outbreak in Singapore. Estimates of the parameters: $\beta = 0.2$, $\alpha = 0.83$, $\gamma = 1$, $\rho = 2.33$, $\phi = 0.6$ and $\mu = 0.1$. The estimated basic reproductive number for this outbreak is $\mathcal{R}_0 = 1.2$. 20
4.9 Data from the 2005 dengue outbreak in Singapore. Estimates of the parameters: $\beta = 1.1$, $\alpha = 1$, $\gamma = 2$, $\rho = 0.04$, $\phi = 0.2$ and $\mu = 0.02$. The estimated basic reproductive number for this outbreak is $\mathcal{R}_0 = 5$. 21

5.1 Caricature of the model. 25
5.2 The equilibria alternate stability, the first and third being stable and the second one being the unstable equilibrium. Graphs of $g(L), c(L)$; $\rho = 15$, $\epsilon = 15$, $a = 0.5$ and $\omega = 0.2$. 31
5.3 Moderate seasonal effects on host and vector transmission rates (α, β and ϵ). The parameter values are: $\mu = 0.00004$, $\mu_e = 0.003$, $\mu_m = 0.03$, $\delta = 0.09$, $\gamma = 0.14$, $\rho = 15$, $\omega = 0.2$, $\epsilon = 15$, $\alpha = 0.5$, $\beta = 0.5$, $a = 0.5$ Initial conditions: $S_0 = 9999$, $I_0 = 1$, $R_0 = 0$ (host population). In this case we show the infected host class ($I(t)$) when seasonal effects take place in the transmission rates (α and β) and control measures (ϵ). For a) and b) α and β are varied simultaneously; a) $\bar{\alpha} = 0.5 + 0.4\sin(\frac{2\Pi t}{180})$ and $\bar{\beta} = 0.5 + 0.4\sin(\frac{2\Pi t}{180})$, b) $\bar{\alpha} = 0.8 + 0.4\sin(\frac{2\Pi t}{180})$ and $\bar{\beta} = 0.8 + 0.4\sin(\frac{2\Pi t}{180})$. For c) and d) ϵ is varied; c) $\bar{\epsilon} = 15 + 5\sin(\frac{2\Pi t}{180})$ and *d)* $\bar{\epsilon} = 15 + 10\sin(\frac{2\Pi t}{180})$. 34

5.4 Moderate seasonal effects on host and vector transmission rates (α, β and ϵ). The parameter values are: $\mu = 0.00004$, $\mu_e = 0.003$, $\mu_m = 0.03$, $\delta = 0.09$, $\gamma = 0.14$, $\rho = 15$, $\omega = 0.2$, $\epsilon = 15$, $\alpha = 0.5$, $\beta = 0.5$, $a = 0.5$ Initial conditions: $S_0 = 9999$, $I_0 = 1$, $R_0 = 0$ (host population). In this case we show the vector population ($V(t)$) when seasonal effects take place in the transmission rates (α and β) and control measures (ϵ). For a) and b) α and β are varied simultaneously; a) $\bar{\alpha} = 0.5 + 0.4\sin(\frac{2\Pi t}{180})$ and $\bar{\beta} = 0.5 + 0.4\sin(\frac{2\Pi t}{180})$, b) $\bar{\alpha} = 0.8 + 0.4\sin(\frac{2\Pi t}{180})$ and $\bar{\beta} = 0.8 + 0.4\sin(\frac{2\Pi t}{180})$. For c) and d) ϵ is varied; c) $\bar{\epsilon} = 15 + 5\sin(\frac{2\Pi t}{180})$ and d) $\bar{\epsilon} = 15 + 10\sin(\frac{2\Pi t}{180})$. The vector begins at the low demographic equilibrium $E_0^{low} = 0.230129$, $V_0^{low} = 0.4099141$ and $J_0^{low} = 0.004318148$ and then jumps to the high equilibrium $E_0^{high} = 5.527807$, $V_0^{high} = 10.99821$, $J_0^{high} = 0.3055878$. In the absence of seasonality $\epsilon = 15$ there is no jump. 35

6.1 Caricature of the model. 39
6.2 Regions of stability when a) $\alpha_1 = \beta_1 = 0.2$, $\alpha_2 = \beta_2 = 0.2$, $\gamma_1 = 0.33$, $\psi = 0.5$, $p = 0.1$. In b) we let $\beta_1 = \beta_2 = 0.5$, $\psi = 0.9$ and $p = 0.9$ while in c) we let $\alpha_2 = \beta_2 = 0.5$, $\psi = 0.5$ and $p = 1$. 43
6.3 Individuals infected with secondary strain (z_1) for three values of the infection rate (ρ_1) from the behavior change class (b_2). 44
6.4 Phase plane of secondary infection (z_1 and z_2). 45
6.5 Time series of first infection (d_1 and d_2). *Parameter values:* $\beta_1 = 0.33$, $\beta_2 = 0.5$, $\gamma_1 = 0.25$, γ_2, $\phi_1 = \phi_2 = 0.1$, $\alpha_1 = 0.5$, $\alpha_2 = 0.33$, $\rho_1 = 1$, $\rho_2 = 4$, $p = 0.1$ and $\psi = 0.5$. *Initial conditions:* $s_0 = 0.98$, $d_1 = 0.01$, $d_2 = 0.01$, $v_0 = 0.98$, $g_1 = 0.01$, and $g_2 = 0.01$. 45
6.6 Time series of behavior change population (b_1 and b_2). *Parameter values:* $\beta_1 = 0.33$, $\beta_2 = 0.5$, $\gamma_1 = 0.25$, γ_2, $\phi_1 = \phi_2 = 0.1$, $\alpha_1 = 0.5$, $\alpha_2 = 0.33$, $\rho_1 = 1$, $\rho_2 = 4$, $p = 0.1$, and $\psi = 0.5$. *Initial conditions:* $s_0 = 0.98$, $d_1 = 0.01$, $d_2 = 0.01$, $v_0 = 0.98$, $g_1 = 0.01$, and $g_2 = 0.01$. 46
6.7 Phase plane of first infection (d_1 and d_2). 47
6.8 Phase plane of behavior change population (b_1 and b_2). 47
6.9 Time series of secondary infection (z_1 and z_2). *Parameter values:* $\beta_1 = 0.33$, $\beta_2 = 0.5$, $\gamma_1 = 0.25$, γ_2, $\phi_1 = \phi_2 = 0.1$, $\alpha_1 = 0.5$, $\alpha_2 = 0.33$, $\rho_1 = 1$, $\rho_2 = 4$, $p = 0.1$ and $\psi = 0.5$. *Initial conditions:* $s_0 = 0.98$, $d_1 = 0.01$, $d_2 = 0.01$, $v_0 = 0.98$, $g_1 = 0.01$, and $g_2 = 0.01$. 48
6.10 Time series of infected mosquito population (g_1 and g_2). *Parameter values:* $\beta_1 = 0.33$, $\beta_2 = 0.5$, $\gamma_1 = 0.25$, γ_2=0.14, $\phi_1 = \phi_2 = 0.1$, $\alpha_1 = 0.5$, $\alpha_2 = 0.33$, $\rho_1 = 1$, $\rho_2 = 4$, $p = 0.1$ and $\psi = 0.5$. *Initial conditions:* $s_0 = 0.98$, $d_1 = 0.01$, $d_2 = 0.01$, $v_0 = 0.98$, $g_1 = 0.01$, and $g_2 = 0.01$. 48
6.11 Phase plane of infected mosquito population (g_1 and g_2). 49
6.12 y_1 when $\mathcal{R}_1 > 1$ and y_2 when $\mathcal{R}_2 < 1$. 50

8.1 Caricature of the model. 78
8.2 Threshold conditions: $\mathcal{R}_c$ and $\mathcal{R}_\phi$. 83
8.3 Histogram for $\mathcal{R}_\phi$. The mean is 3.12 with a standard deviation of 7.39 and 71% of $\mathcal{R}_\phi > 1$. 84
8.4 Histogram of $\frac{\mathcal{R}_c}{\mathcal{R}_\phi}$. The mean is 0.16 with a standard deviation of 0.11 and the median is 0.14 86
8.5 Backward bifurcation and time series of the d-class. Parameter values: $\mu = 0.0000548$, $\phi = 0.2$, $\rho = 0.21$ and $\beta = [0.001, 1.3]$. A time series plot of the system with different initial conditions. *Lower left*: $s = 0.97$, $d = 0.03$ and $r_0 = 0$. *Lower right*: $s = 0.99$, $d = 0.01$ and $r = 0$. *Parameter values*: $\mu = 0.0000548$, $\beta = 0.19$, $\phi = 0.2$ and $\rho = 0.21$. 88
8.6 Problem drinkers (D) vs. ρ. *Parameters:* $\beta = 0.5$, $\phi = 0.2$, and $\mu = 0.0000548$. *Initial conditions:* $s_0 = 0.99$, $d_0 = 0.01$, and $r_0 = 0$. 90
8.7 Problem drinkers (D) vs. ϕ. *Parameters:* $\beta = 0.5$, $\rho = 0.21$, and $\mu = 0.0000548$. *Initial conditions:* $s_0 = 0.99$, $d_0 = 0.01$, and $r_0 = 0$. 91
8.8 Problem drinkers (D) vs. β. *Parameters:* $\rho = 0.21$, $\phi = 0.2$, and $\mu = 0.0000548$. *Initial conditions:* $s_0 = 0.99$, $d_0 = 0.01$, and $r_0 = 0$. 91

9.1 Mean final size of the "problem" drinking population with 1000 nodes, $\langle k \rangle = 6$, $\beta = 0.03$ and $\rho = 0.8$ as a function of the treatment rate ϕ for two extreme values of p (disorder parameter). 95
9.2 Mean final size of the "problem" drinking population with 1000 nodes, $\langle k \rangle = 6$, $\beta = 0.03$ and $\phi = 0.8$ as a function of the relapse rate ρ for two different values of p (disorder parameter). 96
9.3 Mean final size of the "problem" drinking population with 10^3 nodes and $\langle k \rangle = 3$ as a function of the disorder parameter p. *Parameter values:* $\beta = 0.03$, $\rho = 3$, and $\phi = 0.8$. 97
9.4 Mean final size of the "problem" drinking population with 10^3 nodes and $\langle k \rangle = 3$ as a function of the disorder parameter p. *Parameter values:* $\beta = 0.03$, $\rho = 0.4$, and $\phi = 0.8$. 98
9.5 Diagram of transition probabilities. 99
9.6 Histograms of the "problem" drinking population for two values of p when $\rho = 0.4$, $\phi = 0.8$, $\beta = 0.03$ and $\mu = 0.0000548$. 100
9.7 Histograms of the "problem" drinking population for two values of p when $\rho = 3$, $\phi = 0.8$, $\beta = 0.03$ and $\mu = 0.0000548$. 101
9.8 *Left.* Stochastic version of SDR model (100 realizations). *Mean*= 507. *Right.* Deterministic version of SDR model. For these simulations the parameters used were: $\beta = 0.5$, $\rho = 0.21$, $\phi = 0.1$ and $\mu = 0.0000548$ with $\mathcal{R}_\phi = 5$. We started with five drinkers ($D_0 = 5$). *Mean*= 528. 103
9.9 From the stochastic simulations we computed a histogram of the final size of the drinking population at a stoppage time $T = 300$. *Initial conditions: left:* $d_0 = 5$, *right*: $d_0 = 10$. $\mathcal{R}_\phi > 1$. 104

9.10 From the stochastic simulations we computed a histogram of the final size of the drinking population at a stoppage time $T = 2000$. To the right is a zoom of the histogram without the zeros. In this case $\mathcal{R}_\phi < 1$. 105

10.1 Caricature of the model. 109
10.2 Two neighborhoods. *Parameter values:* $\mu = 0.0000548$, $\phi_1 = \phi_2 = 1/30$, $\beta_1 = \beta_2 = 1/5$, $a_1 = a_2 = 15$, $b_2 = 30$, $\tau_1 = \tau_2 = 0.1$, $\rho_1 = 1/5$, $\alpha_1 = 1/30$. *Initial conditions:* $s_0^1 = 0.99$, $o_0^1 = 0$, $m_0^1 = 0.01$, $h_0^1 = 0$, $s_0^2 = 0.95$, $o_0^2 = 0$, $m_0^2 = 0.05$, $h_0^2 = 0$. 117
10.3 Distribution for $\mathcal{R}_0^1$. 120
10.4 Distribution for $\mathcal{R}_0^2$. 120

Chapter 1

Part I: Introduction

It is believed that dengue originated in Africa [42]. During the late 18^{th} century there were the "first" major outbreaks in Asia, Africa, and North America but it is still uncertain as to the exact date (period) when dengue originated. As reported in the CDC the occurrence of these outbreaks on three continents leads to believe that these viruses have been spread worldwide for many years. Dengue fever was not considered to be a fatal disease for those who visited endemic countries [7]. During the late 19^{th} century and early 20^{th} dengue fever was being misdiagnosed with other similar diseases like, scarlatina and rheumatic fever [1, 2, 3, 4].

The first recorded outbreaks were in $1779 - 1780$ in Asia, Africa and North America. Long ago the periods between epidemic outbreaks were long, $10 - 40$ years. Sailing vessels were the preferred mode of vector transport in those times [7]. Dengue fever seems to affect around 100 million people annually. The exact numbers are unknown because not all the cases are reported, cases can reflect flu-like symptoms and many are asymptomatic [50].

There are four different serotypes (DEN-1, DEN-2, DEN-3 and DEN-4). Individuals acquire permanent immunity from each serotype with which they have become infected. Tropical and subtropical regions experiencing high levels of urbanization and increased deforestation are often the areas at the greatest risk for vector-borne disease epidemics [46, 49]. Currently dengue is one of the most serious human infectious diseases [50].

The most severe case of dengue is Dengue Hemorrhagic Fever (DHF) or Dengue Shock Syndrome (DSS). There are two theories that have attempted to explain the

pathogenesis of DHF. One is that virulent dengue virus strains cause DHF while avirulent strains cause DF (Dengue Fever). The other is that DHF is mediated by host immune responses. In other words, the cross-reaction between strains can augment infections [50].

Some important factors that may have contributed to the global emergence of DHF are: lack of effective mosquito control in dengue-endemic countries, uncontrolled urbanization and population growth [7]. A total of $250,000 - 500,000$ cases of DHF are reported annually with a fatality ratio of about 5% [50] (see Figure 1.1 for a world distribution of dengue). Research has shown that $85\% - 90\%$ of DHF cases have been caused by cross-reactions between different strains. DHF can occur in primary or secondary infections but it is more common during a secondary infection [50]. Susceptibility is universal, but children generally have milder ill-

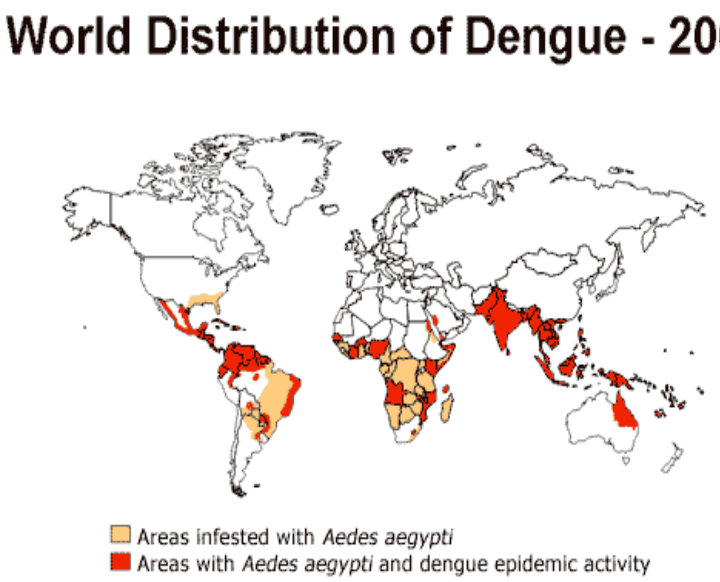

Figure 1.1: World distribution of dengue epidemic [10].

ness than adults. All four dengue serotypes produce flu like symptoms; headache, backache, fatigue, stiffness, anorexia, and chills [42]. The strains are antigenically

distinct, that is, infection with one type does not typically provide immunity to a second type. Instead after infection with a particular strain there is at most 90 days [40, 53]) of partial immunity to other strains.

Recent papers by [19, 43, 41, 58] highlight the concerns of the disease emerging to higher endemic states where it was absent and then reappeared. There are many factors that can contribute to the reappearance of dengue fever:

- Infiltration of a new strain to a mostly susceptible population,
- Loss of immunity in the population,
- Considerable urbanization of rural areas (increases the number of breeding sites),
- Climate variability: temperature fluctuations, floods and droughts.

Current policies and interventions focus on educating people about the seriousness and possibly fatal consequences of dengue fever and its fatal form Dengue Haemorrhagic Fever (DHF) and Dengue Shock Syndrome (DSS). However, these methods have had an negligible effect on dengue endemic countries (see Figure 1.1).

Social dynamics play an important role in the transmission of dengue. Lack of resources, poor living, as well as, lack of knowledge or careless behavior can contribute to new dengue infections. We show that collective behavioral changes can reduce the number of dengue infections. We assume that collective behavior change imply low cost artifacts and rational behavior such as: mosquito repellents, bed nets and screens on windows.

The total economic cost of dengue is difficult to estimate since nearly half the cases are asymptomatic or not reported. Loss wages, work days lost, absenteeism all contribute to the economic impact but are hard to measure accurately.

In Chapter 2 we discuss the epidemiology of dengue. Chapter 3 reviews previous dengue models and their results. In Chapter 4 we explore a single-outbreak model and fit it to data from the most recent outbreaks in Singapore (2001, 2004, and 2005). We make comparisons, estimate parameters and estimate the reproductive number for each outbreak. In Chapter 5, we consider a single strain mathematical model that incorporates the early life-history of the vector allowing for multiple mosquito densities depending on the egg/larvae recruitment function. We incorporate seasonality and illustrate a simple scenario which shows that low mosquito densities can still cause large outbreaks when a new strain is introduced in a mostly susceptible population. In Chapter 6, we look at the effects of social dynamics by incorporating collective behavioral change classes in a two-strain model.

Chapter 2

Epidemiology of dengue

2.1 Ecology of *Aedes aegypti* and *Aedes albopictus*

Two species of mosquitoes are capable of transmitting the dengue virus, *Aedes aegypti* and *Aedes albopictus*. *Aedes albopictus* is found mostly in rural areas. *Aedes aegypti* is mostly found in urban areas where human density is high. *Aedes aegypti* is the main vector/carrier of the dengue virus. The life cycle of *Aedes aegypti* consists of four stages [8]. During the first stage the eggs are laid just above the water line on tree holes, discarded containers, or on the ground where water might fall. Eggs can survive without water for almost a year. *Aedes aegypti* lays up to 150 at once and on average can lay about $1,400$ eggs in its lifetime. The eggs hatch in $1-2$ days and release the larvae. After $7-10$ days the larvae change to pupa in preparation for the adult stage. Days after maturation, the females look for a blood meal and males mate. The males do not ingest blood but feed on plants and flowers. Females can feed on animals or humans but research has shown that they prefer to feed on humans [45, 7]. On average these mosquitoes can live for a period of 12 to 15 days [38]. The females feed every two to three days and lay eggs after the feeding process [56]. *Aedes aegypti* do not usually breed in contaminated waters [42, 5]. This process is highly dependent on temperature.

Aedes aegypti has adapted to live around human environments and eradication has proven impossible. This is mainly due because the breeding sites are in a great part created by humans [48, 30, 42].

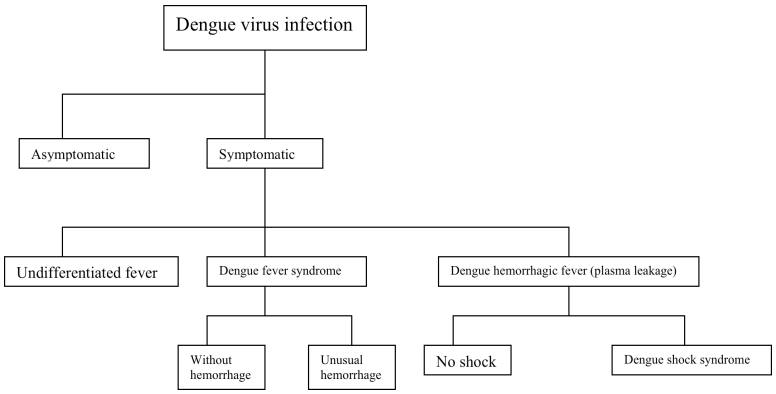

Figure 2.1: Manifestations of the dengue syndrome [42].

2.2 Transmission cycle

Dengue transmission may occur when an uninfected female mosquito feeds on an infected individual or when an infected mosquito bites an uninfected human. Although there has been evidence of vertical transmission of dengue virus by *Aedes aegypti*, typically they can only get infected after biting an infected person. Once the virus is in the mosquito replicates for a period of 8 to 12 days [11]. Humans cannot infect other humans. At the time the individual is infected the virus reproduces and produces symptoms that can last from $3 - 14$ days (see Figure 2.2).

2.3 Treatment and control

Since dengue viruses were isolated, efforts to make a vaccine has failed. There is no vaccine for dengue fever. However, there are efforts in developing attenuated vaccines for dengue fever [25, 20]. These vaccines are in the early stages and human trials have not begun. Hence, it is possible that an effective vaccine will not be available for the next five to ten years.

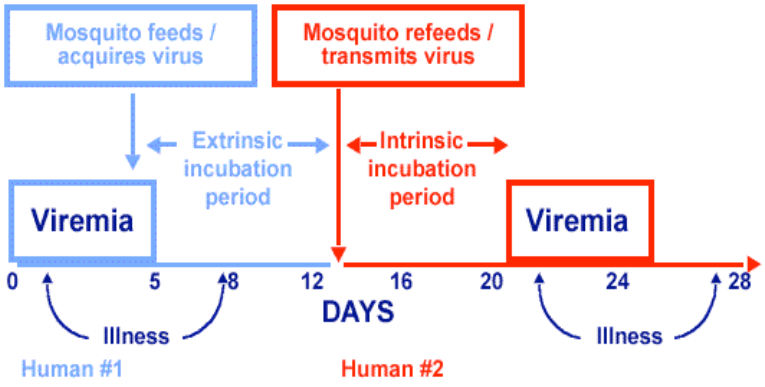

Figure 2.2: Transmission cycle [11].

2.4 Seasonal trends and the effects on dengue transmission

There are many factors that can influence the transmission of dengue fever, e.g. climate, vector movement, vector density among others [42, 26, 54, 39]. There has been significant research on vector-density and there is no clear answer about how low the density of mosquitoes should be in order to prevent large outbreaks. In fact, in Singapore the house index dropped to 1% and outbreaks still occurred [42]. *See Figure 4.1.*

Chapter 3

Review of dengue models and results

Previous dengue models have been developed by [34, 32, 33, 35, 27, 37]. In this chapter I review some of the models previously analyzed and their results.

Most of these papers focus on the ongoing discussion of what causes Dengue Hemorrhagic Fever (DHF) or Dengue Shock Syndrome (DSS) [50, 49, 6, 7, 44]. The main focus in literature was in the immunology of dengue [42, 40, 44, 56, 19, 5]. From previous mathematical modeling few approaches (see [54]) were taken to study reducing the number of breeding sites which could probably be responsible for large epidemic outbreaks. Public policies have been implemented in order to alert communities of the danger of these mosquitoes, however, the strategy works at some level but dengue strains can invade a susceptible population by immigration or loss of immunity as it has happened in Central America, South America, and Puerto Rico [7]. It is widely believed that cross-reaction of strains ($DEN-2$ being the main suspect) is the main catalyst of dengue hemorrhagic fever, DHF.

We reviewed a model for a single strain of dengue [31]. Their model's equations are:

$$\begin{aligned}
S'_H(t) &= \mu_H N_h - \beta_H b \frac{N_v}{N_H+m} S_h \frac{I_v}{N_v} - \mu_H S_H \\
I'_H(t) &= \beta_H b \frac{N_v}{N_H+m} S_H \frac{I_v}{N_v} - (\mu_H + \gamma_H) I_H \\
R'_H(t) &= \gamma_H I_H - \mu_H R_H \\
S'_v(t) &= A - \beta_v b \frac{N_H}{N_H+m} S_v \frac{I_H}{N_h} - \mu_v S_v \\
I'_v(t) &= \beta_v b \frac{N_H}{N_H+m} S_v \frac{I_H}{N_H} - \mu_v I_v
\end{aligned}$$

where $N_H = S_H + I_H + R_H$ and $N_v = S_v + I_v$ represent the host and vector

populations respectively with S_h, S_v denote the susceptible populations, I_H, I_v the infected and R_H the recovered, here assumed with permanent immunity. The parameter values are: $\mu_H = 0.0000457$, $\mu_v = 0.25$, $b = 0.5$, $\beta_H = 0.75$, $\beta_v = 1$, $m = 0$, $\gamma_H = 0.1428$, $N = 10,000$, and $A = 400$.

A single strain dengue model is constructed where they include biting rates and probability of infection (human-mosquito and vice-versa). The analysis of the model turns out to be more complicated but model results and predictions are qualitatively similar to those resulting from our proposed model which includes an egg/larva recruitment function $f(L)$ which is density dependent (L-total mosquito population).

The model looks at the impact of ULV insecticide treatment. The treatment is applied during seven days when there is a low prevalence of the virus. The insecticide does not reduce prevalence of dengue, however, it delays the onset of the epidemic. Essentially, the model looks at vector mortality as a form of control and prevention.

In [35] the competitive dynamics of dengue fever using an ode model is studied. Their objective is to find conditions for or against competitive exclusion. The model is described by the following system of nonlinear differential equations:

$$\begin{aligned}
S'(t) &= h - (B_1 + B_2)S - \mu S, && (3.1)\\
I_1'(t) &= B_1 S - \sigma_2 B_2 I_1 - u I_1, && (3.2)\\
I_2'(t) &= B_2 S - \sigma_1 B_1 I_2 - u I_2, && (3.3)\\
Y_1'(t) &= \sigma_1 B_1 I_2 - (e_1 + u + r) Y_1, && (3.4)\\
Y_2'(t) &= \sigma_2 B_2 I_1 - (e_2 + u + r) Y_2, && (3.5)\\
R'(t) &= r(Y_1 + Y_2) - uR, && (3.6)
\end{aligned}$$

and

$$M'(t) = q - (A_1 + A_2)M - \delta M, \tag{3.7}$$

$$V_1'(t) = A_1 M - \delta V_1, \tag{3.8}$$

$$V_2'(t) = A_2 M - \delta V_2. \tag{3.9}$$

Where $N = S + I_1 + I_2 + Y_1 + Y_2 + R$ and $T = M + V_1 + V_2$ are the total host and vector populations respectively.

To briefly discuss the outline of the model we have the following population classes: S, susceptible hosts, $I_i (i = 1, 2)$, first infection of the host with strain 1 and 2 respectively, $Y_i (i = 1, 2)$, second infection with strain 1 or 2 depending on which strain the host had previously, R, recovered class. The primary infection of the host is given by,

$$B_i = \frac{\beta_i V_i}{c + \omega_h N}.$$

There are two stages for the vector; M, adult vectors, $V_i (i = 1, 2)$, where a host is infected with either strain 1 or 2 at a given rate of,

$$A_i = \frac{\alpha_i (I_i + Y_i)}{c + \omega_v N}.$$

These describe frequency-dependent disease transmission and both are special cases of the Holling type II functional response [24] and are generalizations of the model for Malaria [16], and Chagas disease [59].

The authors incorporate vector-host dynamics in a two-strain dengue model. They carry out numerical simulations to illustrate their results using parameter ranges from the 1991 dengue fever outbreak in Brazil [51]. They estimate the basic reproductive number for both strains (≈ 2 for both). The existence of the interior endemic equilibrium (both strains co-exist) is established via simulations

for $\sigma_i \in (0, 2)$. If σ_i (susceptibility index to strain i) is very small or large only the boundary equilibria exist. The authors were able to establish conditions for the existence of the interior endemic equilibrium for ranges in σ_i. The parameter values used for simulations are: $u = 1/70\ years$, $r = 1/14$, $\alpha_i \in (0, 0.05)$, $\beta_i \in (0, 0.05)$, $\delta = 1/14$, $c = 1$, $\omega = 0.5$, and $\sigma_i \in (0, 5)$.

In the next chapters we constructed dengue fever models that look at a single-outbreak model using current data from Singapore [13], incorporate the early life-stage of the vector, and a multiple strain model that includes collective host behavior changes.

Chapter 4

A case study: a single-outbreak model for dengue outbreaks in Singapore

Singapore a member of Southeastern Asia Islands is located between Malaysia and Indonesia. It has a population of approximately 4.5 million and has an area of 692.7 sq. km [15]. The weather is tropical which makes it an ideal habitat for the vector (*Aedes aegypti* and *Aedes albopictus*) that transmits dengue. Dengue fever has been a problem in Singapore where its public health system has implemented measures but have not impacted dengue transmission. Some of the preventive measures include [13]:

- Clustering of cases by place and time

  -Intensified control actions are implemented in these cluster areas.

- Surveillance control programs

  -Vector control

  -Larval source reduction (search and destroy)

- Health education

  -House to house visits by health officers -Dengue prevention Volunteer Groups (National Environmental Agency (NEA))

- Law enforcement

  -Large fines for facilitating the existence of breeding sites

However, the situation worsen since 2001. Here, we have gathered data from two different outbreaks (2001 and 2004) and use them to estimate model parameters

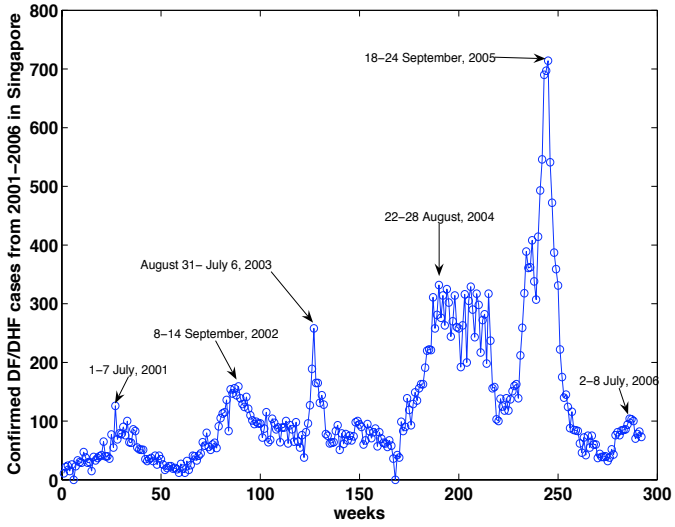

Figure 4.1: Confirmed DF/DHF weekly cases from $2001-2006$ in Singapore [13].

and the basic reproductive number for both years.

In Figure 4.2 we observe that $DEN-1$ and $DEN-2$ have been the prevalent strains in Singapore from $1992-2004$. In particular, using the data provided by [13] we can conclude that $DEN-2$ strain is responsible for the majority of dengue cases from $2001-2003$ (see Figure 4.1). These outbreaks are fairly consistent in their magnitude. Moreover, in 2004 $DEN-1$ took over as the dominant strain and not surprisingly the number of cumulative cases increased significantly. In 2005, $DEN-1$ prevailed as the dominant strain, however, the number of cases caused by strain $DEN-3$ increased. In Figure 4.1 we see that the number of cases for 2006 is significantly lower than for previous years. These sudden drop in the number of dengue cases may be due to the increased immunity in the population. Using geographical data [13] we can see from Figure 4.4 that from $2001-2003$ most dengue cases were scattered along similar regions. However, in 2004, even when it's apparent the most dengue cases occurred in the same regions the concentration

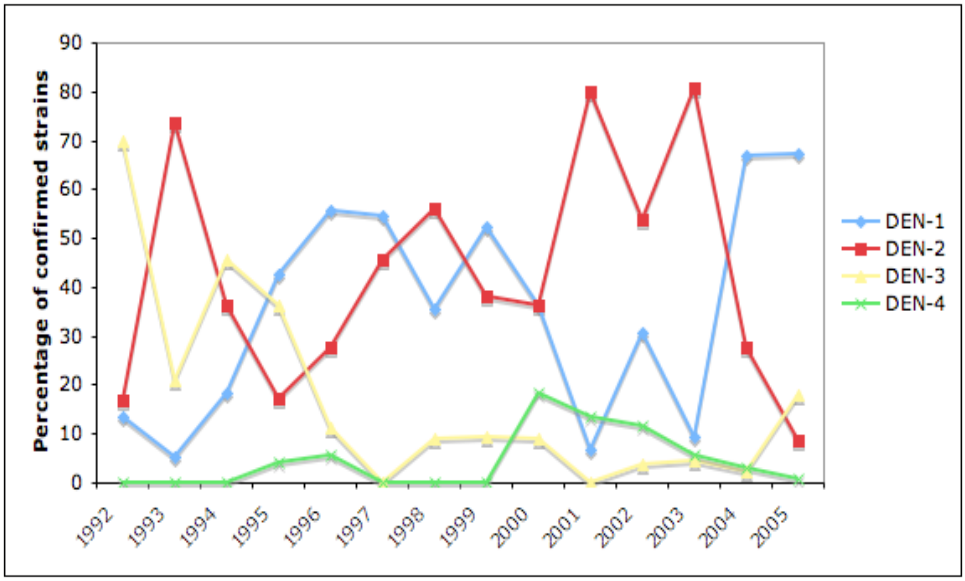

Figure 4.2: Confirmed DF/DHF cases [13].

of the cases seems to be larger than previous years. This is consistent with data on the weekly number of cases (see Figure 4.1). It still remains uncertain how the cases are distributed for 2005. The difference from the 2001 outbreak in comparison with 2005 is of $11,464$ cases. From Figure 4.5 *Aedes aegypti* is mostly found in ornamental and domestic containers. This trend points at the importance of social behavior. It is vital for individuals to reduce the risk of transmission by destroying uncommon artificial breeding sites. The host is mainly responsible for providing "artificial" breeding sites for the mosquitoes and increasing the transmission of dengue. It is worth noting that although anyone can be infected with dengue some age groups are more affected than others. In Figure 4.6 we look at seven different age groups and their respective dengue incidence rates (per$/100,000$). We observe that although incidence has increased steadily in all age groups since 2001 there was a major increase in the $5-14$ age group from 2003 to 2005. This growth can be correlated to the activity level of this age group along with the increased

Figure 4.3: Map of Singapore.

number of "artificial" breeding sites. In fact, dengue incidence rates more than doubled in all age groups from 2003 to 2005.

Laboratory surveillance. Reported cases were serologically confirmed by one or more of laboratory tests; viz. anti-dengue *IgM* antibody enzyme linked immunosorbent assay (ELISA) and the haemagglutination-inhibition test.

4.1 Single-outbreak model

In this chapter we introduce simple single-outbreak mathematical model that describes the dynamics of dengue between hosts and vectors in Singapore. The population is divided as follows: S-susceptible, E-exposed (infected but not infectious), I-infected (presumed infectious) and R-recovered (immune). For the vector we have: V (susceptible mosquitoes), L (latent mosquitoes) and J (infected mosquitoes). The following is the system of nonlinear differential equations that

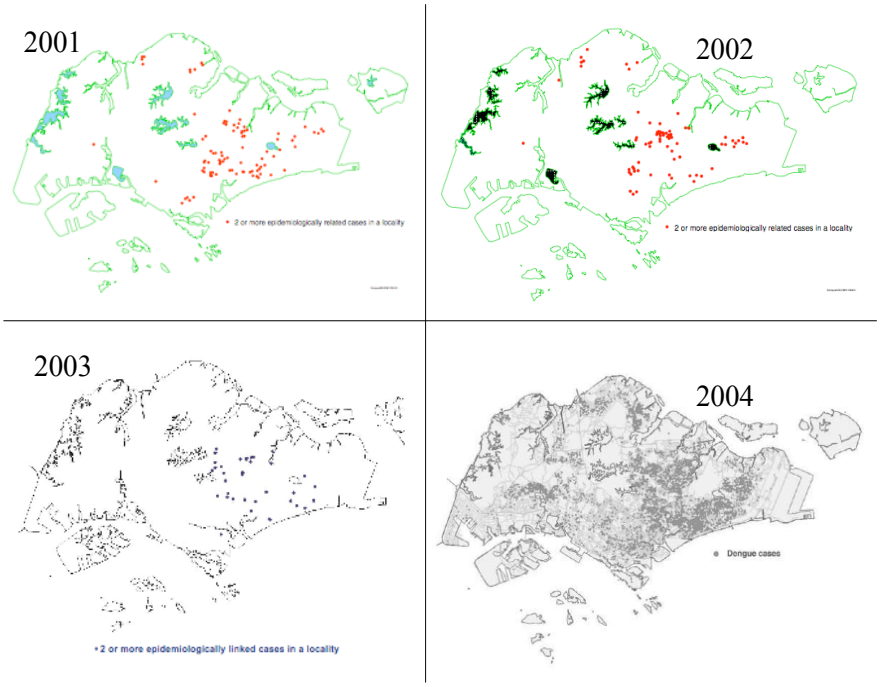

Figure 4.4: Geographical distribution of DF/DHF in Singapore from 2001 − 2004 [13].

we use to model the dynamics of a single outbreak:

$$\begin{aligned} S' &= -\beta S \tfrac{J}{M}, \\ E' &= \beta S \tfrac{J}{M} - \rho E, \\ I' &= \rho E - \gamma I, \\ R' &= \gamma I, \\ V' &= -\alpha V \tfrac{I}{N}, \\ L' &= \alpha V \tfrac{I}{N} - (\mu_m + \phi) L, \\ J' &= \phi L - \mu_m J, \end{aligned} \tag{4.1}$$

where $N = S + E + I + R$ and $M = V + L + J$.

We will compare two outbreaks that occurred in Singapore. We fit our model

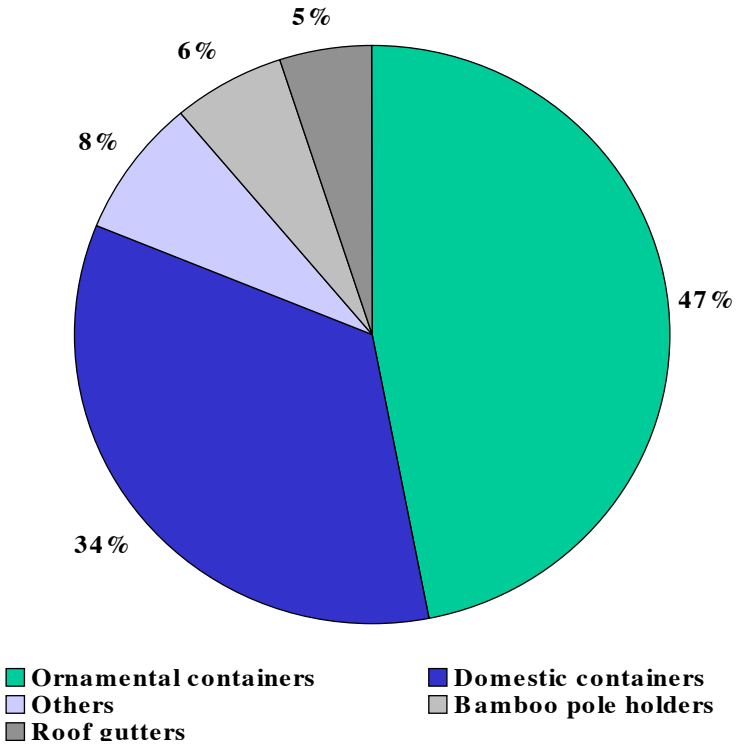

Figure 4.5: Distribution of *Ae. aegpyti* by top five breeding habitats, 2004 [13].

to data and estimate parameters for each outbreak. We will focus on the infectious period ($1/\gamma$) and the transmission (contact) rates for human and vector (β and α, respectively). Parameter definitions can be found in Table 4.1

4.2 Results

The basic reproductive number for the system is given by:

$$\mathcal{R}_0 = \sqrt{\frac{\beta}{\gamma}\frac{\phi}{\mu_m+\phi+d}\frac{\alpha}{\mu_m+d}},$$

where β is the transmission rate from vector to human. $1/\gamma$ represents the average host infectious period. α is the transmission rate from human to vector. $1/(\mu_m+d)$ is the average vector infectious period and $\phi/(\mu_m+\phi+d)$ represent the proportion

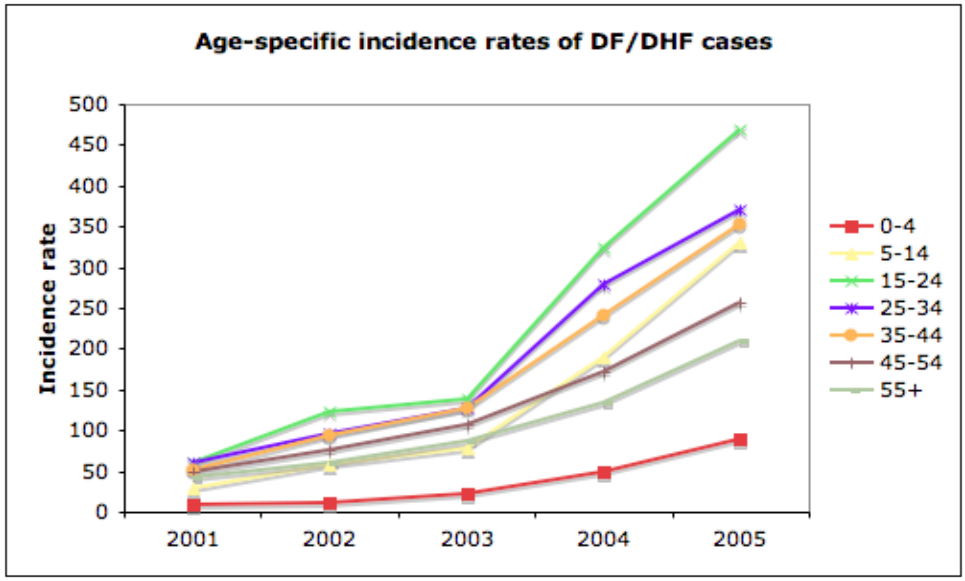

Figure 4.6: Age-specific incidence (per/100,000) rates of DF/DHF cases [13].

of vectors that make it to the infectious class (J).

We used the data from [13] to fit the model, estimate parameters and the basic reproductive number from the 2001, 2004 and 2005 outbreaks. For the 2001 outbreak the dominant strain was $DEN-2$ followed by $DEN-4$, $DEN-1$ and $DEN-3$. However, in 2004 $DEN-1$ surpassed $DEN-2$ as the dominant strain in the population with approximately 70% of the cases (see Figure 4.2). $DEN-2$ followed with approximately 28% of the cases. $DEN-3$ and $DEN-4$ did not play a big role in the 2004 outbreak. In Figure 4.7, 4.8 and 4.9 we show the cumulative number of DF/DHF confirmed cases and the model solution. It is important to notice that the average infectious period (γ) is approximately 1.7 days for 2001 and 7 days for 2004. This implies that the window of opportunity of the mosquito was relatively short in 2004 and much larger in 2005. In 2001 dengue was possibly a mild illness and in 2005 it was likely that the disease was more virulent. In fact, the number of hospitalizations due to dengue has increased since

Table 4.1: Parameter List

Parameters	Description
α	contact rate (human-vector)
β	contact rate (vector-human)
ρ	latent period in humans
ϕ	latent period in mosquito
μ_m	per-capita adult mosquito mortality rate
γ	per-capita recovery rate

2003 [12]. It is not clear if loss of immunity plays a role in the increased virulence

Table 4.2: $\mathcal{R}_0$ estimates for dengue outbreaks in Singapore from $2001 - 2005$.

Year	Value	Dominant strain
2001	1.1	2
2002	2.4	2
2003	4.7	2
2004	1.2	1
2005	5	1

of dengue. Moreover, the 2005 outbreak in which there were more than 700 cases the third week of September, the biggest number of new cases seen in Singapore. Some studies have shown that climate variations such as temperature and rainfall are key components in the transmission of dengue [43, 26]. Furthermore, the 2005 outbreak seems to behave differently. The number of cases increased by $4,659$ from the previous year.

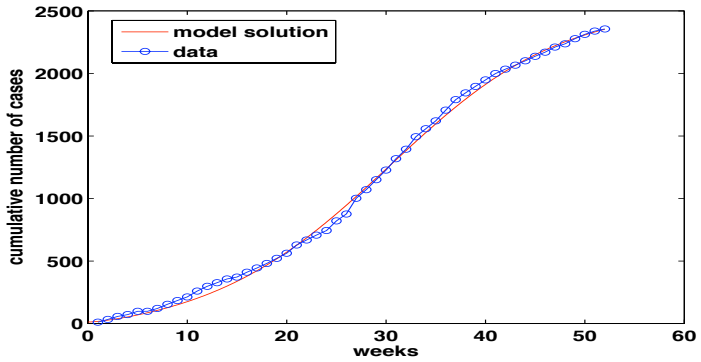

Figure 4.7: Singapore data from the 2001 dengue outbreak. Estimates of the parameters: $\beta = 0.73$, $\alpha = 0.75$, $\gamma = 4.2$, $\rho = 2.3$, $\phi = 0.5$ and $\mu = 0.1$. The estimated basic reproductive number for this outbreak is $\mathcal{R}_0 = 1.1$.

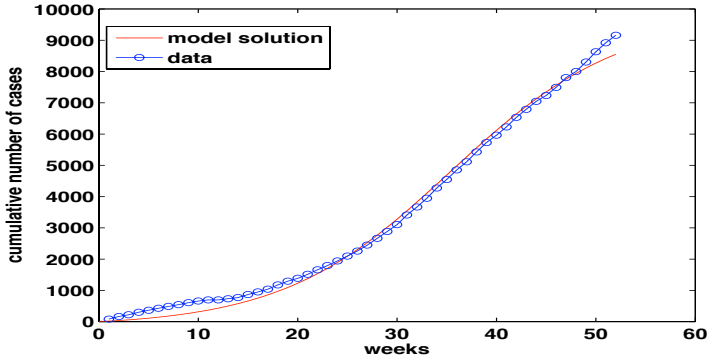

Figure 4.8: Data from the 2004 dengue outbreak in Singapore. Estimates of the parameters: $\beta = 0.2$, $\alpha = 0.83$, $\gamma = 1$, $\rho = 2.33$, $\phi = 0.6$ and $\mu = 0.1$. The estimated basic reproductive number for this outbreak is $\mathcal{R}_0 = 1.2$.

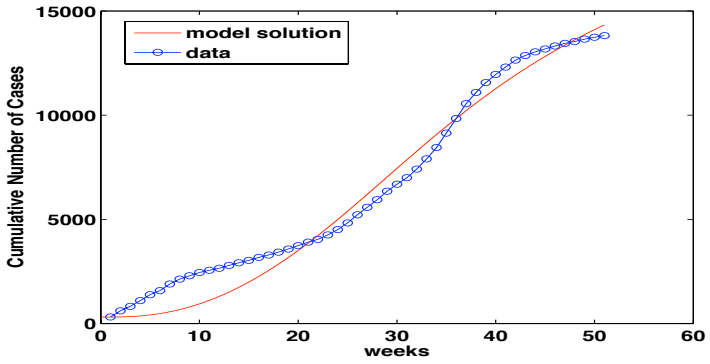

Figure 4.9: Data from the 2005 dengue outbreak in Singapore. Estimates of the parameters: $\beta = 1.1$, $\alpha = 1$, $\gamma = 2$, $\rho = 0.04$, $\phi = 0.2$ and $\mu = 0.02$. The estimated basic reproductive number for this outbreak is $\mathcal{R}_0 = 5$.

4.3 Conclusions

Despite the tremendous efforts of the public health system in Singapore to control dengue the number of confirmed clinical DF/DHF cases has increased over the past five years by $11,464$ new cases. Some factors that could be contributing to the situation in Singapore are: the introduction of new strains, new pool of susceptible individuals (via immigration) and lack of significant reduction in vector population are some of the most important factors.

Other contributing factors are migration and loss of immunity. It was estimated that in 2006 that the migration rate was 9.12 per 1000 individuals [13]. This factor could be contributing to the new cases by displacing the immune individuals (migration) and adding a new pool of susceptible (immigration).

We estimated the basic reproductive number for $2001 - 2005$ outbreaks (see Table 4.2). From the parameter estimates we obtain that the reproductive numbers for each outbreak. We conclude that the difference in the infectious period (γ) gives the vector a bigger window of opportunity to transmit the virus. Also, there are other important factors that could possibly play a major role in transmission such as: immigration and the diffusion of strains in the population.

Other factors can be contributing to the increased virulence and transmissibility of the virus. Some of which will be discussed later.

Chapter 5

Single strain model with vector-life history*

Several models of dengue have been developed in the past [34, 32, 33, 35, 27], with most of them in the tradition of Ross [57]. Knowledge of life history of the vector (closely connected to the distribution, size and dynamics of breeding sites) is the key to the development of potentially effective control measures [36]. Yet, the vector life history has rarely been included by theoreticians. A model that includes a detailed account of the life history of the vector may not be amenable to analysis. Instead, the classical Ross model is expanded to include a simplified version of the vector's life history. The impact of *selective* vector control measures on dengue dynamics is explored. The model assumes that (female) vectors may be found in three states: the egg/larvae state, E; the uninfected vector state, V; and the infected vector state, J. The host (humans) disease dynamics are modeled via an SIR model (see [21, 47, 22, 17, 29]), where $S(t)$ denotes the susceptible human population at time t; $I(t)$ the infected (assumed infectious) host population at time t; and $R(t)$ the recovered individuals (with assumed permanent immunity) at

*Sánchez, F., Engman, M., Harrington, L. and C. Castillo-Chávez. Models for Dengue Transmission and Control. Modeling The Dynamics of Human Diseases: Emerging Paraddigms and Challenges. AMS Contemporary Mathematics Series (in press). Gumel A. (Chief Editor), Castillo-Chávez, C., Clemence, D.P. and R.E. Mickens.

time t. The model is given by following non-linear system:

$$\begin{aligned}
\frac{dE}{dt} &= f(L) - (\mu_e + \delta)E = f_1(E, V, S, R, J, I) \\
\frac{dV}{dt} &= \delta E - \mu_m V - \alpha V \frac{I}{N} = f_2(E, V, S, R, J, I) \\
\frac{dS}{dt} &= \mu N - \beta S \frac{J}{L} - \mu S = f_3(E, V, S, R, J, I) \\
\frac{dR}{dt} &= \gamma I - \mu R = f_4(E, V, S, R, J, I) \\
\frac{dJ}{dt} &= \alpha V \frac{I}{N} - \mu_m J = f_5(E, V, S, R, J, I) \\
\frac{dI}{dt} &= \beta S \frac{J}{L} - (\mu + \gamma)I = f_6(E, V, S, R, J, I)
\end{aligned} \tag{5.1}$$

where $L = V + J$ and $N = S + I + R$ denote the total adult vector and host populations respectively. N is assumed to be constant, a valid assumption when the time scale of interest is short in relation to the life-span of the host but L is not assumed to be constant. In fact, the net egg/larvae recruitment function $f(L)$ is of Kolmogorov type, that is $f(L) = Lg(L)$ with $g : \mathbb{R}^+ \to \mathbb{R}^+$ a differentiable function such that $g(0) > 0$, and $g(\infty) = 0$. Dengue is not assumed to increase vector death rates. Selective control measures (Section 4) are modeled by replacing the more general function g with $g_c(L) \equiv g_0(L) - c(L)$, where $g_0(L)$ represents a (strictly decreasing) per-capita *mosquito fertility rate* and $c(L)$ the per-capita vector death rate that results from selective control efforts. Control efforts are modeled in a phenomenological way via the function $c(L)$ which captures, in a rough manner, the impact of measures geared towards the elimination of the egg/larvae. These measures may include selective spraying of areas where vector density is high. Furthermore, it is assumed that such measures negatively impact the net egg/larvae recruitment functions. Consequently, $g_c^{-1}(y)$ denotes the, possibly multiple valued, inverse image of y under control regime c, that is, shifting vector densities via control measures is a possibility. The parameters used in the model are defined in Table 5.1. Naturally, a reasonable model that includes the life-history of the

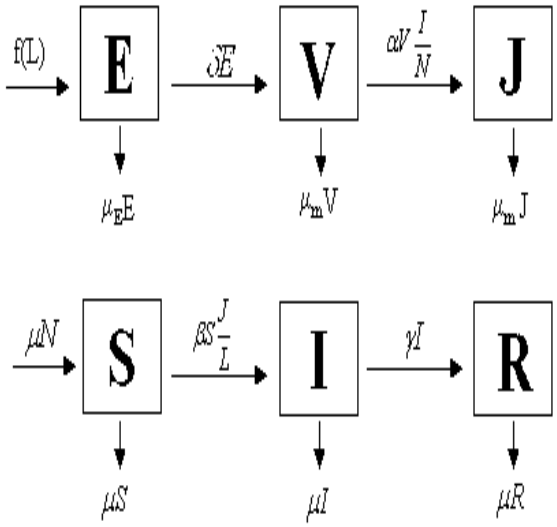

Figure 5.1: Caricature of the model.

vector must be able to support a critical mass of vectors. Enough hosts must also be available for dengue to prosper. Since our focus is primarily on the study of dengue in endemic regions with characteristics similar to those found in Singapore, N is large "enough". Conditions that guarantee the establishment of a "critical" mass of vectors are tied into the nature of $f(L)$. Certainly, such a critical mass exists in places where dengue is endemic (like the Caribbean). The existence of a minimal critical mass of vectors depends on the demographic threshold $\mathcal{R}_d(0)$ (see below). $\mathcal{R}_d(s)$ will govern the existence and stability of vector densities at level s where $s \geq 0$.

In the absence of control measures ($g_c = g_0$) only two vector densities may be possible $L_\infty \equiv 0$ and $L_\infty > 0$. $\mathcal{R}_d(s)$, the vector demographic number at vector density $L_\infty = s$, is given by

$$\mathcal{R}_d(s) = \frac{f'(s)}{\phi} \text{ where } \phi = \frac{(\mu_e + \delta)\mu_m}{\delta}. \tag{5.2}$$

Table 5.1: Parameter List

Parameters	Description
δ	per-capita rate at which viable eggs become adult vectors
α	contact rate (human-vector)
β	contact rate (vector-human)
μ_e	per-capita egg mortality rate
μ_m	per-capita adult mosquito mortality rate
μ	per-capita natural human mortality rate
γ	per-capita recovery rate

Where f is the net egg/larvae recruitment function described above. $\mathcal{R}_d(0)$ denotes the invasion *demographic reproductive number*. $\mathcal{R}_d(0) > 1$ corresponds to the situation where a vector population can successfully invade a habitat. In fact, $\mathcal{R}_d(0) > 1$ guarantees the existence of a critical mass of vectors (positive and stable). It is assumed throughout that $\mathcal{R}_d(0)$ is always greater than one. That is, the possibility of vector extinction is excluded in this study.

The issue of whether or not a disease can invade a host population and remain endemic requires the introduction of a second threshold. Disease invasion and persistence are typically intimately connected to the disease's basic reproductive number $\mathcal{R}_0$. This number or "ratio" is a dimensionless quantity that gives the number of secondary infections generated by a "typical" infectious individual (vector or host) in populations at demographic equilibrium. $\mathcal{R}_0$ involves the parameters that drive the "invasion" process. Hence, its study (sensitivity and uncertainty) helps identify key parameters and evaluate the relative effectiveness of various control measures. $\mathcal{R}_0$ can be computed in various ways. Here, we use

the next generation operator method [23], [28], and obtain that

$$\mathcal{R}_0 = \sqrt{\frac{\alpha\beta}{\mu_m(\mu+\gamma)}}. \tag{5.3}$$

It is shown ($\mathcal{R}_d(0) > 1$) that the disease's basic reproductive number $\mathcal{R}_0$ is the key. The condition $\mathcal{R}_0 < 1$ is, at least, a necessary condition for a globally asymptotically stable disease free state. On the other hand, $\mathcal{R}_0 > 1$ allows the possibility of multiple stable endemic states.

Control is modeled, in the endemic case, as an adult (vectors) harvesting process with a maximal harvesting rate (effort) ϵ. Although, the economics of control are not included, it is implicitly assumed that the cost of increasing ϵ, that is, the cost of eliminating a larger number of adults per unit of time, may grow fast as ϵ increases. Limitations on our ability to implement control efforts (measured by ϵ) may have a severe impact the vector's dynamics, a point that will be illustrated below.

5.1 Disease dynamics and control

In this section it is assumed that the vector has become established, that is, that $\mathcal{R}_d(0) > 1$. We also assumed that we have plenty of hosts, $N >> 0$. The infection-free equilibrium is

$$E_\infty = \frac{\mu_m}{\delta} g_c^{-1}(\phi), L_\infty = V_\infty = g_c^{-1}(\phi), S_\infty = N, R_\infty = J_\infty = I_\infty = 0. \tag{5.4}$$

The "mosquito-free" and "disease-free" state $(0, 0, N, 0, 0, 0)$, is an essential singular point of the system is therefore not considered* (see [18]). Conditions

*However, the use of DDT was probably responsible for the disappearance, over many decades, of dengue in Costa Rica (L. Harrington; personal communication)

for the existence of positive (disease present) equilibria are immediate from the formulae:

$$\begin{aligned} E_\infty &= \tfrac{\mu_m}{\delta} g_c^{-1}(\phi), \\ V_\infty &= \tfrac{\mu+\beta}{\mu\mathcal{R}_0^2+\beta} g_c^{-1}(\phi), \\ S_\infty &= \tfrac{N(\beta+\mu\mathcal{R}_0^2)}{(\mu+\beta)\mathcal{R}_0^2}, \\ R_\infty &= \tfrac{\gamma N\mu_m(\mathcal{R}_0^2-1)}{\alpha(\mu+\beta)}, \\ J_\infty &= \tfrac{\mu(\mathcal{R}_0^2-1)}{\mu\mathcal{R}_0^2+\beta} g_c^{-1}(\phi), \\ I_\infty &= \tfrac{\mu N\mu_m(\mathcal{R}_0^2-1)}{\alpha(\mu+\beta)}, \end{aligned} \tag{5.5}$$

Clearly, positive (endemic) equilibria are possible whenever $\mathcal{R}_0 > 1$. The role of $\mathcal{R}_0$ is fundamental in both the free and "controlled" host-vector system as the following series of results show. The proofs are in the appendix.

Theorem 5.1.1. *Consider the system* (5.1) *with* $f(L) = Lg_c(L)$ *where* g_c, *is differentiable. Assume* $\{g_c^{-1}(\phi)\}$ *is non-empty, and let* $n = card\{g_c^{-1}(\phi)\}$ *(i.e. the number of positive vector densities) then*

a.) *If* $\mathcal{R}_0 \leq 1$ *then the system has n positive disease-free equilibria (at various vector densities) and no endemic equilibria.*

b.) *If* $\mathcal{R}_0 > 1$ *then the system has n positive disease-free equilibria and n endemic equilibria (at distinct vector densities).*

In other words, control measures may support various stable vector densities (a function of the effort and related parameters). Result 4.1 suggests that as long as there is a critical stable mass of vectors (and a large host population) the disease will survive if $\mathcal{R}_0 > 1$. Specific conditions are set in Result 4.2 and 4.3 below.

Theorem 5.1.2. *Let* $\vec{x}_\infty(DF) = (E_\infty, V_\infty, N, 0, 0, 0)$ *be a disease-free equilibrium of* (5.1) *then* $\vec{x}_\infty(DF)$ *is l.a.s. if* $\mathcal{R}_0 < 1$ *and* $\mathcal{R}_d(g_c^{-1}(\phi)) < 1$. *If either of* $\mathcal{R}_0$ *or* $\mathcal{R}_d(g_c^{-1}(\phi))$ *are greater than* 1 *then the corresponding equilibrium is unstable.*

Theorem 5.1.3. *Let* $\vec{x}_\infty = (E_\infty, V_\infty, S_\infty, R_\infty, J_\infty, I_\infty)$ *be an endemic equilibrium of* (5.1) *then* $V_\infty + J_\infty \in \{g_c^{-1}(\phi)\}$, $\mathcal{R}_0 > 1$ *and* $\vec{x}_\infty$ *is locally asymptotically stable if* $\mathcal{R}_d(g_c^{-1}(\phi)) < 1$ *and unstable if* $\mathcal{R}_d(g_c^{-1}(\phi)) > 1$. *Note that* $\mathcal{R}_d(g_c^{-1}(\phi)) < 1$ *simply states that we have a stable vector population (an attractor).*

The condition in Result 4.4 (below) follows from the observation that since $f(L) = Lg_c(L)$ then

$$f'(g_c^{-1}(\phi)) = \phi + g_c^{-1}(\phi)g_c'(g_c^{-1}(\phi)). \tag{5.6}$$

Dividing by $\frac{1}{\phi}$ gives

$$\mathcal{R}_d(g_c^{-1}(\phi)) = 1 + \frac{1}{\phi}g_c^{-1}(\phi)g_c'(g_c^{-1}(\phi)). \tag{5.7}$$

Hence, $\mathcal{R}_d(g_c^{-1}(\phi)) < 1$ if and only if $g_c'(g_c^{-1}(\phi)) < 0$, that is:

Theorem 5.1.4. *Let* $\vec{x}_\infty = (E_\infty, V_\infty, S_\infty, R_\infty, J_\infty, I_\infty)$ *be a (positive disease free or endemic) equilibrium of* (5.1) *then* $\mathcal{R}_d(g_c^{-1}(\phi)) < 1$ *if and only if* $g_c'(V_\infty + J_\infty) < 0$.

In the absence of control measures the system behaves as expected, that is,

Theorem 5.1.5. *Assume that* $c(L) = 0$, *that is,* $f(L) = Lg_0(L)$ *where* $g_0(L)$ *is strictly decreasing. If* $\mathcal{R}_d(0) > 1$ *and* $\mathcal{R}_0 < 1$ *then the unique positive disease-free equilibrium,* $\vec{x}_\infty$, *given by* (5.4), *is globally asymptotically stable in the domain* $\Omega = \{(E, V, S, R, J, I) | E > 0, V > 0, S + I + R = N\} \subset \mathbb{R}^6_+$.

We note that the same result can be obtained under the weaker hypotheses: $card\{g_c^{-1}(\phi)\} = 1$ and $\mathcal{R}_d(g_c^{-1}(\phi)) < 1$.

Vector control is modeled as adult "harvesting" on the "recruitment" function $f(L)$. In fact, if $f(L)$ is replaced by $L(g(L) - c(L))$ then the choice of $c(L)$ can

impact the qualitative dynamics of the system. The following result outlines some possibilities.

Theorem 5.1.6. *Suppose* $\mathcal{R}_d(0) > 1$*, and that* $f(L) = Lg_c(L)$*. Assume that* $g_c(L) = \phi$ *for an increasing, finite sequence* $\{V_\infty^1, V_\infty^2, \cdots, V_\infty^{2n+1}\}$ *where* $g_c'(V_\infty^{2j+1}) < 0$ *for all* $0 \leq j \leq n$ *and* $g_c'(V_\infty^{2j}) > 0$ *for all* $1 \leq j \leq n$*. If* $\mathcal{R}_0 < 1$*, then there are* $n+1$ *locally asymptotically stable positive disease free equilibria for the system* (5.1)*. These equilibria are given by* $\vec{x}_\infty^{2j+1} = (\frac{\mu_m}{\delta} V_\infty^{2j+1}, V_\infty^{2j+1}, N, 0, 0, 0)$*,* $0 \leq j \leq n$ *and the basins of attraction for these equilibria are given by* $\Omega_{2j+1} = \{(E, V, S, R, J, I) | E > 0, V > 0, S + I + R = N, V_\infty^{2j} < V + J < V_\infty^{2j+2}\}$*, for each* $0 \leq j \leq n$*, where, for convenience* V_∞^0 *is defined to be* 0 *and* $V_\infty^{2n+2} = \infty$*.*

Similar results have been obtained before. In [60], Wu and Feng constructed models for Schistosomasis that support alternating stable and unstable equilibria and computed their corresponding basins of attraction.

In order to provide an explicit illustration to the above results, we take $g(L) = \rho e^{-\omega L}$ and $c(L) = \frac{\epsilon L}{a^2 + L^2}$, that is,

$$f(L) = \rho L e^{-\omega L} - \frac{\epsilon L^2}{a^2 + L^2}$$

where ϵ is interpreted as the maximal "harvesting" rate (value of $Lc(L)$ as $L \to \infty$) a^2 is a parameter associated with the time needed to handle of or search for adult vectors, and ρ is the maximal per-capita vector egg-reproduction rate. Equilibria are solutions of

$$\rho e^{-\omega L} - \frac{\epsilon L}{a^2 + L^2} = \phi,$$

that is, this explicit "ϕ" corresponds to the generic ϕ in (5.5). There are at most three positive equilibria. Figure 5.2 illustrates the case when there are three (two stable and one unstable).

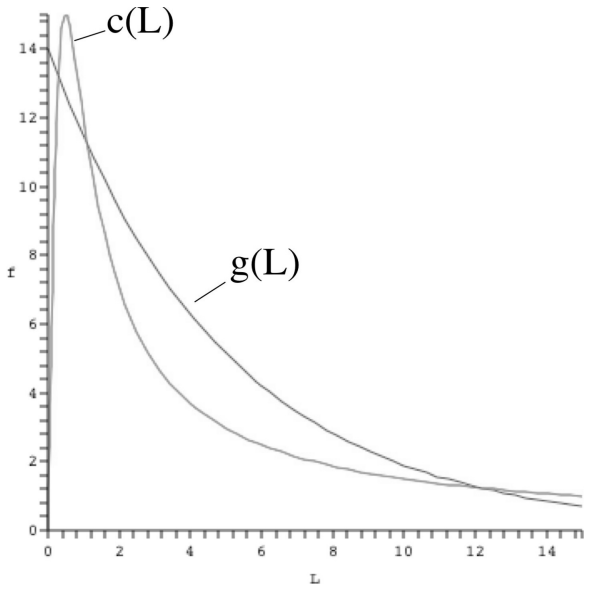

Figure 5.2: The equilibria alternate stability, the first and third being stable and the second one being the unstable equilibrium. Graphs of $g(L), c(L)$; $\rho = 15$, $\epsilon = 15$, $a = 0.5$ and $\omega = 0.2$.

5.2 Effects of seasonal variations

The incorporation of seasonality effects on the transmission dynamics of dengue is important [9], [14]. Seasonality may directly impact host to vector transmission rates (β); the per capita fertility rate (ρ) and possibly the maximal "control" rate (ϵ) (possibly higher when vector densities are higher). Here, we briefly illustrate its potential role on each of these parameters via simulations. Three sets of independent simulations are conducted. The artificial introduction of seasonality effects in $f(L) = \rho L e^{-\omega L} - \frac{\epsilon L^2}{a^2+L^2}$ is as follows: ϵ is replaced by $\bar{\epsilon} = \epsilon_0(\epsilon_1 + \sin(\frac{2\Pi t}{180}))$, β by $\bar{\beta} = \beta_0(\beta_1 + \sin(\frac{2\Pi t}{180}))$ and α is replaced by $\bar{\alpha} = \alpha_0(\alpha_1 + \sin(\frac{2\Pi t}{180}))$. These selections are not driven by particular explicit scenarios or systematically explored. Our objective here is to illustrate the potential role of fluctuations on key parameters.

Seasonal variations in ϵ may derive from the observation that (vectors') "harvesting" efforts may not be equal over the entire year. They may be higher during the rainy (or dry) season. Here, ϵ is varied independently while all the other parameters remain fixed. Simulations that include simultaneous fluctuations on both transmission rates, α and β are also considered.

Figures 5.3c, 5.3d illustrate effects of seasonality on infected host class levels due to regular fluctuations on the intensity of control efforts (ϵ). The vector population exhibits oscillatory behavior with a period of six months (same as that of ϵ). Figures 5.3c and 5.3d illustrate the impact of periodic harvesting effects. The dynamics become regular (oscillatory) after the transients are "gone" (1000 days). Seasonally-dependent harvesting via the control parameter ϵ forces the vector population to jump from the low demographic equilibrium ($V_\infty^{low} = 0.4099141$) to the high ($V_\infty^{high} = 10.99821$) where it remains afterwards. In the absence of seasonality vector levels remain at the lower equilibria. Although vector levels (infected and uninfected) shift the corresponding host-infection levels remain unchanged. That is, the host endemic levels found in Figures 5.3c and 5.3d correspond to both vector levels as illustrated in Figures 5.4c and 5.4d. Moderate, independent or simultaneous changes in transmission rates (α and β) do not drive shifts in vector population levels (from either the low demographic equilibria ($E_0^{low} = 0.230129$, $V_0^{low} = 0.4099141$ and $J_0^{low} = 0.004318148$) to the high ($E_0^{high} = 5.527807$, $V_0^{high} = 10.99821$, $J_0^{high} = 0.3055878$), or vice-versa. In Figure 5.4 there are two sets of simulations a) and b) illustrate that fluctuations on the transmission rates (α and β) do not cause the vector equilibria to "jump" from the low demographic equilibria to the high demographic equilibria. In c) and d) the control parameter (ϵ) is varied and results in the vector density to

move from the low demographic equilibria ($E_0^{low} = 0.230129$, $V_0^{low} = 0.4099141$ and $J_0^{low} = 0.004318148$) to the high demographic equilibria ($E_0^{high} = 5.527807$, $V_0^{high} = 10.99821$, $J_0^{high} = 0.3055878$) for the given set of parameters.

Vector density is started at the low demographic equilibria for all simulations with seasonality to illustrate the effect of the parameters on the vector density.

It is important to re-state that vector density levels may shift from low to high levels and viceversa from the impact of strong fluctuations in control efforts (ϵ), however, simulations suggest that either level of vector density (high or low) leads to approximately the same level of dengue prevalence in human infections (see Figure 5.3).

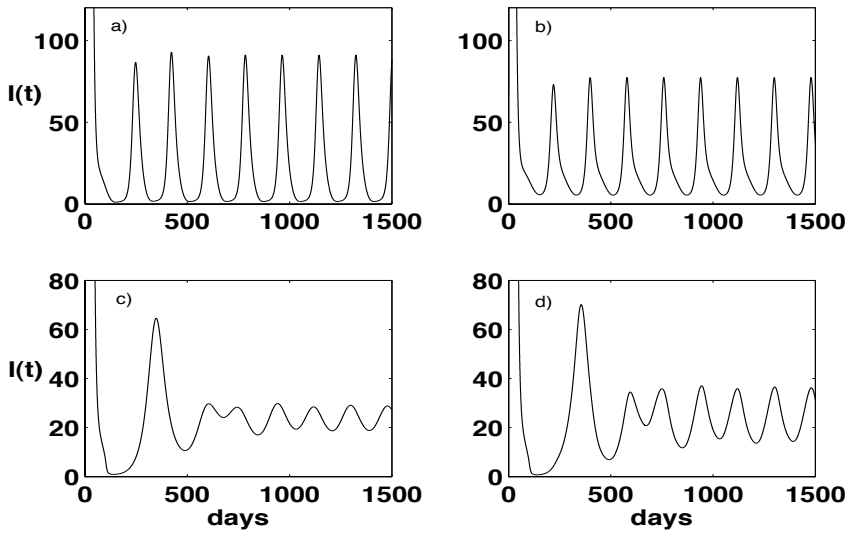

Figure 5.3: Moderate seasonal effects on host and vector transmission rates (α, β and ϵ). The parameter values are: $\mu = 0.00004$, $\mu_e = 0.003$, $\mu_m = 0.03$, $\delta = 0.09$, $\gamma = 0.14$, $\rho = 15$, $\omega = 0.2$, $\epsilon = 15$, $\alpha = 0.5$, $\beta = 0.5$, $a = 0.5$ Initial conditions: $S_0 = 9999$, $I_0 = 1$, $R_0 = 0$ (host population). In this case we show the infected host class ($I(t)$) when seasonal effects take place in the transmission rates (α and β) and control measures (ϵ). For a) and b) α and β are varied simultaneously; a) $\bar{\alpha} = 0.5 + 0.4\sin(\frac{2\Pi t}{180})$ and $\bar{\beta} = 0.5 + 0.4\sin(\frac{2\Pi t}{180})$, b) $\bar{\alpha} = 0.8 + 0.4\sin(\frac{2\Pi t}{180})$ and $\bar{\beta} = 0.8 + 0.4\sin(\frac{2\Pi t}{180})$. For c) and d) ϵ is varied; c) $\bar{\epsilon} = 15 + 5\sin(\frac{2\Pi t}{180})$ and *d)* $\bar{\epsilon} = 15 + 10\sin(\frac{2\Pi t}{180})$.

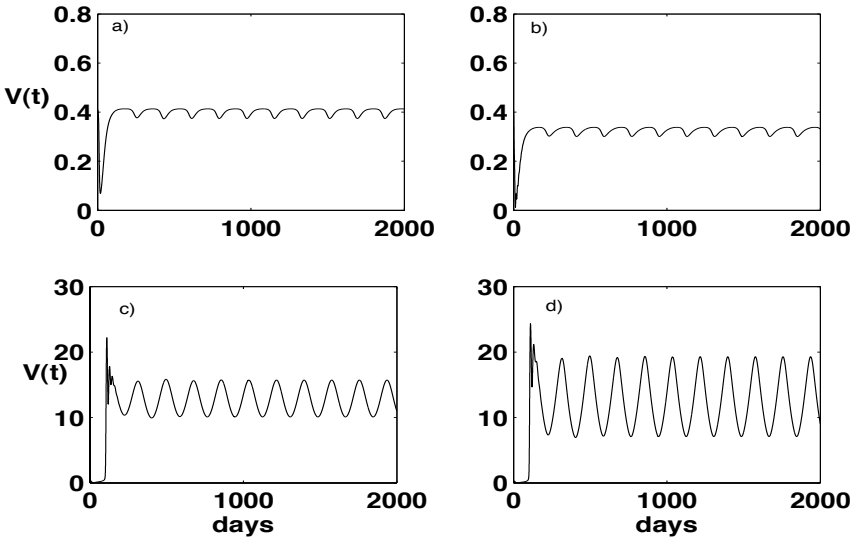

Figure 5.4: Moderate seasonal effects on host and vector transmission rates (α, β and ϵ). The parameter values are: $\mu = 0.00004$, $\mu_e = 0.003$, $\mu_m = 0.03$, $\delta = 0.09$, $\gamma = 0.14$, $\rho = 15$, $\omega = 0.2$, $\epsilon = 15$, $\alpha = 0.5$, $\beta = 0.5$, $a = 0.5$ Initial conditions: $S_0 = 9999$, $I_0 = 1$, $R_0 = 0$ (host population). In this case we show the vector population ($V(t)$) when seasonal effects take place in the transmission rates (α and β) and control measures (ϵ). For a) and b) α and β are varied simultaneously; a) $\bar{\alpha} = 0.5 + 0.4\sin(\frac{2\Pi t}{180})$ and $\bar{\beta} = 0.5 + 0.4\sin(\frac{2\Pi t}{180})$, b) $\bar{\alpha} = 0.8 + 0.4\sin(\frac{2\Pi t}{180})$ and $\bar{\beta} = 0.8 + 0.4\sin(\frac{2\Pi t}{180})$. For c) and d) ϵ is varied; c) $\bar{\epsilon} = 15 + 5\sin(\frac{2\Pi t}{180})$ and d) $\bar{\epsilon} = 15 + 10\sin(\frac{2\Pi t}{180})$. The vector begins at the low demographic equilibrium $E_0^{low} = 0.230129$, $V_0^{low} = 0.4099141$ and $J_0^{low} = 0.004318148$ and then jumps to the high equilibrium $E_0^{high} = 5.527807$, $V_0^{high} = 10.99821$, $J_0^{high} = 0.3055878$. In the absence of seasonality $\epsilon = 15$ there is no jump.

5.3 Conclusions

A model for the transmission dynamics of dengue that includes the egg/larva stage of the vector and control efforts directed towards the adult vector population is considered. The model couples, in a simple way, a modified version of the classical SIR model for the host with a vector model that includes vector life stages (from egg to adult). Sharp conditions for local stability of disease-free and endemic equilibria are computed in the absence and presence of control measures. It is shown that, under the right conditions, the disease-free equilibrium is globally stable provided that $\mathcal{R}_0 < 1$ and $\mathcal{R}_d(0) > 1$ (that is, when a critical mass of vectors exists). Selective control measures geared towards the "elimination" of the adult population ($\mathcal{R}_0 > 1$) can give rise to a landscape that supports multiple stable vector levels. In fact, under some control scenarios, it is possible to establish the local stability of endemic states having $\mathcal{R}_0 > 1$ and $\mathcal{R}_d(g_c^{-1}(\phi)) < 1$.

The possibility of "eliminating" a vector population over sustained periods of time, using drastic policies directed to the adult vectors, seems virtually impossible since reducing vector densities (even significantly) may not seriously impact host-dengue prevalence levels in humans (see example). Control methods that include "attacks" on additional vector-life stages must be implemented. Such efforts should include for example, dramatic reductions on the numbers and sizes of breeding sites.

Currently, in the tradition of Ross, most theoretical work has focused on the use of control efforts aimed at adult vector populations. This is unfortunate. In fact, Ross was clearly aware of the importance of incorporating our knowledge of the ecology and life history of vectors in the development of disease control policies. Ross did not pursue detailed mathematical studies of vector control strategies

because he lacked access to modern computational tools. Frameworks that include vector's life-history dynamics are needed to test control measures that focus on "vulnerabilities" in non-adult vector populations. The introduction of seasonal variation in control measures in a rather artificial setting has helped (we hope) illustrate the view that low vector densities lead to proportionally the same disease host prevalence levels than large vector densities. Methods that focus *only* on controlling adult mosquito populations are simply inadequate. Those that focus (simultaneously) on vector's life-history stages (integrated management approaches) need to be developed, tested and implemented. Finally, eradication of *Aedes aegypti* appears to be the only way to eliminate dengue.

Chapter 6

Two-strain dengue model with collective host behavior change

The mechanisms behind the joint evolutionary dynamics of dengue strains are not well understood despite its high prevalence around the world. Two dengue strains are put in competition in a population where collective host behavior changes can affect the likelihood of repeated infections. Furthermore, we look at collective behavior change after recovery from first infection. This work is based on a previous models by [35, 33, 55, 52].

6.1 The model

Let N and M denote the host and mosquito (assumed constant) populations, respectively. That is, it is assumed that the host/vector ratio remains constant. This common assumption perhaps not accurate in regions where temperature and precipitation activity are highly variable. For mathematical simplicity there is no disease induced mortality. Mortality associated with dengue is low [10]. Hence the per-capita host death and births rates are assumed to be equal to μ. Vectors are also assumed to have the same constant birth and death rates denoted by μ_m. It is assumed that behavioral changes reduce the effective population size, which may alter significantly the likelihood of infection. We let the subscripts i, $k = 1, 2$ where $i \neq k$ denote two distinct strains. The host population is stratified as follows: S, represents susceptible hosts; D_i, represents hosts initially infected with strain i; Z_i, represents hosts experiencing their second dengue infection (strain i); B_i,

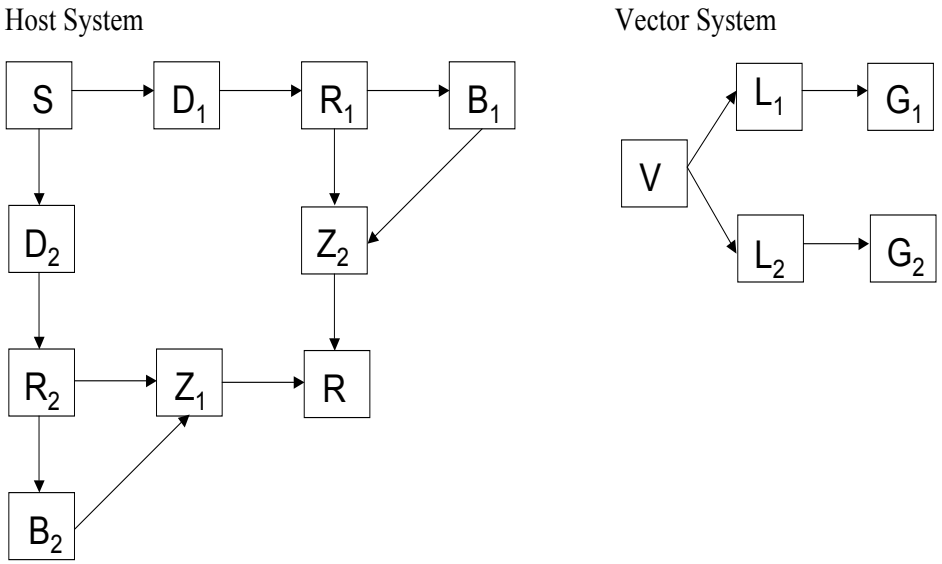

Figure 6.1: Caricature of the model.

represents the class of hosts who change their behavior after infection with strain i; R_i, represents hosts who recover from strain i; R, represents hosts that recover from both strains.

In addition, β_i, represents the transmission rate of strain i from mosquito to host; γ_i represents the recovery rate of hosts infected with strain i; p, represents the rate at which individuals change their behavior.

The vector population is divided as follows: susceptible (adults) mosquitoes, V; mosquitoes infected with strain i but not infectious (latent), L_i; and, mosquitoes infectious with strain i, G_i. Furthermore, α_i, represents the transmission rate of strain i from host to mosquito; ϕ_i represents the rate at which mosquitoes become infectious; and ψ is a measure of the effectiveness of behavioral changes in humans. The transmission dynamics of dengue is modeled by a re-scaled, via the re-introduction of the following dimensionless variables

$s = \frac{S}{N}$, $d_i = \frac{D_i}{N}$, $b_i = \frac{B_i}{N}$, $z_i = \frac{Z_i}{N}$, $r_i = \frac{R_i}{N}$, $r = \frac{R}{N}$, $v = \frac{V}{M}$, $l_i = \frac{L_i}{M}$ and $g_i = \frac{G_i}{M}$,

set of nonlinear differential equations:

$$\begin{aligned} l_i' &= \alpha_i \tfrac{d_i+z_i}{1-\psi(b_i+b_k)}\Big(1-\textstyle\sum_{i=1}^{2} l_i - \sum_{i=1}^{2} g_i\Big) - (\mu_m+\phi_i)l_i, \\ g_i' &= \phi_i l_i - \mu_m g_i, \end{aligned} \tag{6.1}$$

where $v + \sum_{i=1}^{2}(l_i + g_i) = 1$.

$$\begin{aligned} s\prime &= \mu - \beta_i s g_i - \beta_k s g_k - \mu s, \\ d_i' &= \beta_i s g_i - (\mu+\gamma_i)d_i, \\ b_i' &= p r_i - \beta_k b_i g_k - \mu b_i, \\ z_i' &= \beta_i r_k g_i + \beta_i b_k g_i - (\mu+\gamma_i)z_i, \\ r_i' &= \gamma_i d_i - \beta_k r_i g_k - (\mu+p)r_i, \\ r' &= \gamma_i z_i + \gamma_k z_k - \mu r. \end{aligned} \tag{6.2}$$

where $s + \sum_{i=1}^{2}(d_i + b_i + z_i + r_i) + r = 1$. Naturally, the first question focuses on establishing the conditions for disease invasion. The average number of secondary infections caused by a "typical" infectious individual (host or vector) in a mostly susceptible population, that is, when the disease is rare, is denoted by $\mathcal{R}_0$. The, *basic reproductive number*, $\mathcal{R}_0$ of the above system is*:

$$\mathcal{R}_0 = max\{\mathcal{R}_1, \mathcal{R}_2\}, \tag{6.3}$$

where

$$\mathcal{R}_i = \sqrt{\frac{\alpha_i \phi_i}{\mu_m(\mu_m+\phi_i)} \frac{\beta_i}{(\mu+\gamma_i)}}$$

is the i^{th} strain *basic reproductive number*. Here $1/\mu_m$ denotes the average lifespan of the vector; $\phi_i(\mu_m+\phi_i)$ is the proportion of mosquitoes that progress from the latent to the infectious stage; $1/(\mu+\gamma_i)$ is the average infectious period of the host (human); and α_i, β_i are the transmission rates of vectors and hosts, respectively.

*See Appendix for detailed calculation.

Hence, each $\mathcal{R}_i$ is given by the geometric mean of host and vector contributions to secondary infections. In other words, it takes two steps for a vector (host) to generate a secondary vector (host) infection. $\mathcal{R}_0 < 1$ implies the extinction of both strains while $\mathcal{R}_0 > 1$ implies that at least one strain will survive (see Appendix).

6.2 Disease invasion and persistence

The system has a disease-free equilibrium, ξ_0^*; two boundary equilibria, ξ_1^* and ξ_2^*, where only one of the strains is present and an endemic state. They are:

$$\begin{aligned} \xi_0^* &= (1,0,0,0,0,0,0,0,0,0,0,0,0,0), \\ \xi_1^* &= (s^*,d_1^*,0,0,0,r_1^*,0,b_1^*,0,l_1^*,0,g_1^*,0), \\ \xi_2^* &= (s^*,0,d_2^*,0,0,0,r_2^*,0,b_2^*,0,l_2^*,0,g_2^*), \end{aligned} \tag{6.4}$$

where

$$\begin{aligned} l_i^* &= \tfrac{\mu\mu_m(\mathcal{R}_i-1)}{\beta_i\phi_i(1-\delta_i+\nu_i)}, \\ g_i^* &= \tfrac{\mu(\mathcal{R}_i-1)}{\beta_i(1-\delta_i+\nu_i)}, \\ s^* &= \tfrac{\nu_i+1-\delta_i}{\nu_i+\mathcal{R}_i-\delta_i}, \\ d_i^* &= \tfrac{\mu(\mathcal{R}_i-1)}{(\mu+\gamma_i)(\mathcal{R}_i-\delta_i+\nu_i)}, \\ b_i^* &= \tfrac{p\gamma_i(\mathcal{R}_i-1)}{(\mu+p)(\mu+\gamma_i)(\mathcal{R}_i-\delta_i+\nu_i)}, \\ r_i^* &= \tfrac{\mu\gamma_i(\mathcal{R}_i-1)}{(\mu+\gamma_i)(\mu+p)(\mathcal{R}_i-\delta_i+\nu_i)}, \end{aligned} \tag{6.5}$$

$$\delta_i = \frac{p\psi\gamma_i}{(\mu+p)(\mu+\gamma_i)},$$

and

$$\nu_i = \frac{\alpha_i}{\mu_m}\frac{\mu}{\mu+\gamma_i}.$$

δ_i represents the risk of becoming infected with a second strain after behavioral changes and ν_i represents the efficacy of human transmission of dengue to mosquitoes. The factors in δ_i are: ψ, the effectiveness of behavior change;

$\gamma_i/(\mu+\gamma_i)$, the proportion of individuals who survive from the infection to the recovered class; and $p/(\mu+p)$, the proportion of individuals who change behavior and survive. The factors in ν_i are: $\mu/(\mu+\gamma_i)$, the proportion of humans who die in the infected class; α_i, the transmission rate of infection from humans to mosquitoes; and $1/\mu_m$, the average life span of mosquitoes. The stability properties of these equilibria are stated in the following proposition:

Theorem 6.2.1. *Let* $\vec{\xi}_0^* = (1,0,0,0,0,0,0,0,0,0,0,0,0,0)$ *be the positive disease-free equilibrium of* (6.1)-(6.2) *then it is locally asymptotically stable if and only if* $\mathcal{R}_0 < 1$.

Proposition 6.2.2. *A necessary condition for the local asymptotic stability of the endemic equilibria is that (for* $i,k = 1,2$, $i \neq k$*)*

$$\mathcal{R}_i^2 < \left[\frac{1-(\mathcal{R}_k^2-1)\frac{\delta_k}{(\nu_k+\mathcal{R}_k^2-\delta_k)}}{1-(\mathcal{R}_k^2-1)\mu\frac{\mu_m+\phi_k}{\beta_k\phi_k(\nu_k+1-\delta_k)}}\right]\left[\frac{(\nu_k+\mathcal{R}_k^2-\delta_k)}{\frac{\gamma_k(\mathcal{R}_k^2-1)}{(\mu+\gamma_k)}+(\nu_k+1-\delta_k)}\right] \tag{6.6}$$

See Appendix for a proof of Proposition 6.6.

Theorem 6.2.3. *Assume* $\beta_i = \rho_k$, *for* $i \neq k$, *where* $\psi = 0$ *and* $\mathcal{R}_0 < 1$, *then the positive disease-free equilibrium given by 6.4 is globally asymptotically stable on the domain* $\Omega = \{(s,d_i,b_i,z_i,r_i,r,v,l_i,g_i) | x + \sum_{i=1}^{2}(d_i+b_i+z_i+r_i)+r = 1, v+\sum_{i=1}^{2} l_i + \sum_{i=1}^{2} g_i = 1\} \subset \mathbb{R}_+^{15}$ *for* $i = 1,2$.

See Appendix for a proof of Theorem 6.2.3.

Four distinct regions of stability are described in Figure 6.2. "DF" represents the disease-free equilibrium which is globally asymptotically stable when $\mathcal{R}_0 < 1$. Region I represents the region where local stability of the boundary equilibrium associated with strain 1 ($\mathcal{R}_1 > 1$) is locally asymptotically stable; and region

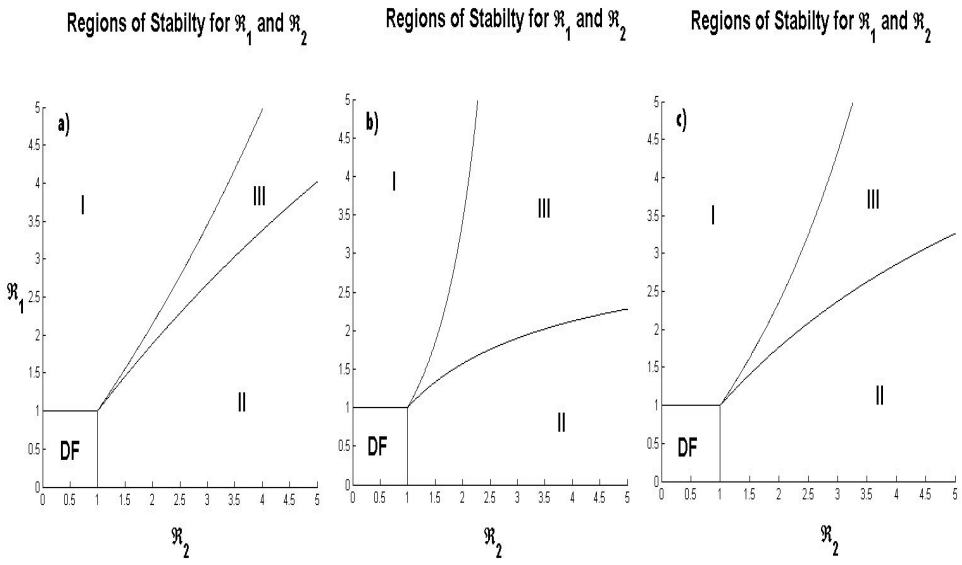

Figure 6.2: Regions of stability when a) $\alpha_1 = \beta_1 = 0.2$, $\alpha_2 = \beta_2 = 0.2$, $\gamma_1 = 0.33$, $\psi = 0.5$, $p = 0.1$. In b) we let $\beta_1 = \beta_2 = 0.5$, $\psi = 0.9$ and $p = 0.9$ while in c) we let $\alpha_2 = \beta_2 = 0.5$, $\psi = 0.5$ and $p = 1$.

II represents the analogous case for the secondary boundary equilibria ($\mathcal{R}_2 > 1$). Region III represents the region of strain coexistence. Parameter values can greatly affect the size of region III, but not the overall qualitative behavior.

6.3 Numerical simulations

For the numerical simulations we v the parameters α_i, β_i, ρ_k, p, and ψ were varied while maintaining μ, μ_m, ϕ_i, and γ_i constant. Parameter values and initial conditions are chosen to be biologically accurate as to display the behavior of our model. The parameters μ, and μ_m were determined from dengue outbreak studies [32, 33].

In Figure 6.3 we look at the secondary infection for different values of ρ_1. ρ_i

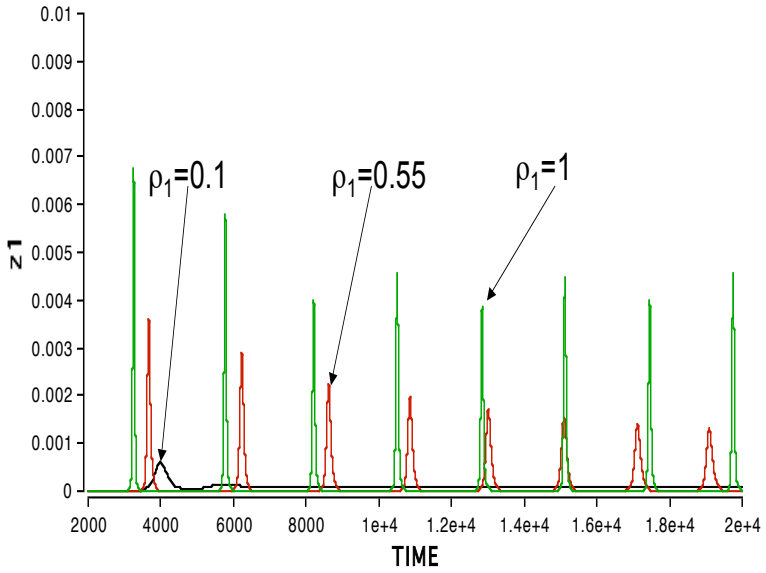

Figure 6.3: Individuals infected with secondary strain (z_1) for three values of the infection rate (ρ_1) from the behavior change class (b_2).

represents the reduced transmission rate from the behavior change class. When $\rho_1 = 0.1$ the system takes longer to take off and then stabilizes at a very low level. This implies that effective preventive measure by the population can have a significant impact on the transmission dynamics of dengue. It is also important to note that most of these measures are inexpensive and can easily be implemented, however, cultural differences and poverty can play a role in the implementation of these measures. When $\rho_1 = 0.55$ the number of secondary infections grows faster and does not reach an endemic equilibrium but oscillates at low levels. When $\rho_1 = 1$ the number of secondary infections grows faster and at higher levels and does not stabilize. Over the long term dynamics the system oscillates a low levels (see Figure 6.4). In Figures 6.5, 6.6, 6.9, 6.10 we show the time series of the system. For these scenarios we let strain two be the more virulent strain. From Figure 6.5 we can see that strain two, the more virulent strain, takes off faster

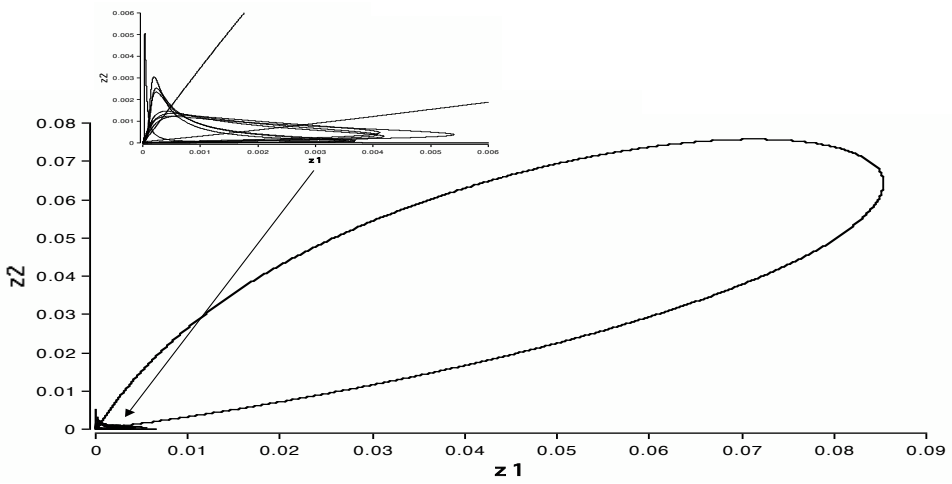

Figure 6.4: Phase plane of secondary infection (z_1 and z_2).

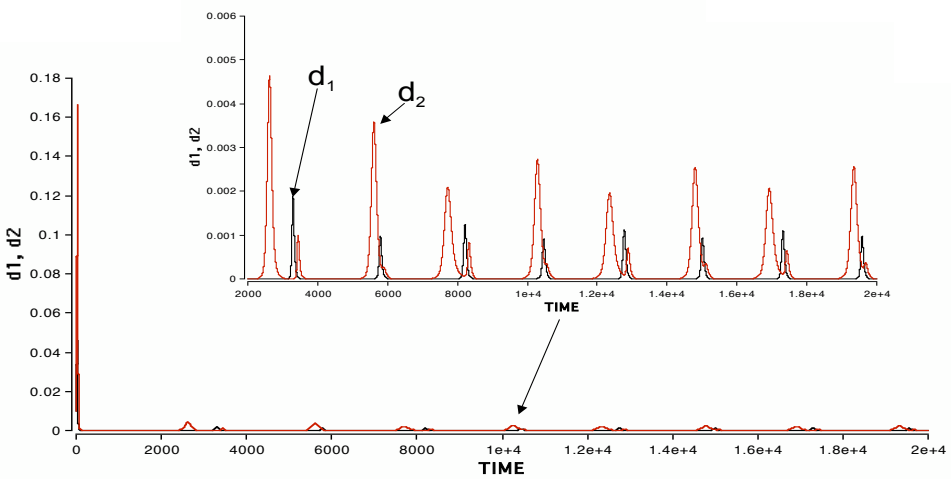

Figure 6.5: Time series of first infection (d_1 and d_2). *Parameter values:* $\beta_1 = 0.33$, $\beta_2 = 0.5$, $\gamma_1 = 0.25$, γ_2, $\phi_1 = \phi_2 = 0.1$, $\alpha_1 = 0.5$, $\alpha_2 = 0.33$, $\rho_1 = 1$, $\rho_2 = 4$, $p = 0.1$ and $\psi = 0.5$. *Initial conditions:* $s_0 = 0.98$, $d_1 = 0.01$, $d_2 = 0.01$, $v_0 = 0.98$, $g_1 = 0.01$, and $g_2 = 0.01$.

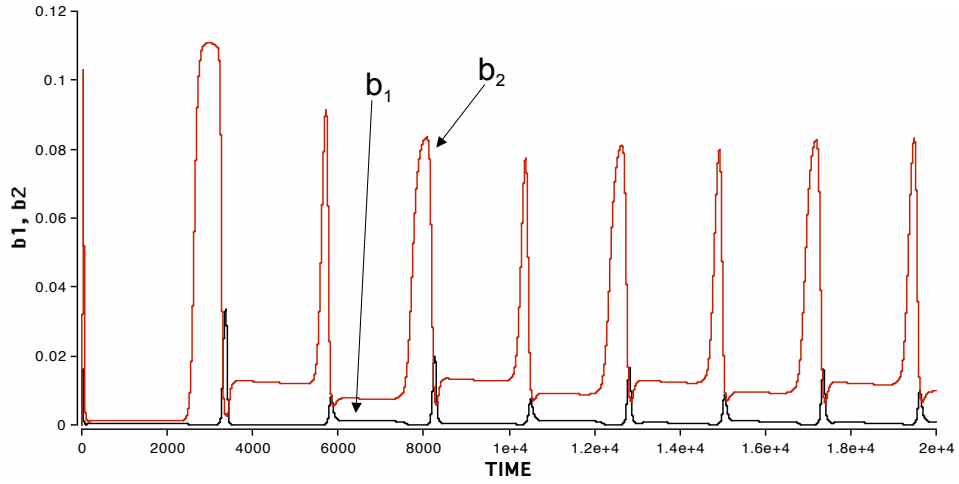

Figure 6.6: Time series of behavior change population (b_1 and b_2). *Parameter values:* $\beta_1 = 0.33$, $\beta_2 = 0.5$, $\gamma_1 = 0.25$, γ_2, $\phi_1 = \phi_2 = 0.1$, $\alpha_1 = 0.5$, $\alpha_2 = 0.33$, $\rho_1 = 1$, $\rho_2 = 4$, $p = 0.1$, and $\psi = 0.5$. *Initial conditions:* $s_0 = 0.98$, $d_1 = 0.01$, $d_2 = 0.01$, $v_0 = 0.98$, $g_1 = 0.01$, and $g_2 = 0.01$.

and has a larger effect on infected host population. In this case we have sustained oscillations (see Figure 6.7). In Figure 6.6 it is not surprising that b_2 is larger than b_1. This indicates that the more virulent strain has a more significant effect on the population that has been previously infected with strain two. See Figure 6.8 for limit cycle of the behavior change class. There is a correlation between the virulence of the strain and the way the population reacts to the disease. When larger outbreaks occur the population (collectively) tend to pay more attention to the risks involved. However, if the outbreak is "insignificant", i.e., not many confirmed cases due to asymptomatic cases, the population tend to ignore the risks and take less caution. In the mosquito population the system also shows sustained oscillations (see Figure 6.11). Although strain two is the more virulent strain, strain one has the larger impact on the infected mosquito population.

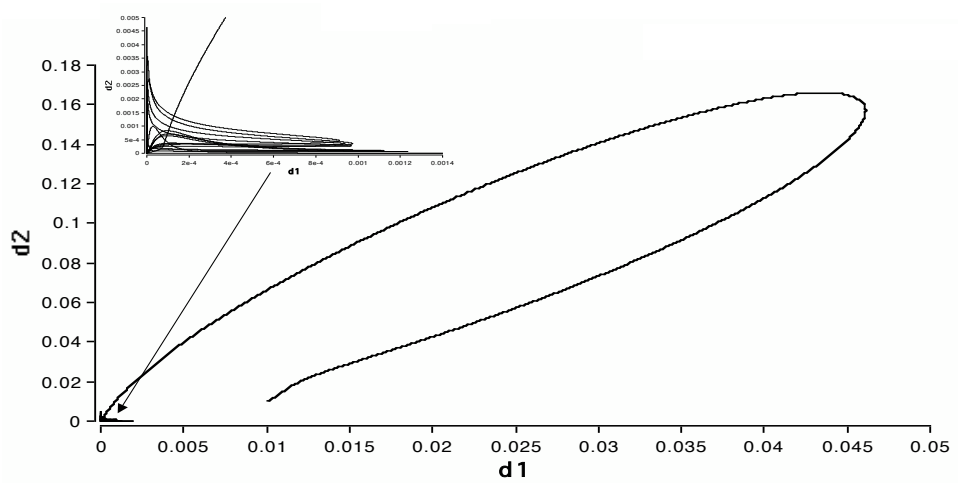

Figure 6.7: Phase plane of first infection (d_1 and d_2).

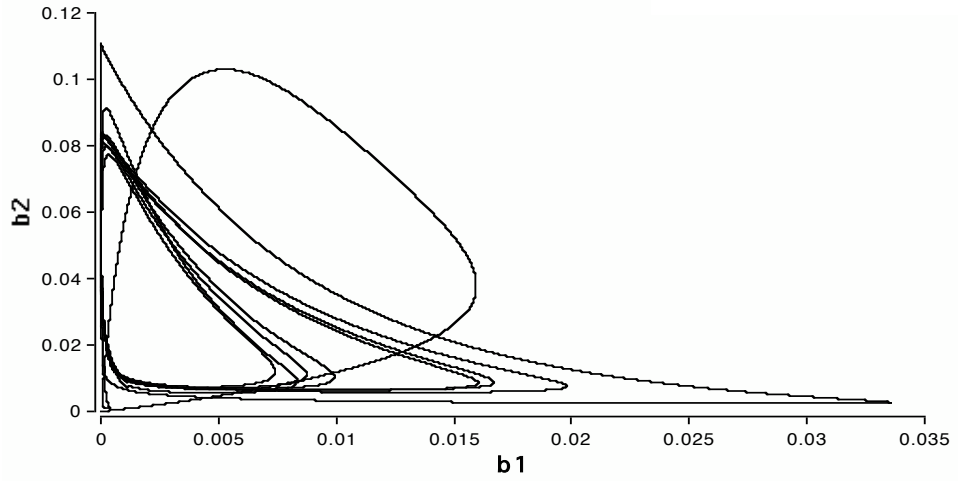

Figure 6.8: Phase plane of behavior change population (b_1 and b_2).

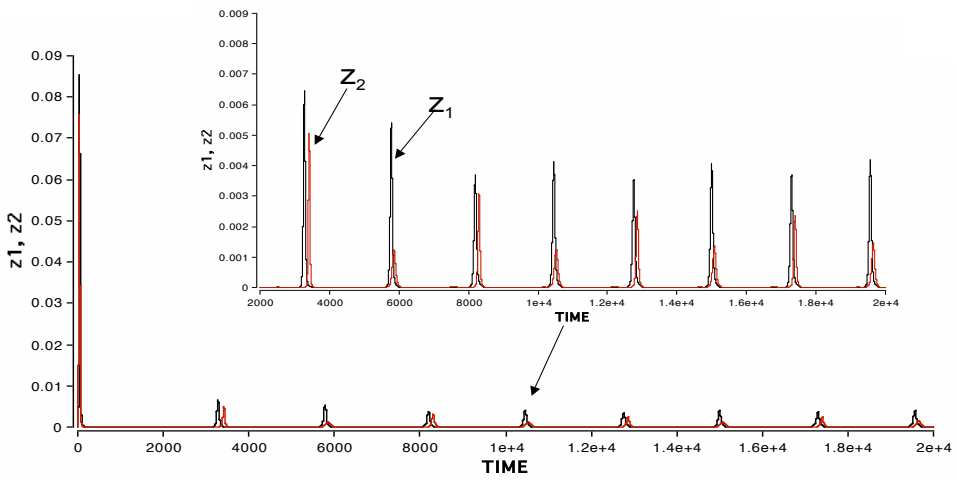

Figure 6.9: Time series of secondary infection (z_1 and z_2). *Parameter values:* $\beta_1 = 0.33$, $\beta_2 = 0.5$, $\gamma_1 = 0.25$, γ_2, $\phi_1 = \phi_2 = 0.1$, $\alpha_1 = 0.5$, $\alpha_2 = 0.33$, $\rho_1 = 1$, $\rho_2 = 4$, $p = 0.1$ and $\psi = 0.5$. *Initial conditions:* $s_0 = 0.98$, $d_1 = 0.01$, $d_2 = 0.01$, $v_0 = 0.98$, $g_1 = 0.01$, and $g_2 = 0.01$.

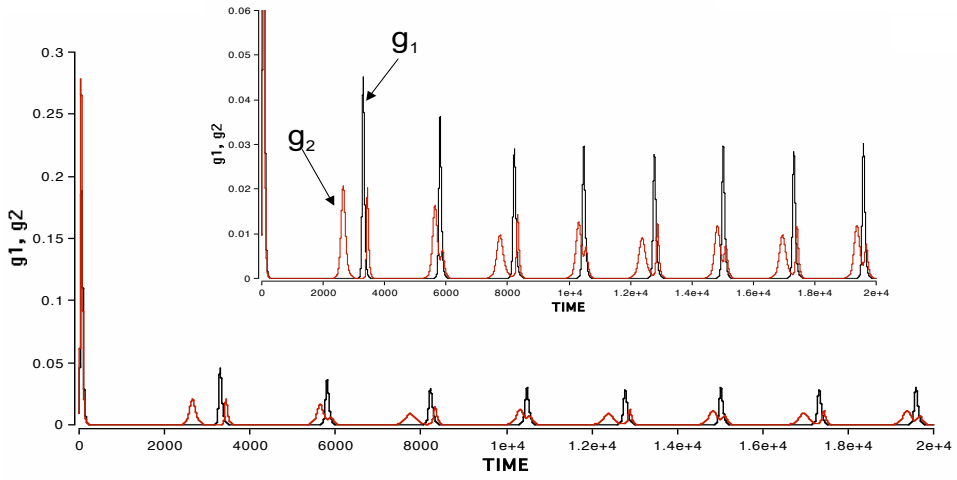

Figure 6.10: Time series of infected mosquito population (g_1 and g_2). *Parameter values:* $\beta_1 = 0.33$, $\beta_2 = 0.5$, $\gamma_1 = 0.25$, γ_2=0.14, $\phi_1 = \phi_2 = 0.1$, $\alpha_1 = 0.5$, $\alpha_2 = 0.33$, $\rho_1 = 1$, $\rho_2 = 4$, $p = 0.1$ and $\psi = 0.5$. *Initial conditions:* $s_0 = 0.98$, $d_1 = 0.01$, $d_2 = 0.01$, $v_0 = 0.98$, $g_1 = 0.01$, and $g_2 = 0.01$.

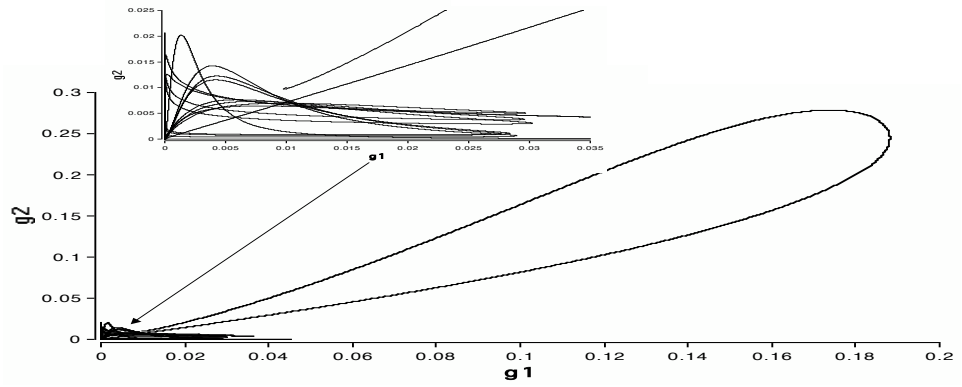

Figure 6.11: Phase plane of infected mosquito population (g_1 and g_2).

This is mostly related to the short infectious period of strain one ($\gamma_1 = 1/4$). The more virulent strain (strain two) has an infectious period of $\gamma_2 = 1/7$. The longer infectious period relates the virulence of the strain. Typically, if individuals get a highly virulent strain the effects of the disease are more prevalent and last longer.

Simulations with Seasonality. The introduction of seasonality requires four control parameters: η_0 which controls the growth of the mosquito population, η_1 which controls the strength of the seasonality, ω which controls the frequency of oscillation and ϕ which controls the phase of oscillations. The control parameters play a large role in determining the dynamics of the system. η_0 dictates whether the population will eventually die out, go unbounded, or reach a steady mean value. Oscillations in both mosquito and host classes can be induced by η_1 and ω can determine the nature of the oscillations while ϕ is the phase shift. The most important feature, however, is that the seasonality term is an explicit function of time. That is, the system of equations is now non-autonomous. This adds a great deal of complexity to the analysis and numerical solutions were sought in order to address this issue. Figure 6.12 is a summary of our results. We see that adding

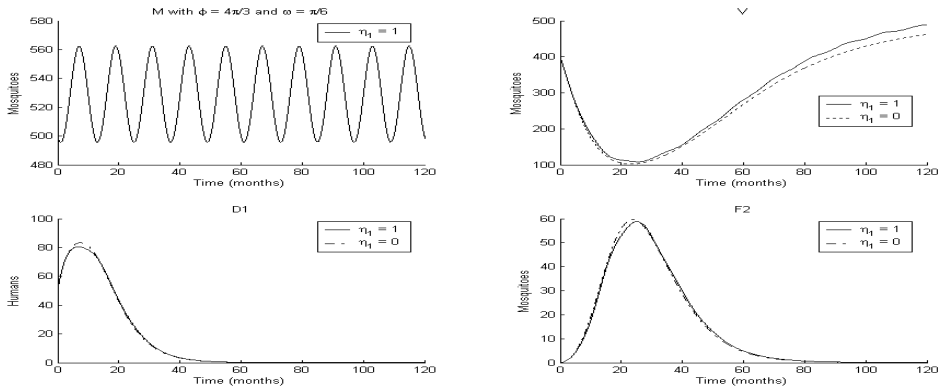

Figure 6.12: y_1 when $\mathcal{R}_1 > 1$ and y_2 when $\mathcal{R}_2 < 1$.

the seasonality term has a tremendous impact on the total mosquito population. It was previously assumed that the mosquito population was constant and that allowed for the re-scaling of the system of equations, transforming them into a very tractable form. Figure 6.12 (a) clearly shows that the total mosquito population is not constant and in fact is periodic in time. In Figure 6.12 (b) we see that while these periodic oscillations are also evident in the number of susceptible mosquitoes, the dynamics of that class are dominated by the initial growth and decay terms. The oscillations are of very low amplitude and do not effect the overall dynamics significantly. Looking at Figure 6.12 (c) and (d), there is little change between the two systems.

6.4 Conclusions

A model for the transmission dynamics of two strains of dengue, a mosquito-transmitted disease, were formulated and analyzed with the incorporation of a behavioral change class. In a region where two serotypes of dengue are present, the incorporation of a behavioral change class may be essential to more accurately

model host and mosquito populations in efforts to implement ideas for control methods. After a primary infection and the severe medical complications that may accompany the infection, a once primary infected individual may change his/her behavior to prevent a possible secondary infection. The model shows that the rate of secondary infections is influenced greatly through the incorporation of a behavioral change class.

The local and global stability of the disease-free equilibria and the co-existence of strains was established (numerically). Our results support the necessity of a behavioral change class to model the transmission dynamics of dengue. A behavioral change constitutes any control methods implemented by a once primarily infected, susceptible population. Any proportion of that population implementing control methods results in a dramatic decrease of the infectious and infected mosquito population rates. Control methods instituted by those individuals (collective behavior) may be an effective method to control dengue outbreaks. Heighten control methods implemented continuously may also be an effective method to lessen the rate of dengue outbreaks.

Social behavior plays a major role in the evolution of infectious diseases. There are tremendous challenges in modeling social dynamics. Innovative methods of modeling that incorporate social dynamics are needed in order to have a bigger impact on emerging infectious diseases.

Appendices

Appendix A

Jacobians and Characteristic Equations for the single strain model

Using the fact that N is constant, it is a straightforward computation to obtain the Jacobian of the system (5.1). It is given by

$$J(\vec{x}) = \begin{bmatrix} -(\mu_e+\delta) & f'(L) & 0 & 0 & f'(L) & 0 \\ \delta & -(\mu_m+\frac{\alpha I}{N}) & 0 & 0 & 0 & -\frac{\alpha V}{N} \\ 0 & \frac{\beta SJ}{L^2} & -\frac{\beta J}{L}-\mu & 0 & -\frac{\beta SV}{L^2} & 0 \\ 0 & 0 & 0 & -\mu & 0 & \gamma \\ 0 & \frac{\alpha I}{N} & 0 & 0 & -\mu_m & \frac{\alpha V}{N} \\ 0 & -\frac{\beta SJ}{L^2} & \frac{\beta J}{L} & 0 & \frac{\beta SV}{L^2} & -(\mu+\gamma) \end{bmatrix}. \quad \text{(A.1)}$$

At a disease free equilibrium $\vec{x}_\infty(DF) = (E_\infty, V_\infty, N, 0, 0, 0)$ it reduces to the simple form

$$J(\vec{x}_\infty(DF)) = \begin{bmatrix} -(\mu_e+\delta) & f'(V_\infty) & 0 & 0 & f'(V_\infty) & 0 \\ \delta & -\mu_m & 0 & 0 & 0 & -\frac{\alpha V_\infty}{N} \\ 0 & 0 & -\mu & 0 & -\frac{\beta N}{V_\infty} & 0 \\ 0 & 0 & 0 & -\mu & 0 & \gamma \\ 0 & 0 & 0 & 0 & -\mu_m & \frac{\alpha V_\infty}{N} \\ 0 & 0 & 0 & 0 & \frac{\beta N}{V_\infty} & -(\mu+\gamma) \end{bmatrix}.$$

Due to the block diagonal form of the Jacobian its eigenvalues are those of the upper left and lower right 3×3 matrices whose characteristic equations are

$$(\mu+\lambda)[\lambda^2 + (\mu_m+\mu_e+\delta)\lambda + (\mu_m(\mu_e+\delta) - \delta f'(g_c^{-1}(\phi))] = 0 \quad \text{(A.2)}$$

and

$$(\mu+\lambda)[\lambda^2+(\mu+\mu_m+\gamma)\lambda+(\mu_m(\mu+\gamma)-\alpha\beta)]=0. \tag{A.3}$$

Writing the characteristic polynomial, in a useable form, for the Jacobian at an endemic equilibrium requires more work.

Proposition A.0.1. *The characteristic polynomial of the Jacobian* (A.1) *at the equilibrium* (5.5) *is given by*

$$\begin{aligned}
&\det(J(\vec{x}_\infty)-\lambda I)= \\
&\qquad (\mu+\lambda)\left[\lambda^2+(\mu_m+\mu_e+\delta)\lambda+\mu_m(\mu_e+\delta)-\delta f'(g_c^{-1}(\phi))\right] \\
&\qquad\cdot\left\{\lambda^3+\left[(\mu+\gamma)+\frac{\mu_m(\mu\mathcal{R}_0^2+\beta)}{\beta+\mu}+\frac{\mu(\mu+\beta)\mathcal{R}_0^2}{\beta+\mu R_0^2}\right]\lambda^2\right. \\
&\left.+\left[\mu_m\mu\mathcal{R}_0^2+(\mu+\gamma)\left(\frac{\mu_m\mu(\mathcal{R}_0^2-1)}{\mu+\beta}+\frac{\mu(\mu+\beta)\mathcal{R}_0^2}{\beta+\mu\mathcal{R}_0^2}\right)\right]\lambda+\mu(\mu+\gamma)\mu_m(\mathcal{R}_0^2-1)\right\}
\end{aligned} \tag{A.4}$$

Proof. We first expand $\det(J(\vec{x})-\lambda I)$ along the $4th$ column then subtract column 4 from column 2 and add row 5 to row 3 in the resultant 5×5 sub-determinant to arrive at

$$\det(J(\vec{x})-\lambda I)=(-\mu-\lambda)\times$$

$$\begin{vmatrix}
-(\mu_e+\delta)-\lambda & 0 & 0 & f'(L) & 0 \\
\delta & -(\mu_m+\frac{\alpha I}{N})-\lambda & 0 & 0 & -\frac{\alpha V}{N} \\
0 & 0 & -(\mu+\lambda) & 0 & -(\mu+\gamma+\lambda) \\
0 & \frac{\alpha I}{N}+\mu_m+\lambda & 0 & -\mu_m-\lambda & \frac{\alpha V}{N} \\
0 & -\frac{\beta S}{L} & \frac{\beta J}{L} & \frac{\beta SV}{L^2} & -(\mu+\gamma)-\lambda
\end{vmatrix}\cdot$$

We now add row 2 to row 4 and expand along the $4th$ row to get

$$\det(J(\vec{x}) - \lambda I) = (-\mu - \lambda)\times$$
$$\left\{ \delta \begin{vmatrix} 0 & 0 & f'(L) & 0 \\ -(\mu_m + \frac{\alpha I}{N}) - \lambda & 0 & 0 & -\frac{\alpha V}{N} \\ 0 & \mu + \lambda & 0 & \mu + \gamma + \lambda \\ -\frac{\beta S}{L} & \frac{\beta J}{L} & \frac{\beta SV}{L^2} & -(\mu + \gamma) - \lambda \end{vmatrix} + (\mu_m + \lambda)\times \right.$$
$$\left. \begin{vmatrix} -(\mu_e + \delta) - \lambda & 0 & 0 & 0 \\ \delta & -(\mu_m + \frac{\alpha I}{N}) - \lambda & 0 & -\frac{\alpha V}{N} \\ 0 & 0 & \mu + \lambda & \mu + \gamma + \lambda \\ 0 & -\frac{\beta S}{L} & \frac{\beta J}{L} & -(\mu + \gamma) - \lambda \end{vmatrix} \right\}.$$

It is not difficult to see that after expansion of both 4×4 determinants along their top rows, a common factor which is a 3×3 determinant emerges. Upon substitution of the equilibrium values, this 3×3 determinant yields the cubic factor of (A.4) and the rest accounts for the quadratic factor. □

Proof of Theorem 5.1.2

Theorem 5.1.2. *Let $\vec{x}_\infty(DF) = (E_\infty, V_\infty, N, 0, 0, 0)$ be a positive disease free equilibrium of (5.1) then $\vec{x}_\infty(DF)$ is locally asymptotically stable if $\mathcal{R}_0 < 1$ and $\mathcal{R}_d(g_c^{-1}(\phi)) < 1$. If one of $\mathcal{R}_0$ or $\mathcal{R}_d(g_c^{-1}(\phi))$ is greater than one then the equilibrium is unstable.*

Proof. The characteristic polynomial for the Jacobian at $\vec{x}_\infty(DF)$ contains the quadratic factor

$$\lambda^2 + (\mu_m + \mu_e + \delta)\lambda + (\mu_m(\mu_e + \delta) - \delta f'(g_c^{-1}(\phi))$$

so that the negativity of the real parts of its roots requires, that

$$(\mu_m(\mu_e + \delta) - \delta f'(g_c^{-1}(\phi)) > 0,$$

but this is equivalent, by definition, to $\mathcal{R}_d(g_c^{-1}(\phi)) < 1$. The characteristic polynomial at the disease free equilibrium contains a factor

$$\lambda^2 + (\mu + \mu_m + \gamma)\lambda + [\mu_m(\mu + \gamma) - \alpha\beta],$$

so that these roots have negative real part if and only if $\mu_m(\mu+\gamma)-\alpha\beta > 0$, which is equivalent to $\mathcal{R}_0 < 1$. □

Proof of Theorem 5.1.3

Theorem 5.1.3. *Let $\vec{x}_\infty = (E_\infty, V_\infty, S_\infty, R_\infty, J_\infty, I_\infty)$ be an endemic equilibrium of (5.1) then $V_\infty + J_\infty \in \{g_c^{-1}(\phi)\}$, $\mathcal{R}_0 > 1$, and $\vec{x}_\infty$ is locally asymptotically stable if $\mathcal{R}_d(g_c^{-1}(\phi)) < 1$ and unstable if $\mathcal{R}_d(g_c^{-1}(\phi)) > 1$.*

Proof. $V_\infty + J_\infty \in \{g_c^{-1}(\phi)\}$ follows immediately from the sum of equations V_∞ and J_∞. From I_∞ we see that endemicity requires $\mathcal{R}_0 > 1$. Now, the roots of the quadratic factor of equation all have negative real part if and only if

$$(\mu_m(\mu_e + \delta) - \delta f'(g_c^{-1}(\phi)) > 0$$

but, by definition, this is equivalent to $\mathcal{R}_d(g_c^{-1}(\phi)) < 1$. It remains only to verify that all the zeros of the cubic factor of,

$$\begin{aligned}
&\lambda^3 + \left[(\mu+\gamma) + \frac{\mu_m(\mu\mathcal{R}_0^2 + \beta)}{\beta + \mu} + \frac{\mu(\mu+\beta)\mathcal{R}_0^2}{\beta + \mu\mathcal{R}_0^2}\right]\lambda^2 \\
&+ \left[\mu_m\mu\mathcal{R}_0^2 + (\mu+\gamma)\left(\frac{\mu_m\mu(\mathcal{R}_0^2-1)}{\mu+\beta} + \frac{\mu(\mu+\beta)\mathcal{R}_0^2}{\beta+\mu\mathcal{R}_0^2}\right)\right]\lambda + \mu(\mu+\gamma)\mu_m(\mathcal{R}_0^2-1),
\end{aligned} \tag{A.5}$$

have, under these conditions, negative real parts. For this we use the Routh-Hurwitz criteria. With a_1, a_2, a_3 defined as the coefficients of the second, first and zeroth degree terms respectively, we clearly have $a_1 > 0$, and $a_3 > 0$ when $\mathcal{R}_0 > 1$. We now multiply the first terms of a_1 and a_2 and observe that the products of all the other terms are positive since $\mathcal{R}_0 > 1$. Therefore

$$a_1 a_2 - a_3 = \mu_m \mu(\mu + \gamma)\mathcal{R}_0^2 + \text{positive terms} - \mu_m \mu(\mu + \gamma)(\mathcal{R}_0^2 - 1)$$

$= \mu_m \mu(\mu + \gamma)(\mathcal{R}_0^2 - (\mathcal{R}_0^2 - 1))+$ positive terms

and hence $a_1 a_2 - a_3 > 0$. Hence, the Routh-Hurwitz criteria are satisfied and the result is proved. □

Proof of Theorem 5.1.5

Theorem 5.1.5. *Assume that $c(L) = 0$, that is, $f(L) = Lg_0(L)$ where $g_0(L)$ is strictly decreasing. If $\mathcal{R}_d(0) > 1$ and $\mathcal{R}_0 < 1$ then the unique positive disease-free equilibrium, $\vec{x}_\infty$, given by (5.4), is globally asymptotically stable in the domain $\Omega = \{(E, V, S, R, J, I) | E > 0, V > 0, S + I + R = N\} \subset \mathbb{R}^6_+$.*

Proof. The condition $\mathcal{R}_d(0) > 1$ together with the fact that $g_0(L)$ is strictly decreasing implies$g_0(L) = \phi$ has a unique positive solution proving the existence and, in this case, uniqueness of the equilibrium.

Now, let $(E(t), V(t), S(t), R(t), J(t), I(t))$ be any solution of the system (5.1) with initial condition $(E_0, V_0, S_0, R_0, J_0, I_0) \in \Omega$. The sum of the differential equations V' and J' together with E' gives the reduced, two dimensional system in E and $L = V + J$

$$\frac{dE}{dt} = f(L) - (\mu_e + \delta)E = F(E, L) \tag{A.6}$$

$$\frac{dL}{dt} = \delta E - \mu_m L = G(E, L) \tag{A.7}$$

on $\mathbb{R}^2_+$.

Both $(0,0)$ and $(E_\infty, L_\infty) = \left(\frac{\mu_m}{\delta} g_0^{-1}(\phi), g_0^{-1}(\phi)\right)$ are equilibria of (A.6), (A.7), but a short calculation shows that the condition $\mathcal{R}_d(0) > 1$ implies that $(0,0)$ is a saddle point whose stable manifold does not intersect $\mathbb{R}^2_+ \setminus \{(0,0)\}$. It is also easy to see that $\mathbb{R}^2_+ \setminus \{(0,0)\}$ is positively invariant. As a result, no positive semi-orbits starting in $\mathbb{R}^2_+ \setminus \{(0,0)\}$ can converge to $(0,0)$. On the other hand (E_∞, L_∞) is locally asymptotically stable by Result 4.2 since g_0 strictly decreasing implies $\mathcal{R}_d(g_0^{-1}(\phi)) < 1$. The divergence of the vector field defining the flow for (A.6), (A.7) is negative on all of $\mathbb{R}^2_+$. Hence, by Bendixson's theorem there is no periodic orbit.

Integration of (A.6) yields

$$E(t) \leq e^{-(\mu_e+\delta)t} E_0 + \frac{M}{(\mu_e+\delta)}(1 - e^{-(\mu_e+\delta)t})$$

where M is the upper bound for $f(L)$ and, therefore, $E(t)$ is bounded for $t > 0$. A similar argument, together with the boundedness of $E(t)$, proves that $L(t)$ is bounded for $t > 0$.

The Poincaré-Bendixson theorem now applies as follows: Since $(E(t), L(t))$ is a bounded semi-orbit in a region which contains no periodic orbit and only one, asymptotically stable equilibrium, then the limit set of the semi-orbit must contain nothing but the equilibrium (E_∞, L_∞). In other words, all semi-orbits of the full system must enter the invariant set

$$\{(E, V, S, R, J, I) | E > 0, V > 0, E = E_\infty, V + J = L_\infty, S + I + R = N\}.$$

Now, we need only compute the limits for S, R, J and I, and the limit of V will follow from the constraint $V + J = L_\infty$. To this end, we integrate equations $J'(t)$

and $I'(t)$ to obtain:

$$I(t) = e^{-(\mu+\gamma)t} I_0 + \frac{\beta}{e^{(\mu+\gamma)t}} \int_0^t e^{(\mu+\gamma)\tau} \frac{S(\tau)J(\tau)}{L(\tau)} d\tau \tag{A.8}$$

and

$$J(t) = e^{-\mu_m t} J_0 + \frac{\alpha}{N e^{\mu_m t}} \int_0^t e^{\mu_m \tau} I(\tau) V(\tau) d\tau. \tag{A.9}$$

Clearly,

$$S(t) \leq N, I(t) \leq N, \frac{J(t)}{L(t)} \leq 1, \text{ and } V(t) \leq L(t) \tag{A.10}$$

and now that we have proved that $L(t)$ approaches a finite limit, by (A.10), all of $V(t)$, $I(t)$, $S(t)$, and $J(t)$ must also be bounded. Computing lim sup of both (A.8) and (A.9) and using L'Hôpital's rule, we have

$$\limsup_{t\to\infty} I(t) \leq \frac{\beta}{\mu+\gamma} \limsup_{t\to\infty} \frac{J(t)}{L(t)} \limsup_{t\to\infty} S(t) \tag{A.11}$$

and

$$\limsup_{t\to\infty} J(t) \leq \frac{\alpha}{\mu_m N} \limsup_{t\to\infty} I(t) \limsup_{t\to\infty} V(t) \tag{A.12}$$

We now claim that

$$\limsup_{t\to\infty} J(t) = \lim_{t\to\infty} J(t) = 0.$$

If $\limsup_{t\to\infty} V(t) = 0$ then by (A.12) $\limsup_{t\to\infty} J(t) = \lim_{t\to\infty} J(t) = 0$ and the claim is established. Now assume $\limsup_{t\to\infty} V(t) > 0$ and suppose $\limsup_{t\to\infty} J(t) > 0$ for the purpose of proving the claim by contradiction. Since $\limsup_{t\to\infty} L(t) = \lim_{t\to\infty} L(t) = L_\infty > 0$ exists

$$\limsup_{t\to\infty} \frac{J(t)}{L(t)} = \frac{1}{L_\infty} \limsup_{t\to\infty} J(t) \tag{A.13}$$

but also $V(t) \leq L(t)$ for all t so that

$$\frac{1}{\limsup_{t\to\infty} V(t)} \geq \frac{1}{L_\infty}. \tag{A.14}$$

Combining (A.13) and (A.14) gives

$$\limsup_{t\to\infty} \frac{J(t)}{L(t)} \leq \frac{\limsup_{t\to\infty} J(t)}{\limsup_{t\to\infty} V(t)} \tag{A.15}$$

Substituting (A.15) into (A.11) gives us

$$\limsup_{t\to\infty} I(t) \leq \frac{\beta}{\mu+\gamma} \frac{\limsup_{t\to\infty} J(t)}{\limsup_{t\to\infty} V(t)} \limsup_{t\to\infty} S(t) \tag{A.16}$$

And then, finally substituting (A.16) into (A.12) and using the definition for $\mathcal{R}_0$ we arrive at

$$\limsup_{t\to\infty} J(t) \leq \frac{\mathcal{R}_0^2}{N} \limsup_{t\to\infty} J(t) \limsup_{t\to\infty} S(t)$$

but since $\limsup_{t\to\infty} S(t) \leq N$ this leads to the contradiction $\mathcal{R}_0 \geq 1$. Hence we must have

$$\lim_{t\to\infty} J(t) = 0.$$

Now from (A.11) and (A.13) it follows that $I(t) \to 0$. Since $L = V + J$ and $J(t) \to 0$ we must have $V(t) \to L_\infty = g_0^{-1}(\phi)$. Finally, by integrating $R'(t)$ and using the fact that $I(t) \to 0$ we get $R(t) \to 0$ and since $S + I + R = N$, $S(t) \to N$.

This completes the proof. □

Proof of Theorem 5.1.6

Theorem 5.1.6. *Suppose $\mathcal{R}_d(0) > 1$, and that $f(L) = Lg_c(L)$. Assume that $g_c(L) = \phi$ for an increasing, finite sequence $\{V_\infty^1, V_\infty^2, \cdots, V_\infty^{2n+1}\}$ where $g_c'(V_\infty^{2j+1}) < 0$ for all $0 \leq j \leq n$ and $g_c'(V_\infty^{2j}) > 0$ for all $1 \leq j \leq n$. If $\mathcal{R}_0 < 1$, then there are $n+1$ locally asymptotically stable positive disease free equilibria for the system (5.1). These equilibria are given by $\vec{x}_\infty^{2j+1} = (\frac{\mu_m}{\delta} V_\infty^{2j+1}, V_\infty^{2j+1}, N, 0, 0, 0)$, $0 \leq j \leq n$ and the basins of attraction for these equilibria are given by $\Omega_{2j+1} = \{(E, V, S, R, J, I) | E > 0, V > 0, S + I + R = N, V_\infty^{2j} < V + J < V_\infty^{2j+2}\}$, for each $0 \leq j \leq n$, where, for convenience V_∞^0 is defined to be 0 and $V_\infty^{2n+2} = \infty$.*

Proof. Result 4.6 implies that the condition $g_c'(V_\infty^{2j+1}) < 0$ is equivalent to the condition $\mathcal{R}_d(g_c^{-1}(\phi)) < 1$. The proof follows by observing that the conditions in the comment after Theorem 5.1.5 hold in each set Ω_{2j+1}. That is, in sets that exclude unstable equilibria (V_∞^{2j} and V_∞^{2j+2}). □

Appendix B

Jacobian and proofs of two strain model of dengue

Using the next generation operator approach of [23] to calculate $\mathcal{R}_0$, the Jacobian of the infectious classes (d_i, z_i, g_i where $i = 1, 2$) is as follows:

$$\mathcal{A} = \begin{bmatrix} -(\mu+\gamma_1) & 0 & 0 & 0 & \beta_1 s & 0 \\ 0 & -(\mu+\gamma_2) & 0 & 0 & 0 & \beta_2 s \\ 0 & 0 & -(\mu+\gamma_1) & 0 & \beta_1 r_2 & 0 \\ 0 & 0 & 0 & -(\mu+\gamma_2) & 0 & \beta_2 r_1 \\ \frac{\alpha_1\phi_1 v}{\mu_m+\phi_1} & 0 & \frac{\alpha_1\phi_1 v}{\mu_m+\phi_1} & 0 & -\mu_m\mu_m & 0 \\ 0 & \frac{\alpha_2\phi_2 v}{\mu_m+\phi_2} & 0 & \frac{\alpha_2\phi_2 v}{\mu_m+\phi_2} & 0 & -\mu_m \end{bmatrix}. \tag{B.1}$$

The *basic reproductive number*, $\mathcal{R}_0$, for each strain is calculated from the eigenvalues of the matrix $\mathcal{M} \cdot \mathcal{D}^{-1}$ where $\mathcal{M}$ and $\mathcal{D}$ are the decomposition of $\mathcal{A}$ such that $\mathcal{D}$ consists of the diagonal elements of $\mathcal{A}$ where $\mathcal{A} = \mathcal{M} - \mathcal{D}$ with $\mathcal{M}$ and $\mathcal{D} > 0$.

The Jacobian of the system (6.1) - (6.2) is given by,

$$J(\vec{\xi}) = \begin{bmatrix} J_1 & J_2 \\ J_3 & J_4 \end{bmatrix}$$

where,

$a_1 = \frac{\alpha_2 v(d_2+z_2)\psi}{(1-\psi(b_1+b_2))^2}$, $a_2 = -\frac{\alpha_2(d_2+z_2)}{1-\psi(b_1+b_2)} - (\mu_m + \phi_2)$, $a_3 = \frac{\alpha_1 v(d_1+z_1)\psi}{(1-\psi(b_1+b_2))^2}$, and $a_4 = -\frac{\alpha_1(d_1+z_1)}{1-\psi(b_1+b_2)} - (\mu_m + \phi_1)$. Then,

$$J_1 = \begin{bmatrix} -(\mu+\gamma_2) & 0 & 0 & 0 & \beta_2 s & 0 & 0 \\ \gamma_2 & -(\beta_1 g_1+\mu+p) & 0 & 0 & 0 & 0 & 0 \\ 0 & p & -(\rho_2 g_1+\mu) & 0 & 0 & 0 & 0 \\ \frac{\alpha_2 v}{1-\psi(b_1+b_2)} & 0 & a_1 & a_2 & -\frac{\alpha_2(d_2+z_2)}{1-\psi(b_1+b_2)} & \frac{\alpha_2 s}{1-\psi(b_1+b_2)} & 0 \\ 0 & 0 & 0 & \phi_2 & -\mu_m & 0 & 0 \\ 0 & 0 & 0 & 0 & \beta_2 r_1+\rho_1 b_1 & -(\mu+\gamma_2) & 0 \\ 0 & 0 & 0 & 0 & 0 & 0 & -(\mu+\gamma_1) \end{bmatrix},$$

$$J_2 = \begin{bmatrix} 0 & 0 & 0 & 0 & 0 & \beta_2 g_2 \\ 0 & 0 & 0 & 0 & -\beta_1 r_2 & 0 \quad 0 \\ 0 & 0 & 0 & -\rho_2 u_2 & 0 & 0 \\ 0 & \frac{\alpha_2 v(d_2+z_2)\psi}{(1-\psi(b_1+b_2))^2} & -\frac{\alpha_2(d_2+z_2)}{1-\psi(b_1+b_2)} & -\frac{\alpha_2(d_2+z_2)}{1-\psi(b_1+b_2)} & 0 & 0 \\ 0 & 0 & 0 & 0 & 0 & 0 \\ 0 & 0 & 0 & \beta_1 s & 0 & \beta_1 g_1 \end{bmatrix}$$

$$J_3 = \begin{bmatrix} 0 & 0 & 0 & 0 & 0 & 0 \\ 0 & 0 & 0 & 0 & -\beta_2 r_1 & 0 \\ 0 & 0 & 0 & 0 & -\rho_1 b_1 & 0 \\ 0 & 0 & \frac{\alpha_1 v(d_2+z_2)\psi}{(1-\psi(b_1+b_2))^2} & -\frac{\alpha_1(d_1+z_1)}{1-\psi(b_1+b_2)} & -\frac{\alpha_1(d_1+z_1)}{1-\psi(b_1+b_2)} & 0 \\ 0 & 0 & 0 & 0 & 0 & 0 \\ 0 & \beta_1 g_1 & \rho_2 g_1 & 0 & 0 & 0 \\ 0 & 0 & 0 & 0 & -\beta_2 s & 0 \end{bmatrix}$$

$$J_4 = \begin{bmatrix} -(\mu+\gamma_1) & 0 & 0 & 0 & \beta_1 s & 0 & \beta_1 g_1 \\ \gamma_1 & -\beta_2 g_2-(\mu+p) & 0 & 0 & 0 & 0 & 0 \\ 0 & p & -\rho_1 g_2-\mu & 0 & 0 & 0 & 0 \\ \frac{\alpha_1 v}{1-\psi(b_1+b_2)} & 0 & a_3 & a_4 & \frac{\alpha_1(d_1+z_1)}{1-\psi(b_1+b_2)} & \frac{\alpha_1 v}{1-\psi(b_1+b_2)} & 0 \\ 0 & 0 & 0 & \phi_1 & -\mu_m & 0 & 0 \\ 0 & 0 & 0 & 0 & \beta_1 r_2+\rho_2 b_2 & -(\mu+\gamma_1) & 0 \\ 0 & 0 & 0 & 0 & -\beta_1 s & 0 & -\beta_1 g_1-\beta_2 g_2-\mu \end{bmatrix}$$

Also, for convenience the order of the system in the Jacobian matrix is, $\vec{\xi} = (d_2, r_2, b_2, l_2, g_2, z_2, d_1, r_1, b_1, l_1, g_1, z_1, s)$.

At the DFE, $\vec{\xi^*}(DF) = (0,0,0,0,0,0,0,0,0,0,0,0,1)$, it reduces to

$$J(\vec{\xi^*}(DF)) = \begin{bmatrix} -(\mu+\gamma_2) & 0 & 0 & 0 & \beta_2 & 0 & 0 & 0 & 0 & 0 & 0 & 0 & 0 \\ \gamma_2 & -(\mu+p) & 0 & 0 & 0 & 0 & 0 & 0 & 0 & 0 & 0 & 0 & 0 \\ 0 & p & -\mu & 0 & 0 & 0 & 0 & 0 & 0 & 0 & 0 & 0 & 0 \\ \alpha_2 & 0 & 0 & -(\mu_m+\phi_2) & 0 & \alpha_2 & 0 & 0 & 0 & 0 & 0 & 0 & 0 \\ 0 & 0 & 0 & \phi_2 & -\mu_m & 0 & 0 & 0 & 0 & 0 & 0 & 0 & 0 \\ 0 & 0 & 0 & 0 & \beta_2 & -(\mu+\gamma_2) & 0 & 0 & 0 & 0 & 0 & 0 & 0 \\ 0 & 0 & 0 & 0 & 0 & 0 & -(\mu+\gamma_1) & 0 & 0 & 0 & 0 & 0 & 0 \\ 0 & 0 & 0 & 0 & 0 & 0 & \gamma_1 & -(\mu+p) & 0 & 0 & 0 & 0 & 0 \\ 0 & 0 & 0 & 0 & 0 & 0 & 0 & p & -\mu & 0 & 0 & 0 & 0 \\ 0 & 0 & 0 & 0 & 0 & 0 & \alpha_1 & 0 & 0 & -(\mu_m+\phi_1) & 0 & \alpha_1 & 0 \\ 0 & 0 & 0 & 0 & 0 & 0 & 0 & 0 & 0 & \phi_1 & -\mu_m & 0 & 0 \\ 0 & 0 & 0 & 0 & 0 & 0 & 0 & 0 & 0 & 0 & 0 & -(\mu+\gamma_1) & 0 \\ 0 & 0 & 0 & 0 & -\beta_2 & 0 & 0 & 0 & 0 & 0 & -\beta_1 & 0 & -\mu \end{bmatrix}.$$

The Jacobian matrix corresponding to the endemic equilibria is as follows, where $\vec{\xi} = (d_2, z_2, b_2, r_2, l_2, g_2, d_1, z_1, b_1, r_1, l_1, g_1, s)$:

$$J(\vec{\xi^*}(EE)) = \begin{bmatrix} G1 & * \\ 0 & G2 \end{bmatrix}.$$

where,

$$G1 = \begin{bmatrix} \frac{-\mu(\mathcal{R}_2-1)}{\nu_2+1-\delta_2}-\mu & 0 & 0 & 0 & 0 & 0 & \frac{-\beta_2(\nu_2+1-\delta_2)}{\nu_2+\mathcal{R}_2-\delta_2} \\ \frac{\mu(\mathcal{R}_2-1)}{\nu_2+1-\delta_2} & -(\mu+\gamma_2) & 0 & 0 & 0 & 0 & \frac{-\beta_2(\nu_2+1-\delta_2)}{\nu_2+\mathcal{R}_2-\delta_2} \\ 0 & 0 & -(\mu+\gamma_2) & 0 & 0 & 0 & 0 \\ 0 & 0 & 0 & -\mu & p & 0 & 0 \\ 0 & \gamma_2 & 0 & 0 & -(\mu+p) & 0 & 0 \\ 0 & h_1 & h_1 & h_2 & 0 & h_3 & h_4 \\ 0 & 0 & 0 & 0 & 0 & \phi_2 & -\mu_m \end{bmatrix}$$

and,

$$G2 = \begin{bmatrix} -(\gamma_1+\mu) & 0 & 0 & 0 & 0 & \frac{\beta_1(\nu_2+1-\delta_2)}{\nu_2+\mathcal{R}_2-\delta_2} \\ 0 & -(\gamma_1+\mu) & 0 & 0 & 0 & h_6 \\ 0 & 0 & \frac{-\rho_1\mu(\mathcal{R}_2-1)}{\beta_2(\nu_2+1-\delta_2)}-\mu & p & 0 & 0 \\ \gamma_1 & 0 & 0 & \frac{-\mu(\mathcal{R}_2-1)}{\nu_2+1-\delta_2}-p-\mu & 0 & 0 \\ h_6 & h_6 & 0 & 0 & -(\mu_m+\phi_1) & 0 \\ 0 & 0 & 0 & 0 & \phi_1 & -\mu_m \end{bmatrix}.$$

The following values are found in $J(\vec{\xi^*}(EE))$,

$$\begin{aligned} h_1 &= \frac{\alpha_2(1-\frac{\mu_m\mu(\mathcal{R}_2-1)}{\beta_2\phi_2(\nu_2+1\delta_2)}\frac{\mu(\mathcal{R}_2-1)}{\beta_2(\nu_2+1-\delta_2)})}{1-\frac{\delta_2(\mathcal{R}_2-1)}{\nu_2+\mathcal{R}_2-\delta_2}} \\ h_2 &= \frac{\alpha_2\mu\psi(\mathcal{R}_2-1)(1-\frac{\mu_m\mu(\mathcal{R}_2-1)}{\beta_2\phi_2(\nu_2+1-\delta_2)}-\frac{\mu(\mathcal{R}_2-1)}{\beta_2(\nu_2+1\delta_2)}}{(\mu+\gamma_2)(\nu_2+\mathcal{R}_2-\delta_2)(1-\frac{\delta_2(\mathcal{R}_2-1)}{\nu_2+\mathcal{R}_2-\delta_2})^2} \\ h_3 &= -\frac{\alpha_2\mu(\mathcal{R}_2-1)}{(\mu+\gamma_2)(\nu_2+\mathcal{R}_2-\delta_2)(1-\frac{\delta_2(\mathcal{R}_2-1)}{\nu_2+\mathcal{R}_2-\delta_2})}-(\phi_2+\mu_m) \\ h_4 &= -\frac{\alpha_2\mu(\mathcal{R}_2-1)}{(\mu+\gamma_2)(\nu_2+\mathcal{R}_2-\delta_2)(1-\frac{\delta_2(\mathcal{R}_2-1)}{\nu_2+\mathcal{R}_2-\delta_2})} \\ h_5 &= \frac{\beta_1\mu\delta_2(\mathcal{R}_2-1)}{p\psi(\nu_2+\mathcal{R}_2-\delta_2)}+\frac{\rho_2\delta_2(\mathcal{R}_2-1)}{\psi(\nu_2+\mathcal{R}_2-\delta_2)} \\ h_6 &= \frac{\alpha_1(1-\frac{\mu_m\mu(\mathcal{R}_2-1)}{\beta_2\phi_2(\nu_2+1-\delta_2)}-\frac{\mu(\mathcal{R}_2-1)}{\beta_2(\nu_2+1-\delta_2)}}{1-\frac{\delta_2(\mathcal{R}_2-1)}{\nu_2+\mathcal{R}_2-\delta_2}} \end{aligned}$$

Proof of Theorem 6.2.1

Theorem 6.2.1. *Let* $\vec{\xi}_0^* = (1,0,0,0,0,0,0,0,0,0,0,0,0,0)$ *be the positive disease-free equilibria of* (6.1)-(6.2) *then it is locally asymptotically stable if and only if* $\mathcal{R}_0 < 1$.

Proof. The analysis follows from the eigenvalues of the Jacobian* matrix eval-

*See Appendix

uated at the the disease-free equilibrium. They are: $-1($ of multiplicity two $)$, $-\mu($ of multiplicity three $)$, $-(\mu+\gamma_1)$, $-(\mu+\gamma_2)$ and the roots of the cubic equation:

$$\lambda^3+(2\mu_m+\gamma_i+\phi_i+\mu)\lambda^2+(\mu_m(\mu_m+\phi_i)+(\mu+\gamma_i)(2\mu_m+\phi_i))\lambda+ \\ \mu_m(\mu_m+\phi_i)(\mu+\gamma_i)(1-\mathcal{R}_i)=0, \quad \text{(B.2)}$$

which are of the form

$$\lambda^3+a_1\lambda^2+a_2\lambda+a_3=0.$$

Clearly $a_1>0$ and $a_3>0$ whenever $\mathcal{R}_0<1$. Then we are left to verify the condition $a_1a_2-a_3>0$, or whether or not

$$(2\mu_m+\gamma_i+\phi_i+\mu)(\mu_m(\mu_m+\phi_i)+(\mu+\gamma_i)(2\mu_m+\phi_i)) \\ >\mu_m(\mu_m+\phi_i)(\mu+\gamma_i)(1-\mathcal{R}_0), \quad \text{(B.3)}$$

and,

$$2\mu_m(2\mu_m+\phi_i)(\mu+\gamma_i)+(pos.terms)>\mu_m(\mu_m+\phi_i)(\mu+\gamma_i). \quad \text{(B.4)}$$

where $i=1,2$. They both hold when $\mathcal{R}_0<1$ □

Proof of Theorem 6.2.3

Theorem 6.2.3. *Assume $\beta_i=\rho_k$, for $i\neq k$, where $\psi=0$ and $\mathcal{R}_0<1$, then the positive disease-free equilibrium given by 6.4 is globally asymptotically stable on the domain $\Omega=\{(s,d_i,b_i,z_i,r_i,r,v,l_i,g_i)|x+\sum_{i=1}^{2}(d_i+b_i+z_i+r_i)+r=1, v+\sum_{i=1}^{2}l_i+\sum_{i=1}^{2}g_i=1\}\subset\mathbb{R}^{15}_{+}$ for $i=1,2$.*

Proof. We construct the following Lyapunov function, where $i,k=1,2$ and $i\neq k$.

$$\mathcal{L}=\sum_{i=1}^{2}\Big(\frac{\beta_i}{\mu_m(\mu_m+\phi_i)}g_i+l_i+i_i+z_i\Big)\geq 0,$$

where the orbital derivative is given by

$$\dot{\mathcal{L}} = \sum_{i=1}^{2} \Bigg(-(\mu+\gamma_i)(i_i+z_i)\Big[1-\mathcal{R}_0\Big(1-\sum_{i=1}^{2} l_i - \sum_{i=1}^{2} z_i\Big)\Big] \\ -\phi_i l_i(\frac{\beta_i}{\mu_m}-1) + \beta_i g_i(1-(i_k+z_k))\Bigg) \leq 0 \quad \text{(B.5)}$$

By inspection and with β_i sufficiently small (which basically indicates that the transmission rate is small) but greater than μ_m, $\dot{\mathcal{L}} \leq 0$. □

Proof of Proposition 6.6

Proposition 6.6. *A necessary condition for the local asymptotic stability of the endemic equilibria is that (for $i,k = 1,2$, $i \neq k$)*

$$\mathcal{R}_i^2 < \left[\frac{1-(\mathcal{R}_k^2-1)\frac{\delta_k}{(\nu_k+\mathcal{R}_k^2-\delta_k)}}{1-(\mathcal{R}_k^2-1)\mu\frac{\mu_m+\phi_k}{\beta_k\phi_k(\nu_k+1-\delta_k)}}\right]\left[\frac{(\nu_k+\mathcal{R}_k^2-\delta_k)}{\frac{\gamma_k(\mathcal{R}_k^2-1)}{(\mu+\gamma_k)}+(\nu_k+1-\delta_k)}\right] \quad \text{(B.6)}$$

Proof. It must be shown that all eigenvalues of the sub-matrix $G2$ have negative real part whenever (B.6) holds. The problem reduces to the study of the roots of the characteristic polynomial,

$$p(\lambda) = \lambda^3 + (2\mu_m + \mu + + \gamma_1 + \phi_1)\lambda^2 + [(\mu_m+\phi_1)(\mu+\gamma_1) + \mu_m(\mu+\gamma_1+\mu_m+\phi_1)]\,\lambda \\ + \left[\mu_m(\mu_m+\phi_1)(\mu+\gamma_1) - h_5(h_6\phi_1 + \frac{\beta_1\phi_1(\nu_2+1-\delta_2)}{\nu_2+\mathcal{R}_2-\delta_2}\right], \quad \text{(B.7)}$$

of this sub-matrix.

With a_1, a_2, and a_3 the quadratic, linear, and constant coefficients, respectively. It is easy to see that a_1,a_2 are positive, and that $a_1a_2 - a_3 > 0$ when (B.6) holds. The inequality of the proposition is, after substitution of the expressions of h_5 and h_6, equivalent to the condition that $a_3 > 0$.

□

BIBLIOGRAPHY

[1] Dengue fever. The Lancet, May 1872.

[2] Dengue fever. The Lancet, October 1872.

[3] Para-scarlet and dengue fevers. The Lancet, February 1920.

[4] Dengue fever. The Lancet, December 1928.

[5] Biology of plasmodium parasites and anopheles mosquitos. http://www-micro.msb.le.ac.uk/224/Bradley/Biology.html, 1996, Accessed 2004.

[6] Cdc: Dengue outbreak associated with multiple serotypes – puerto rico. http://www.cdc.gov/mmwr/preview/mmwrhtml/00055624.htm, November 1998.

[7] Center for disease control (cdc): Dengue fever. http://www.cdc.gov/ncidod/dvbid/dengue/index.htm, June 2001, Accessed 2006.

[8] Mosquito control around the home and in communities. http://www.ces.ncsu.edu/depts/ent/notes/Urban/mosquito.htm, July 2001, Accessed 2006.

[9] Geography. http://welcome.topuertorico.org/geogra.shtml, 2003, Accessed 2006.

[10] Center for disease control. http://www.cdc.gov/ncidod/dvbid/dengue/map-distribution-2003.htm, June 2006, Accessed 2006.

[11] Center for disease control (cdc): Clinical and public health aspects. http://www.cdc.gov/ncidod/dvbid/dengue/slideset/set1/i/slide02.htm, February 2006, Accessed 2006.

[12] Ministry of health singapore. health facts singapore. http://www.moh.gov.sg/corp/publications/statistics/top10.do, August 2006, Accessed 2006.

[13] Ministry of health: Statistics, publications & resources. http://www.moh.gov.sg, Accessed 2006.

[14] U.s. department of the interior. u.s. geological survey. u.s. geological survey programs in puerto rico. http://water.usgs.gov/pubs/fs/FS-051-96/, Accessed 2006.

[15] The world fact book. http://www.cia.gov/cia/publications/factbook, Accessed 2006.

[16] J. Aron and R. May. *The population dynamics of Malaria*. Chapman and Hall, 1982.

[17] N. Bailey. *The Mathematical Theory of Infectious Diseases*. Griffin, 1975.

[18] F. Berezovsky, G. Karev, B. Song, and C. Castillo-Chávez. Simple epidemic models with surprising dynamics. *Mathematical Biosciences and Engineering*, 1, 2004.

[19] W. Black IV, E. Bennett, N. Gorrochotegui-Escalante, C. Barillas-Mury, I. Fernández-Salas, M. Muñoz, J. Farfan-Ale, K. Olson, and B. Beaty. Flavivirus susceptibility in aedes aegypti. *Archives of Medical Research*, 22:379–388, 2002.

[20] J. Blaney, A. Durbin, B. Murphy, and S. Whitehead. Development of a live attenuated dengue virus vaccine using reverse genetics. *Viral Immunology*, 19(1):10–32, 2006.

[21] F. Brauer and C. Castillo-Chávez. *Mathematical Models in Population Biology and Epidemiology*, volume 40 of *Texts in Applied Mathematics*. Springer-Verlag, 2001.

[22] S. Busenberg and K. Cooke. *Vertically Transmitted Diseases*, volume 23 of *Biomathematics*. Springer-Verlag, 1993.

[23] C. Castillo-Chávez, Z. Feng, and W. Huang. On the computation of r_0 and its role on global stability. *In: Mathematical Approaches for emerging and re-emerging infectious diseases, Part II, IMA*, 125:224–250, 2002.

[24] C. Castillo-Chávez, J. Velasco-Hernández, and S. Fridman. Modelling contact structures in biology. *Lecture Notes in Biomathematics*, 100:454–492, 1995.

[25] P. Chanthavanich, C. Luxemburger, C. Sirivichayakul, K. Lapphra, K. Pengsaa, S. Yoksan, A. Sabchareon, and J. Lang. Short report: Immune response and occurence of dengue infection in thai children three to eight years after vaccination with live attenuated tetravalent dengue vaccine. *American Journal of Tropical Medicine and Hygiene*, 75(1):26–28, 2006.

[26] G. Chowell and F. Sánchez. An outbreak of dengue in mexico, 2003: Quantifying the role of interventions. *Journal of Environmental Health*, 68(10):40–44, June 2006.

[27] M. Derouich and A. Boutayeb. Dengue fever: Mathematical modelling and computer simulation. *Applied Mathematics and Computation*, 177:528–544, 2006.

[28] O. Diekmann, J. Heesterbeek, and J. Metz. On the definition and the computation of the basic reproduction ratio r_0 in models for infectious diseases in heterogeneous populations. *Journal of Mathematical Biology*, 28:365–382, 1990.

[29] K. Dietz. Transmission and control of arbovirus diseases in: D. ludwig *et al.* (eds.). *Epidemiology, Proceedings of the Society for Industrial and Applied Mathematics*, page 104, 1974.

[30] J. Edman, T. Scott, A. Costero, A. Morrison, L. Harrington, and G. Clark. *Aedes aegypti* (diptera: Culicidae) movement influenced by availability of oviposition sites. *Journal of Medical Entomology, Traub Memorial Issue*, 35(4):578–583, 1998.

[31] L. Esteva and C. Vargas. Analysis of a dengue disease transmission model. *Mathematical Biosciences*, 150(2):131–151, June 1998.

[32] L. Esteva and C. Vargas. A model for dengue disease with variable human population. *Journal of Mathematical Biology*, 38:220–240, 1999.

[33] L. Esteva and C. Vargas. Coexistence of different serotypes of dengue virus. *Journal of Mathematical Biology*, 46:31–47, 2002.

[34] M. Esteva-Peralta. Modelos matematicos de la enfermedad del dengue. 1996.

[35] Z. Feng and J. Velasco-Hernández. Competitive exclusion in a vector-host model for the dengue fever. *Journal of Mathematical Biology*, 35:523–544, 1997.

[36] D. Focks, R. Brenner, J. Hayes, and E. Daniels. Transmission thresholds for dengue in terms of *aedes aegypti* pupae per person with discussion of their utility in source reduction efforts. *American Journal of Tropical Medicine and Hygiene*, 62(1):11–18, 2000.

[37] D. Focks, E. Daniels, D. Haile, and J. Keesling. A simulation model of the epidemiology of urban dengue fever: Literature analysis, model development, preliminary validation, and samples of simulation results. *American Journal of Tropical Medicine and Hygiene*, 53:489–506, 1995.

[38] B. Gerade, S. Lee, T. Scott, J. Edman, L. Harrington, S. Kitthawee, J. Jones, and J. Clark. Field validation of aedes aegypti (diptera: Culicidae) age estimation by analysis of cuticular hydrocarbons. *Journal of Medical Entomology*, 41(2):231–238, 2004.

[39] A. Getis, A. Morrison, K. Gray, and T. Scott. Characteristics of the spatial pattern of the dengue vector, *aedes aegypti*, in iquitos, peru. *American Journal of Tropical Medicine and Hygiene*, 69(5):494–505, 2003.

[40] D. Gubler. *The arbovirus: Epidemiology and Ecology*, volume II. CRC press, 1986.

[41] D. Gubler. Cities spawn epidemic dengue viruses. *Nature Medicine*, 10(2):129–130, 2004.

[42] D. Gubler and G. Kuno. *Dengue and Dengue Hemorrhagic Fever*. CABI, 1997.

[43] D. Gubler, P. Reiter, K. Ebi, W. Yap, R. Nasci, and J. Patz. Climate variability and change in the united states: Potential impacts on vector and rodent-borne diseases. *Environmental Health Perspectives*, 109(2):223–233, 2001.

[44] L. Harrington, J. Buonaccorsi, J. Edman, A. Costero, P. Kittayapong, G. Gary, and T. Scott. Analysis of survival of young and old aedes aegypti (diptera: Culicidae) from puerto rico and thailand. *Journal of Medical Entomology*, 38(4):537–547, 2001.

[45] L. Harrington, J. Edman, and T. Scott. Why do female *aedes aegypti* (diptera: Culicidae) feed preferentially and frequently on human blood. *Journal of Medical Entomology*, 38(3):411–422, 2001.

[46] L. Harrington, T. Scott, K. Lerdthusnee, R. Coleman, A. Costero, G. Clark, J. Jones, S. Kitthawee, P. Kittayapong, R. Sithiprasasna, and J. Edman. Dispersal of the dengue vector *aedes aegypti* within and between rural communities. *American Journal of Tropical Medicine and Hygiene*, 72(2):209–220, 2005.

[47] H. Hethcote. The mathematics of infectious diseases. *SIAM Review*, 42(4):599–653, December 2000.

[48] P. Kaufman, L. Harrington, J. Waldron, and D. Rutz. The importance of agricultural tire habitats for mosquitoes of public health importance in new york state. *Journal of the American Mosquito Control Association*, 21(2):171–176, 2005.

[49] J. Keating. An investigation into the cyclical incidence of dengue fever. *Social Science & Medicine*, 53:1587–1597, 2001.

[50] I. Kurane and T. Takasaki. Dengue fever and dengue hemorrhagic fever: challenges of controlling an enemy still at large. *Reviews in Medical Virology*, 11:301–311, 2001.

[51] C. Marques, O. Foratini, and E. Masad. The basic reproductive number for dengue fever n sao paulo state, brazil 1990-1991 epidemic. *Transactions of the Royal Society of Tropical Medicine and Hygiene*, 88:58–59, 1994.

[52] J. Mena-Lorca, J. Velasco-Hernández, and C. Castillo-Chávez. Superinfection, virulence and density dependent mortality in an epidemic model. *Biometrics Unit, Cornell University*, BU 1299-M, 1995.

[53] J. Mendez Galvan and R. Castellanos. Manual para la vigilancia epidemiologica del dengue, 1994, Accessed 2004.

[54] A. Morrison, K. Gray, A. Getis, H. Astete, M. Sihuincha, D. Focks, D. Watts, J. Stancil, J. Olson, P. Blair, and T. Scott. Temporal and geographic patterns of *aedes aegypti* (diptera: Culicidae) production in iquitos, peru. *Journal of Medical Entomology*, 41(6):1123–1142, 2004.

[55] M. Nowak and R. May. Superinfection and the evolution of parasite virulence. *Proceedings of the Royal Society of London B*, 255:81–89, 1994.

[56] A. Ponlawat and L. Harrington. Blood feeding patterns of *aedes aegypti* and *aedes albopictus* in thailand. *Journal of Medical Entomology*, 42(5):844–849, 2005.

[57] R. Ross. The prevention of malaria. 1911.

[58] A. Tran, X. Deparis, P. Dussart, J. Morvan, P. Rabarison, F. Remy, L. Polidori, and J. Gardon. Dengue spatial and temporal patterns, french guiana, 2001. *Emerging Infectious Diseases*, 10(4):615–621, April 2004.

[59] J. Velasco-Hernández. A model for chagas disease involving transmission by vectors and blood transfusion. *Theoretical Population Biology*, 46(1):1–31, 1994.

[60] J. Wu and Z. Feng. Mathematical models for schistosomiasis with delays and multiple definitive hosts. *In: Mathematical Approaches for emerging and re-emerging infectious diseases, Part II, IMA*, 126:215–229, 2002.

Chapter 7

Part II: Introduction

Alcohol abuse has been a problem in the United States and around the world for decades. There are nearly 14 million people in the United States (1 in every 13 adults) who abuse alcohol or are alcoholic. Some of the more common complications of alcohol abuse include: HIV, sexually transmitted diseases (STD's), violent acts leading to injury/death, less productivity (economic burden), liver diseases (Cirrhosis), date rape among others [1, 28]. There is no cure for alcohol abuse or alcoholism.

Formulating drinking behavior models by itself can give rise to many insights and questions. The process naturally raises and instigates questions that often help sharpen the focus of the research and on occasion identify directions that require attention or reformulation. For example, during the process of developing a population model of the "spread" of drinking behaviors through contacts between humans mixing in "appropriate" environments a variety of questions arise including: What is a *drink*? What are safe drinking levels? What is an occasional drinker? Of course, the answers are different for each individual but we must use averages. How does one average? The impact of using "averages" to describe a population of drinkers has its own pitfalls since our aggregated models are not derived explicitly from individual based models. In an ideal world, we would have not only good data but individuals based and time series data that capture the dynamics of drinking over "legitimate" time horizons. The use of models (their simulation and analysis) as a tool that enhances understanding by suggesting or identifying new directions and hypotheses or by closing down unproductive paths

or identifying wrong turns, is not only necessary but fundamental. But what type of models? Typically in fields where models have become established (ecology, genetics, epidemiology, etc.) the model is not thought of as a description that captures as much detail as it can from a complex system but actually it is thought of as a tool designed to answer sharp, focused, specific questions. Hence, the level of detail or information that it is incorporated in a model should be just enough to guarantee that the question under consideration can be addressed in a non-obvious and useful setting. This is why in many areas of ecology and epidemiology (particularly where data are available) the goal has often been to use as simple models as possible (but not simpler) as one attempts to address a specific question. Deterministic models have many advantages and can often give solid insights into processes where data are limited ([11, 12, 10]). The introduction of models with high degree of complexity is sometimes possible and its analyses often possible ([26, 33, 8]).

The question requires the use of a model that includes two levels of heterogeneity: "local" and "global". We are able to formulate a modeling framework that captures the impact of two contact mixing levels driven by average residence times and drinking activity per unit of time. We hope to use this complex setting (still a highly aggregated model) to study the interactions between "global" drinking environments and local drinking networks and their effect of such interactions on the short- and the long-term dynamics of drinking at the population level.

There are many factors that contribute to individuals becoming problem drinkers: peer pressure from other drinkers, stress level, type of environment, relationships, among others. It is difficult to take into account many of the factors that could contribute to the problem.

There are many different treatments that include medication or psychological help or a combination of both. One of the main problems is that individuals that recover could relapse even after being sober for a long time. How this process occurs is what interests us. We look at the impact of "problem" drinkers on the population of temporarily recovered and the impact of fast recovery. Also, education plays a big role in most social and disease dynamics [17], however, educational programs or rehabilitation programs usually target individuals who typically have strong self motivation to get better. Moreover, individuals who really need help are usually timid and rarely seek any type of help.

In Chapter 8 we will focus on the influence of other drinkers on the temporarily recovered and look at two different types of environments (local and global). We explored a simple mathematical model (deterministic, networks and stochastic) that looks at the impact of influence of other drinkers, temporary recovery and relapse. In Chapter 9 we look at different types of environments play a role in drinking dynamics. We also look at a more detailed model that includes different classes of drinkers (abstainers, occasional, moderate, heavy) in a local and global environments. We study the effects of these environments in the light drinking classes (abstainer and occasional).

Chapter 8

Drinking as an epidemic–a simple mathematical model with recovery and relapse*

The outcomes (patterns) associated with various biological and sociological processes are often the result of interactions or contacts between individuals, groups, sub-populations or populations. For example, some aspects associated with the process of language acquisition can be thought of as the result of non-specified contacts between those who speak the language and those who have yet to acquire it. Although contacts between individuals in different states are at the heart of these processes, the definition of "contact" (effective contact) is highly dependent on context and difficult to define. Gonorrhea transmission, for example, is most often the result of intimate sexual contacts (intercourse) between infected and non-infected partners. Tuberculosis (TB) or influenza infections are most often the result of "casual" contacts (handshakes or kissing) or the result of sharing close environments, for long-enough periods of time with infected individuals.

Starting with the pioneering work of Ross and his students [29], researchers who conduct studies of social and health problems in which data are scarce have often relied on simple mean field deterministic models to generate insights and understanding. The analysis of such mathematical models is used to generate hy-

*Fabio Sánchez, Xiahong Wang, Carlos Castillo-Chávez, Paul Gruenewald and Dennis Gorman. Drinking as an epidemic–a simple mathematical model with recovery and relapse. Evidence Based Relapse Prevention. Edited by Katie Witkiewitz and G. Alan Marlatt, 2006 (to appear in).

potheses or to gain insights (with limited data) on the "transmission" process and its control [11, 12, 10]. Challenges arise from the fact that the dynamics of social processes are highly non-linear. Tuberculosis, for example, can be transmitted through casual interactions (e.g. in public transportation systems) or through the type of close contacts that take place among household members or close friends. While it has been difficult to measure explicitly the contribution of each of these transmission routes in the case of TB, it has been possible to show that both routes are necessary for the pathogen's survival [15, 3]. In epidemiology, the result of contacts between susceptible and infectious individuals may alter temporarily or permanently an individual's health status. Flu infections are short ($3-6$ days on the average), TB infections are life-long (most infected individuals remaining "forever" in a latent state) and HIV infections are progressive (especially in the absence of treatment) and life-long.

In addition to studying infectious disease transmission processes, epidemiological contact models have also been applied to the study of the dynamics of social and behavioral processes such as eating disorders, drug addictions and violence [16, 34, 30, 14, 27]. There are clearly differences in the generation of addictive behaviors and the transmission of infectious diseases. However, the fact remains that the acquisition of both can be modeled (in the context of specific questions) as the likely result of contacts between individuals in given environments. For example, the development of alcohol use among young people and the influence of "supportive environments" on the development and maintenance of heavy drinking, alcohol abuse, dependence and problems among adults, are predicated upon the combined effects of social influence and access to alcohol [18, 35, 36, 37]. Thus, additional understanding of the dynamics of drinking behaviors may result from

the use of a perspective that models drinking as the result of contacts of susceptibles with individuals in distinct drinking states.

8.1 Simple SDR drinking model

Drinking is modeled as an "acquired" state, the result of frequent (i.e., high number of contacts) or intense (i.e., high likelihood of conversion) interactions between individuals in three drinking states (susceptible, regular drinkers and temporarily recovered) within an (implicitly) assumed fixed drinking environment.

This is the first time this approach is used to model drinking dynamics. The goal of the model is to identify mechanisms (quantitatively speaking) that facilitate or limit the conversion of a population of non-drinkers to one of drinkers. The process of quantification helps to understand the role of social forces on the time evolution of drinking. Knowledge of these factors may be useful in the development of effective drinking control policies and in the evaluation of treatment interventions.

We describe the dynamics of drinking within the context of the classic SIR (Susceptible-Infected-Recovered) epidemiological framework [6]. The population in question is divided into the following drinking classes: occasional and moderate drinkers (S); problem drinkers or "infectious" (D); and temporarily recovered (R). It is assumed that the population size remains constant, that is, that the time scale of interest is such that the total population size does not change significantly over the length of the study. New recruits join the population as occasional and moderate drinkers (S) and mix at random (i.e., homogeneous mixing) with the rest of the members of the population. Uniform or homogeneous mixing means that the likelihood of coming into contact with members of each class is either $\frac{S}{N} = s$,

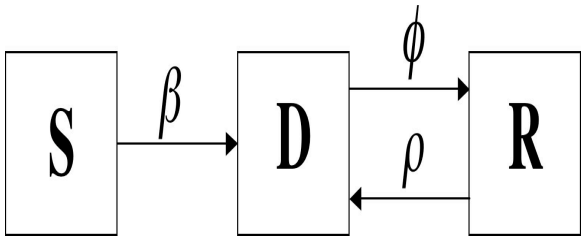

Figure 8.1: Caricature of the model.

$\frac{D}{N} = d$ or $\frac{R}{N} = r$ where $N = S + D + R$. Under these assumptions, the process of transmitting "drinking behaviors" is modeled via the following re-scaled (that is, we work with proportions) system of nonlinear differential equations:

$$\begin{aligned} \dot{s} &= \mu - \beta sd - \mu s, \\ \dot{d} &= \beta sd + \rho rd - (\mu + \phi)d, \\ \dot{r} &= \phi d - \rho rd - \mu r, \\ 1 &= s + d + r. \end{aligned} \tag{8.1}$$

The rate of conversion from the susceptible state (occasional drinker) to the regular drinking state is assumed to be proportional to the size of the susceptible population, the likelihood of interacting with a randomly selected drinking partner and the magnitude and intensity of the contacts. The rate of relapse is the result of similar forces that involve contacts between r and d individuals.

The fact that individuals can transition to the D class from the S and R classes suggests that "conversion" may be the result of "group" rather than individual processes. The "first" transfer of individuals to the drinking class is the result of a nonlinear process modeled via a function of S and D, $B(S, D)$. This function must satisfy the following conditions: $B(0, D) = B(S, 0) = 0$ (in the absence of susceptible or problem drinkers there is no transmission). Homogeneous mixing means that $B(S, D)$ can be modelled as $\beta S\frac{D}{N}$ or $B(s, d) = \beta sd$ (in re-scaled vari-

ables). Here β is a measure of the average number of effective interactions between susceptible and problem drinkers per unit of time. The rate of transfer from R to D is the result of a nonlinear process modeled via the function $G(D, R)$ with $G(0, R) = G(D, 0) = 0$. Here, we choose to model the total nonlinear relapse rate by $\rho R\frac{D}{N}$ or ρrd (in re-scaled variables) where the parameter ρ is a measure of the average number of effective contacts per unit of time between drinkers and temporarily recovered individuals. This nonlinear process assumes that R and D individuals (as well as S-individuals) share the same environments.

From the analysis of the "drinking-free" equilibrium, that is, the state where drinking is not part of the culture, we compute the model's basic reproductive number

$$\mathcal{R}_0 = \frac{\beta}{\mu}$$

which corresponds to the case when, $\phi = 0$ (no treatment). $\mathcal{R}_0$ is the number of secondary cases generated by a "typical" regular drinker in a non-drinking population, that is, a population where problem drinkers are so rare that their numbers are "insignificant" and where treatment is not available. That is, $\mathcal{R}_0$ is computed in the situation when the R-class does not exist.

$\mathcal{R}_0$ measures the growth of drinking behaviors per generation and is the product of the average D-residence time, namely $\frac{1}{\mu}$ ("infectious" window) and the D-transmission rate β. It is worth noting that $\mathcal{R}_0$ decreases if either $\frac{1}{\mu}$ (average drinking "life-span") or β (transmission rate) or both decrease.

The basic reproductive number with recovery is given by

$$\mathcal{R}_\phi = \frac{\beta}{\mu + \phi},$$

with $\mathcal{R}_{\phi=0} \equiv \mathcal{R}_0$. In this case, the SD model dynamics are well known. In fact, if $\mathcal{R}_0 < 1$ then the introduction of any number of drinkers does not result in the

Table 8.1: Description of parameters and parameter distribution functions. All rates are *per-capita*.

Parameters	Description	Min	Max	Median	Std	Distribution Function
β	transmission rate	0.0012	1.3	0.6434	0.3710	$Unif(0.001, 0.4)$
ρ	relapse rate	0.0001	0.5	0.2553	0.1437	$Unif(0.5, 1)$
ϕ	recovery rate	$5.43e^{-4}$	0.4646	0.1033	0.0736	$Beta(a = 2, b = 15)$
μ	departure rate	$5e^{-8}$	$3.39e^{-4}$	$3.83e^{-5}$	$5.46e^{-5}$	$exp(5.48e^{-3})$

establishment of a culture of drinking ($D(t) \to 0$ as $t \to \infty$). On the other hand, if $\mathcal{R}_0 > 1$ even the introduction of a single drinker will lead to the establishment of a culture of drinkers ($D(t) \to D^* > 0$ as $t \to \infty$). The results here are not typical. $\mathcal{R}_\phi < 1$ does not guarantee that the "epidemic" will die out. Furthermore, when $\mathcal{R}_\phi > 1$ the "epidemic" takes off and reaches a "permanent" endemic state (i.e., persistence of a regular drinking class over time is guaranteed).

8.2 Population dynamics of drinking under high relapse rates

Here the relationship between recovery (ϕ) and relapse (ρ) rates are explored. Ideally, effective treatments should increase recovery and reduce relapse rates to the extent that an "epidemic" of heavy drinking is reduced or stopped. However, it appears from an analysis of the basic drinking reproductive number (with recovery), $\mathcal{R}_\phi$, that this may be a difficult task. We have the trivial equilibrium (no drinking state) given (in proportions) by $(s^*, d^*, r^*) = (1, 0, 0)$. Positive solutions $(s^* > 0, d^* > 0, r^* > 0)$, that is, solutions where drinking may become established are solutions of the quadratic equation

$$f(d) = d^2 - Bd + C = 0,$$

where $B = 1 - \frac{1}{\mathcal{R}_0} - \frac{1}{\mathcal{R}_\rho}$ and $C = \frac{1}{\mathcal{R}_0}\left[\frac{1}{\mathcal{R}_\rho} - \frac{\beta}{\rho}\right]$ with $\mathcal{R}_\rho = \frac{\rho}{\mu+\phi}$. Two positive solutions d_1^*, d_2^* in $(0, 1)$ exist whenever $B > 0, C > 0$, $f'(1) > 0$ and $B^2 - 4C > 0$. From the definition of C it follows that $C > 0$ whenever $\mathcal{R}_\phi < 1$. The positivity of the discriminant ($B^2 - 4C > 0$) requires the following conditions: $\mathcal{R}_\rho > 1$ and $0 < \mathcal{R}_c < \mathcal{R}_\phi < 1$ ($\mathcal{R}_c > 0$ whenever $\mathcal{R}_\phi < 1$) where

$$\mathcal{R}_\rho = \frac{\rho}{\mu + \phi}$$

Table 8.2: Description of threshold conditions.

Thresholds	Description
$\mathcal{R}_0$	Number of secondary cases generated by a "typical" problem drinker in a non-drinking population.
$\mathcal{R}_\phi$	Basic reproductive number with recovery.
$\mathcal{R}_\rho$	Number of secondary cases generated by a "typical" problem drinker in a population of "temporarily" recovered individuals.
$\mathcal{R}_c$	Critical value to where drinking communities can be under control.

and

$$\mathcal{R}_c = \frac{\rho}{\beta}\left[\frac{1}{1+\frac{1}{\mathcal{R}_0}} - 2\sqrt{\frac{1}{\mathcal{R}_0} - \frac{\mu}{\rho}}\right].$$

If both $0 < \mathcal{R}_c < \mathcal{R}_\phi < 1$ and $\mathcal{R}_\rho < 1$ then drinking dies out. However, whether or not a culture of drinking becomes established ($0 < \mathcal{R}_c < \mathcal{R}_\phi < 1$ and $\mathcal{R}_\rho > 1$) depends on initial conditions (see Figure 8.5c, 8.5d). That is, where the system ends up (including the rapid growth and establishment of a d-class or its elimination) depends on the size of the initial proportion of problem drinkers. In fact, a rapid and large "outbreak" is possible whenever the number (or proportion) of initial drinkers is high. Such an outbreak, the model predicts, will result in the long-term survival of a regular drinking culture despite the fact that $\mathcal{R}_\phi < 1$. Furthermore, in this last case a community of drinkers not only becomes established but may be nearly impossible to eliminate. In fact, parameters must be modified so that the value of $\mathcal{R}_0$ is lower than that of $\mathcal{R}_c$. This result is "unexpected" since the system has in place parameters that represent the effects of highly effective treatment programs (that is, $\mathcal{R}_\phi < 1$). Using current drinking literature pertaining to recovery, relapse and the social interpersonal influences upon drinking behavior [23]-[22], we have estimated several of the parameters necessary to the initial specification of a

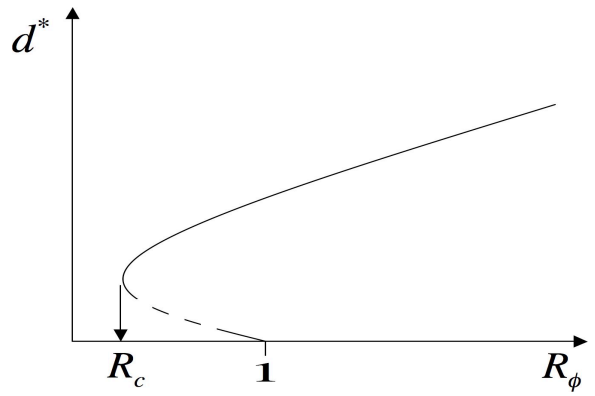

Figure 8.2: Threshold conditions: $\mathcal{R}_c$ and $\mathcal{R}_\phi$.

simple SDR model of drinking behavior (see Table 8.1).

8.3 Uncertainty and sensitivity analysis

The exact measurement of key behavioral and drinking parameters is difficult since precise data pertaining to these are not readily available. Thus, in order to better estimate the impact of variation in parameter ranges on dynamical outcomes, we conduct an uncertainty analysis on $\mathcal{R}_\phi$, $\frac{\mathcal{R}_c}{\mathcal{R}_\phi}$ and $\mathcal{R}_\rho$ (see Table 8.2 for description). We assigned probability distribution functions to each of the parameters (see Table 8.1) in $\mathcal{R}_\phi$, $\frac{\mathcal{R}_c}{\mathcal{R}_\phi}$ and $\mathcal{R}_\rho$ based on our reading of the relevant literature pertaining to the initiation, maintenance and cessation of alcohol use, and proceeded to study their impact on the corresponding $\mathcal{R}_\phi$ and $\frac{\mathcal{R}_c}{\mathcal{R}_\phi}$ distributions.

The level of uncertainty in the model's parameter values is explored via Monte Carlo simulations (based on 1000 realizations). Figures 8.3 and 8.4 show the resulting histograms $\mathcal{R}_\phi$ and $\frac{\mathcal{R}_c}{\mathcal{R}_\phi}$.

$\frac{\mathcal{R}_c}{\mathcal{R}_\phi} < 1$ provides a necessary condition for the possibility of having two drinking steady states ($d_1^* > 0, d_2^* > 0$). In other words, the number of problem drinkers in

the population plays a major role in the "spreading" of the drinking culture and establishment of drinking environments. That is, for any given set of parameter values there is a critical mass of drinkers that can cause the drinking community to grow or disappear. This happens when $0 < \mathcal{R}_c < \mathcal{R}_0 < 1$. Figure 8.4 illustrates the fact that $\frac{\mathcal{R}_c}{\mathcal{R}_\phi} < 1$ using the distributions from Table 8.1 as well as having the two positive "drinking" steady states.

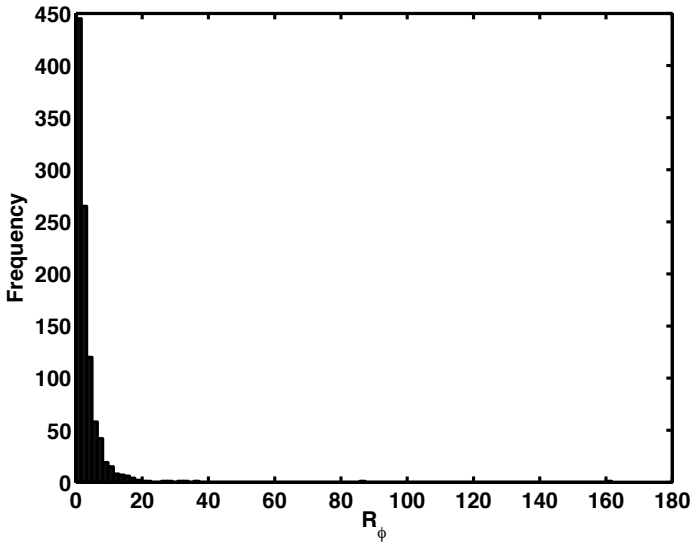

Figure 8.3: Histogram for $\mathcal{R}_\phi$. The mean is 3.12 with a standard deviation of 7.39 and 71% of $\mathcal{R}_\phi > 1$.

The quantities $\mathcal{R}_\phi$, $\mathcal{R}_c$ and $\mathcal{R}_\rho$ are functions of parameters. Here, we analyzed the sensitivity of $\mathcal{R}_\phi$, $\frac{\mathcal{R}_c}{\mathcal{R}_\phi}$ and $\mathcal{R}_\rho$ to parameter variations. Using the partial rank correlation coefficient (PRCC) we determined the qualitative relationship between the parameters and the threshold quantities previously described. The analysis showed that the alcohol recovery rate was the most significant (sensitive) parameter. Furthermore, if ϕ (recovery rate) is not small and the relapse rate ρ is high enough then the situation can actually worsen despite treatment effectiveness. In

Table 8.3: Partial Rank Correlation Coefficient of $\mathcal{R}_\phi$, $\mathcal{R}_\rho$ and $\mathcal{R}_c/\mathcal{R}_\phi$ with their respective p-values.

$\mathcal{R}_\phi$			$\mathcal{R}_\rho$			$\mathcal{R}_c/\mathcal{R}_\phi$		
Parameter	PRCC	p-value	Parameter	PRCC	p-value	Parameter	PRCC	p-value
β	-0.263	0.000	β	—	—	β	-0.085	0.007
ρ	—	—	ρ	-0.673	0.000	ρ	-0.909	0.000
ϕ	0.213	0.000	ϕ	0.079	0.013	ϕ	0.984	0.000
μ	0.066	0.036	μ	-0.031	0.036	μ	0.021	0.500

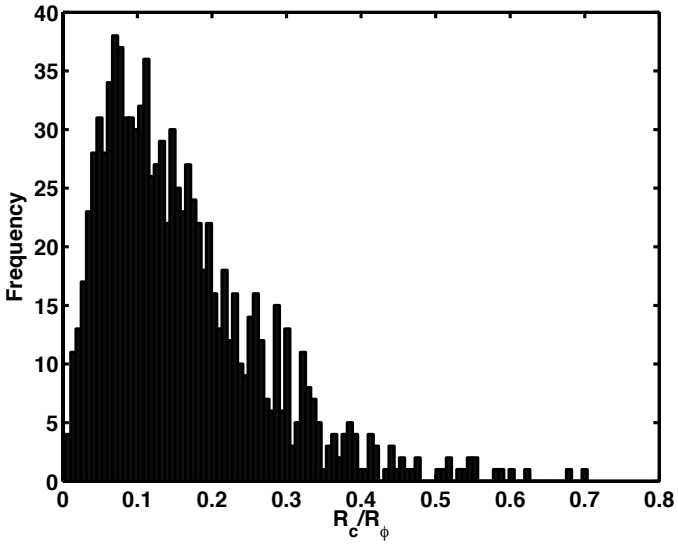

Figure 8.4: Histogram of $\frac{\mathcal{R}_c}{\mathcal{R}_\phi}$. The mean is 0.16 with a standard deviation of 0.11 and the median is 0.14

other words, if both the initial rate of recovery from treatment and the subsequent relapse rate are high this will create a critical mass of vulnerable individuals that can re-enter the problem drinker class. The PRCC value indicates the effect of the parameter in the quantities $\mathcal{R}_\phi$, $\frac{\mathcal{R}_c}{\mathcal{R}_\phi}$ and $\mathcal{R}_\rho$.

From Table 8.3 the transmission rate (β) has a "negative" effect on $\mathcal{R}_\phi$ and $\mathcal{R}_c/\mathcal{R}_\phi$. In other words, it decreases both quantities but it has a greater effect on $\mathcal{R}_\phi$. The relapse rate (ρ) has a "negative" effect on $\mathcal{R}_\rho$ and $\mathcal{R}_c/\mathcal{R}_\phi$. It has a relatively large effect on both quantities, however, the treatment rate (ϕ) has the biggest (positive) effect on $\mathcal{R}_c/\mathcal{R}_\phi$. It increases $\mathcal{R}_c/\mathcal{R}_\phi$. In other words, if $\frac{\mathcal{R}_c}{\mathcal{R}_\phi} > 1$ the drinking community becomes established.

Table 8.4: Estimates of $\mathcal{R}_\phi$, $\frac{\mathcal{R}_c}{\mathcal{R}_\phi}$ and $\mathcal{R}_\rho$ from 10 Monte Carlo simulations.

	$\mathcal{R}_\phi$				$\mathcal{R}_c/\mathcal{R}_\phi$				$\mathcal{R}_\rho$		
Realization	Mean	Std	$\Pr(\mathcal{R}_\phi > 1)$	Realization	Mean	Std	Median	Realization	Mean	Std	$\Pr(\mathcal{R}_\rho > 1)$
1	3.71	22.24	0.72	1	0.1549	0.1079	0.1278	1	3.68	5.56	0.77
2	3.27	7.80	0.70	2	0.1665	0.1166	0.1382	2	4.26	8.43	0.79
3	3.11	6.11	0.69	3	0.1677	0.1145	0.1399	3	4.07	12.22	0.76
4	2.79	3.86	0.70	4	0.1662	0.1133	0.1403	4	3.89	6.13	0.78
5	3.00	4.47	0.73	5	0.1687	0.1168	0.1413	5	4.07	9.98	0.76
6	3.00	7.23	0.70	6	0.1657	0.1161	0.1373	6	4.30	12.23	0.75
7	2.93	4.07	0.69	7	0.1642	0.1149	0.1364	7	3.71	6.74	0.75
8	2.95	4.96	0.71	8	0.1659	0.1130	0.1397	8	4.22	7.58	0.76
9	3.20	6.43	0.73	9	0.1620	0.1115	0.1363	9	3.78	7.53	0.75
10	3.23	6.73	0.72	10	0.1597	0.1094	0.1354	10	3.73	5.74	0.77
Mean	3.12	7.39	0.71	Mean	0.1642	0.1134	0.1373	Mean	3.97	8.21	0.76
SE	0.0812	1.7049	0.0053	SE	0.0042	0.0003	0.0039	SE	0.0771	0.7880	0.0042
CV	0.0823	0.7296	0.0235	CV	0.0255	0.0267	0.0281	CV	0.0614	0.3034	0.0173

8.4 Numerical simulations

Numerical simulations are used to illustrate our model results on drinking dynamics. The most general model can support two positive equilibria (backward bifurcation) when $\mathcal{R}_\phi < 1$, $\frac{\mathcal{R}_c}{\mathcal{R}_\phi} < 1$ and $\mathcal{R}_\rho > 1$ where $\mathcal{R}_\rho = \frac{\rho}{\beta}(1 - \mathcal{R}_\phi)$ with $\rho > \beta$. The probability that $\mathcal{R}_\phi > 1$ is high (see Table 8.4), that is, it is highly likely that drinking becomes established. Individuals who recover then relapse at the total

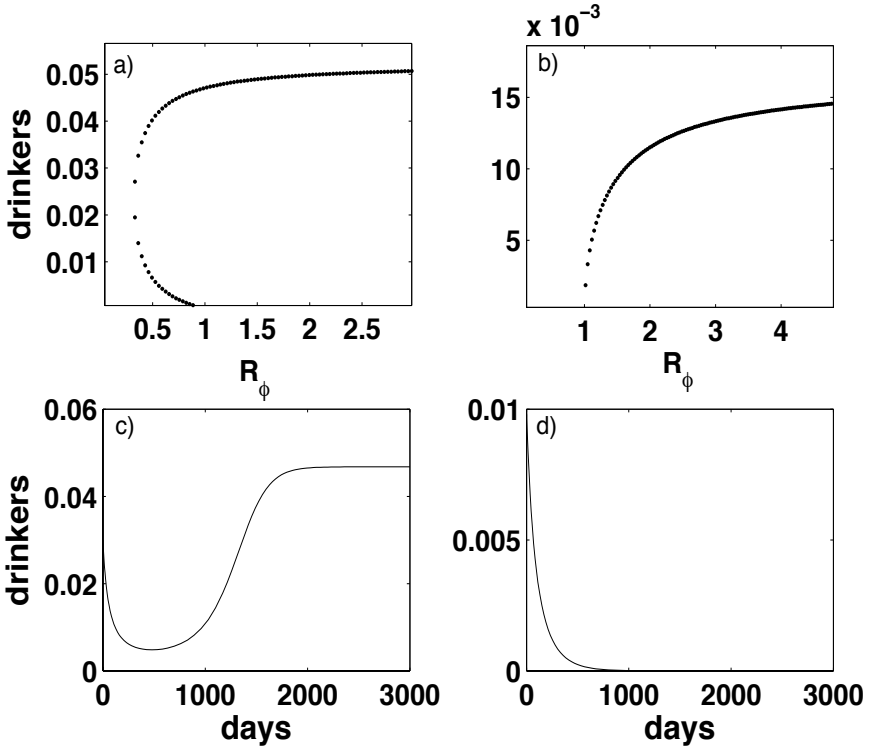

Figure 8.5: Backward bifurcation and time series of the d-class. Parameter values: $\mu = 0.0000548$, $\phi = 0.2$, $\rho = 0.21$ and $\beta = [0.001, 1.3]$. A time series plot of the system with different initial conditions. *Lower left*: $s = 0.97$, $d = 0.03$ and $r_0 = 0$. *Lower right*: $s = 0.99$, $d = 0.01$ and $r = 0$. *Parameter values*: $\mu = 0.0000548$, $\beta = 0.19$, $\phi = 0.2$ and $\rho = 0.21$.

rate ρdr (nonlinear relapse). If this rate is high, then the probability that we enter the region ($\mathcal{R}_\phi < 1$ and multiple positive steady states) where the development of successful treatment programs is unlikely is increased. This implies that once a drinking culture is established it is difficult to bring it to a low enough level to completely eliminate it. As soon as a drinking culture is established, the effectiveness of treatment (ϕ) becomes a critical factor in limiting and curtailing its influence. High rates of recovery with high relapse rates will not affect reductions in problem drinking. In fact, a new pool of high-risk "susceptible" previous problem drinkers can become part of such a drinking community and problem drinking become difficult to eradicate.

In Figure 8.5a) we illustrate a backward bifurcation where drinking behavior can become quickly established and getting it under control would require a tremendous effort ($\mathcal{R}_c = 0.33$). We used a range of parameter values that allows for the possibility of multiple steady states ($\mathcal{R}_\phi < 1$, $\frac{\mathcal{R}_c}{\mathcal{R}_\phi} < 1$ and $\mathcal{R}_\rho > 1$). In the case in which recovery and relapse rates are equal ($\phi = \rho = 0.2$), $\mathcal{R}_\phi < 1$ is a sufficient condition to bring the drinking culture under control (Figure 8.5b).

The number of initial problem drinkers introduced in the population play a crucial role in the establishment of the drinking community. Figure 8.5c illustrates the role of initial conditions (initial number of occasional and moderate drinkers, problem drinkers and recovered individuals) in the presence of two drinking endemic states (a backward bifurcation). Setting the initial parameter for problem drinkers within the population at just 3% is sufficient to establish a community of drinkers. Such a situation might occur, for example, when a new class of freshmen arrive at college. The critical proportion of problem drinkers may determine whether or not a drinking culture becomes endemic (established) even under un-

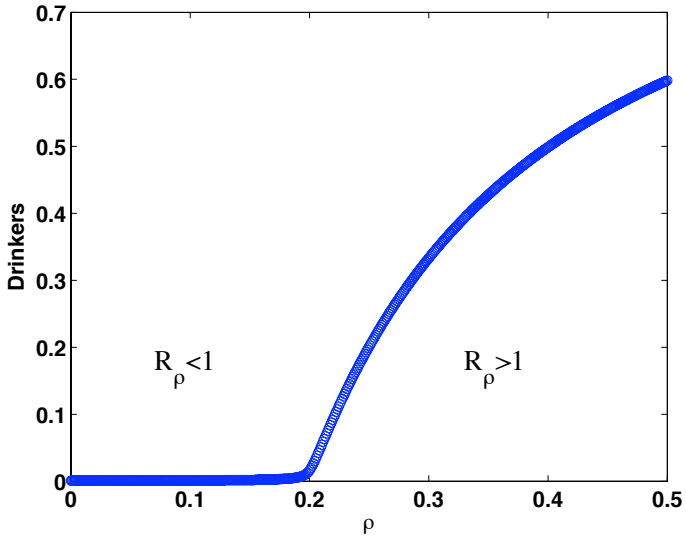

Figure 8.6: Problem drinkers (D) vs. ρ. *Parameters:* $\beta = 0.5$, $\phi = 0.2$, and $\mu = 0.0000548$. *Initial conditions:* $s_0 = 0.99$, $d_0 = 0.01$, and $r_0 = 0$.

favorable conditions ($\mathcal{R}_\phi < 1$). In contrast, when we start with less than 3% of the population as problem drinkers then the drinking community is "eliminated" (see Figure 8.5d). In Figure 8.6 we can see a phase transition that occurs as the relapse rate (ρ) increases and becomes larger than the treatment rate (ϕ). This phase transition is correlated with the quantity $\mathcal{R}_\rho$. When the number of secondary conversions from the temporarily recovered population is bigger than one the proportion of problem drinkers increases. In contrast, in Figure 8.7 we observe the opposite. As the treatment rate (ϕ) increases the proportion of problem drinkers decreases. This happens as the treatment of problem drinkers becomes more effective the number of secondary cases starts decreasing ($\mathcal{R}_\phi < 1$) and the proportion of problem drinkers decrease. In the case where the "conversion" rate (β) (see Figure 8.8) is varied the proportion of problem drinkers stays at zero until it crosses $\beta = 0.19$. This occurs when $\mathcal{R}_\phi = 1$.

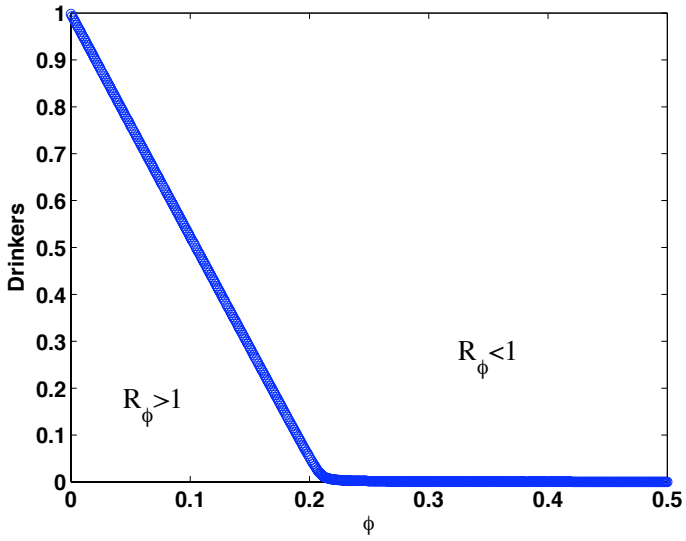

Figure 8.7: Problem drinkers (D) vs. ϕ. *Parameters:* $\beta = 0.5$, $\rho = 0.21$, and $\mu = 0.0000548$. *Initial conditions:* $s_0 = 0.99$, $d_0 = 0.01$, and $r_0 = 0$.

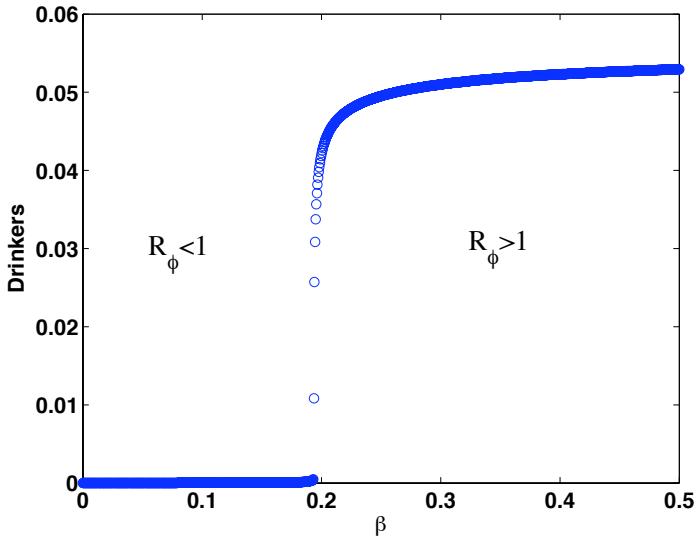

Figure 8.8: Problem drinkers (D) vs. β. *Parameters:* $\rho = 0.21$, $\phi = 0.2$, and $\mu = 0.0000548$. *Initial conditions:* $s_0 = 0.99$, $d_0 = 0.01$, and $r_0 = 0$.

8.5 Conclusions

We introduced a simple mathematical model to describe the dynamics of drinking behaviors generated from contacts between individuals in drinking environments. This simple model, despite its limitations, has generated some useful insights. $\mathcal{R}_\phi$, the basic reproductive number (as a function of treatment), is not always the key. In fact, in situations where recovery and relapse rates are high $\mathcal{R}_\phi < 1$ does not guarantee the successful elimination of drinking from the population. High relapse rates will occur when treatment programs only have short-term positive effects.

Model results and analyses show that the propagation of drinking behaviors is the result of two conversion processes: s to d as determined by $\mathcal{R}_\phi$ and r to d. Furthermore, in contrast to classic epidemiology, outbreaks (sudden growth in the number of problem drinkers) are possible when $\mathcal{R}_\phi < 1$. In this last situation, initial conditions play an essential role on the establishment of drinking communities. The case $\mathcal{R}_\phi < 1$ and $\mathcal{R}_\rho > 1$ is enhanced by intervention programs with high relapse rates. Under this scenario the control of problem alcohol use via treatment may be extremely difficult. It may be more effective to try to limit the average resident times of s-individuals in drinking environments (i.e., the average time they spend in places in which alcohol is available and drinking is commonplace). Indeed, this may be the most efficient way to proceed until treatments with more sustained effects are identified and widely implemented.

Chapter 9

Drinking model in a small-world network and a Markov chain model

9.1 Small-world networks

The fact that several processes (like drinking) are highly dependent on the contact of individuals on a given population has driven theoreticians to the study of epidemics on networks. Initially, most studies have been carried out using distinct static network structures [25, 24]. These graphs (networks) were brought to light by the work of Erdős and Rényi in the $1960's$ [5].

In 1998 Watts-Strogatz introduced an algorithm that generates small-world networks. The algorithm constructs a one-dimensional ring lattice of N nodes connected to its $2k$ (k=average number of connections) nearest neighbors. With probability p some edges are selected and "rewired" to a randomly selected node. The algorithm prevents two nodes from having more than one edge running between them, and there cannot be self-connections from the nodes in this lattice [38].

These type of networks were classified by the level of randomness (clustering) which is modeled by p. A regular network has a value of $p = 0$. Every node in the network is connected to its nearest two neighbors (to the right and left, $k = 2$). In a random network which has $p = 1$, every node has equal probability to be connected to any node in the network.

The novelty of their work came from the fact that having a small number of randomly connected nodes ($p \simeq 0.01$) reduces the distance between any two nodes in the network. For our purposes, this facilitates the spread of drinking behavior.

These type of networks have shown to support high levels of clustering. Networks having these two characteristics (clustering and short average distance between nodes) are known as the small-world effect, a phenomena that has been observed in various social and other networks [38].

9.2 Drinking behavior on small-world networks

If nodes represent individuals in the population and the edges describe their contacts with other individuals then epidemics on networks can be used to evaluate the role of contact/social structure in the spread of drinking behavior.

In this setting, individuals can be in one of three distinct states: susceptible (light drinker), drinkers ("problem" drinker), and "temporarily" recovered (SDR). A susceptible individual in contact with a "problem" drinker (D) may become a "problem" drinker with probability βD where β is the risk of "infection" per unit time. In the same way, problem drinkers can recover with probability ϕ where $\frac{1}{\phi}$ is the average time spent in the "problem" drinking class. After recovery, former drinkers (R) can relapse into the "problem" drinking class with probability ρD. Note that this probability assumes that former drinkers (R) relapse via contacts with "problem" drinkers (D) (see Figure 9.5 for transition probabilities). Five nodes were predetermined to be "problem" drinkers and chosen from the network uniformly at random. In all cases throughout this section we averaged 30 realizations over a period of 10^4 units of time and 52 values of the disorder parameter p. In Figure 9.1 we determined the mean final size of the spread of drinking behaviors for $p = 0$ and $p = 1$, i.e., very few random connections and connections completely random, respectively. The final size is almost the same for both values of p.

In Figure 9.2 we do the same tests but there is a significant difference in the final

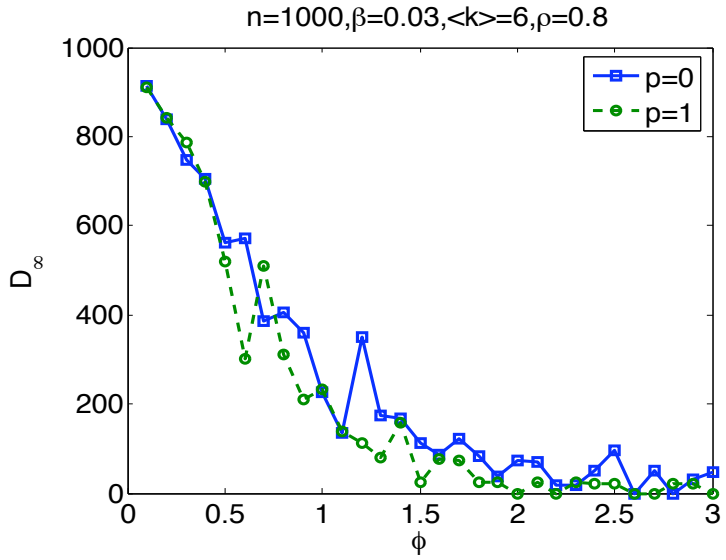

Figure 9.1: Mean final size of the "problem" drinking population with 1000 nodes, $\langle k \rangle = 6$, $\beta = 0.03$ and $\rho = 0.8$ as a function of the treatment rate ϕ for two extreme values of p (disorder parameter).

size of the drinking community. When $p = 1$ the community becomes established at the highest prevalence level (on average between 40% and 55%). From Figure 9.3 we observe that the population of problem drinkers oscillates between 300 and 600 with not much fluctuation for all values of p (disorder parameter). In other words, the structure of the network does not play a role in the "spread" of the drinking behavior. Few random connections have the same effect as the probability of having many random connections being high. This leads to the conclusion that the system is robust for a particular parameter range, that is, when the relapse rate (ρ) is larger than the treatment rate (ϕ), i.e., treatment is not effective. We also computed histograms from extreme values of p (0 ad 1). See Figure 9.7. Figures 9.6, 9.7, we show different distributions for the cases previously discussed of "problem" drinkers for two values of the disorder parameter p.

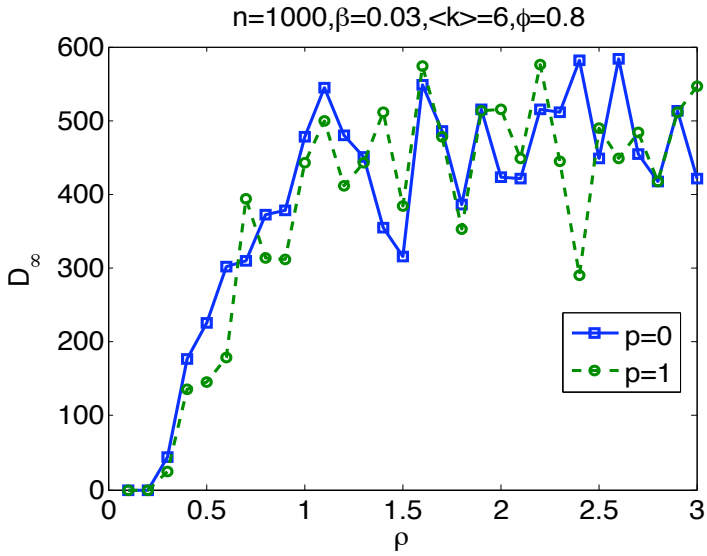

Figure 9.2: Mean final size of the "problem" drinking population with 1000 nodes, $\langle k \rangle = 6$, $\beta = 0.03$ and $\phi = 0.8$ as a function of the relapse rate ρ for two different values of p (disorder parameter).

9.3 Conclusions

In this study, we look at the role of social structure on drinking dynamics. The setting is provided by networks parametrized via a disorder parameter "p". For $p = 0$, we have a situation where individuals only interact "locally", that is, only with the nearest neighbors while when $p = 1$ they interact with everybody in the network.

It is not surprising to see that drinking dynamics are enhanced when $p = 1$. On the other hand, it is surprising to see that network structure does not significantly impact population drinking levels.

In addition, in this section we explored the role of varying the treatment rate (ϕ) and the relapse rate (ρ) for two different values of the disorder parameter ($p = 0$

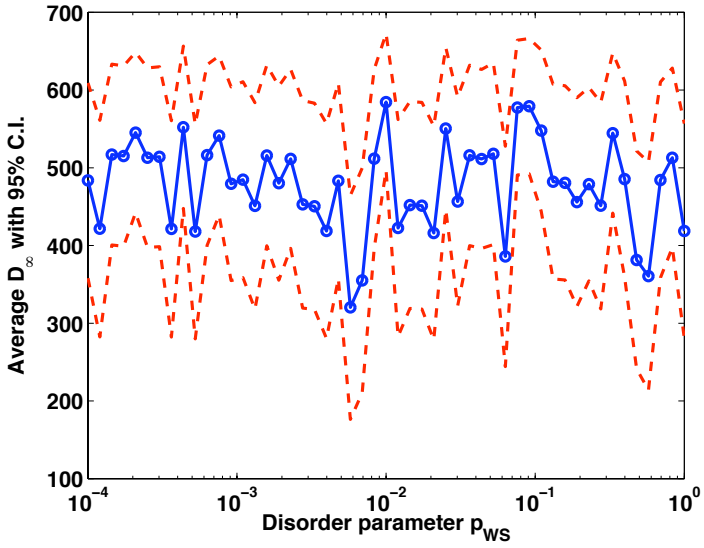

Figure 9.3: Mean final size of the "problem" drinking population with 10^3 nodes and $\langle k \rangle = 3$ as a function of the disorder parameter p. *Parameter values:* $\beta = 0.03$, $\rho = 3$, and $\phi = 0.8$.

and $p = 1$). In the case of ϕ we find that network structure has no effect on the final size of the drinking community. However, as the treatment rate increases (more effective treatment) the final size of the drinking community decreases regardless of network structure for a fixed relapse rate ($\rho = 0.8$).

In the case of the relapse rate (ρ), the final size of the drinking community is not affected by network structure. Moreover, as the relapse rate (ρ) increases the final size of the drinking community also increases for a fixed treatment rate, $\phi = 0.8$.

In Figure 9.3 the relapse rate is larger than the treatment rate ($\rho = 3, \phi = 0.8$), i.e., ineffective treatment. The drinking community is established at around 50%. Network structure does not impact the size of the drinking community. In Figure 9.4 the treatment rate is larger than the relapse rate ($\phi = 0.8, \rho = 0.4$), i.e., effective

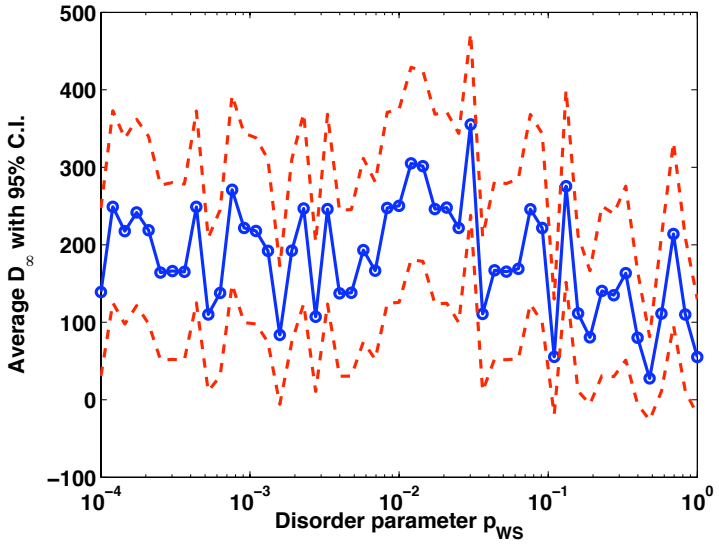

Figure 9.4: Mean final size of the "problem" drinking population with 10^3 nodes and $\langle k \rangle = 3$ as a function of the disorder parameter p. *Parameter values:* $\beta = 0.03$, $\rho = 0.4$, and $\phi = 0.8$.

treatment. The drinking community is established at around 20%. Despite the fact that network structure does not impact the size of the drinking community, an effective treatment program can lead to the decrease of the final size of the drinking community.

In our study we find that for large relapse rates the prevalence of the drinking community is high and it is very difficult to reduce. Effective treatment rates are necessary to control and reduce the prevalence of drinking communities.

Also, our simulations show that the number of long-distance connections do not play a significant role in the establishment and maintenance of such communities.

Treatment programs must develop individual follow-up programs designed to keep vulnerable individuals from relapse into drinking. Clearly, there are some issues that need to be addressed (economics) and many well established treat-

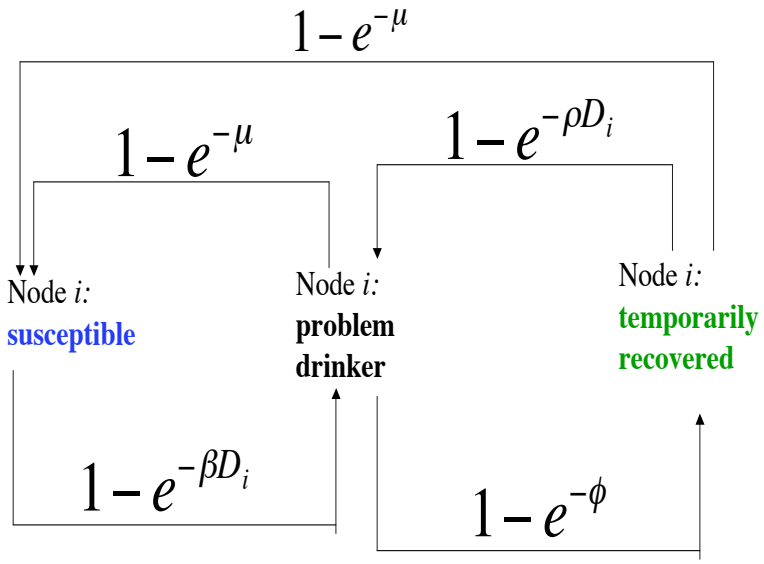

Figure 9.5: Diagram of transition probabilities.

ment facilities that need to re-evaluate their traditional sometimes non-effective programs.

9.4 Drinking behavior: a continuous Markov chain approach

In this section we look at the stochastic version of the simple SDR model described in Chapter 8 (see [31]) using a continuous time Markov chain model. We are particularly interested in explaining the role of stochasticity on the backward bifurcation region and compare it to its deterministic counterpart [2]. We showed that the mean of the stochastic realizations and the deterministic model match. We compute final size distributions at a fixed time horizon for $\mathcal{R}_\phi < 1$ and $\mathcal{R}_\phi > 1$.

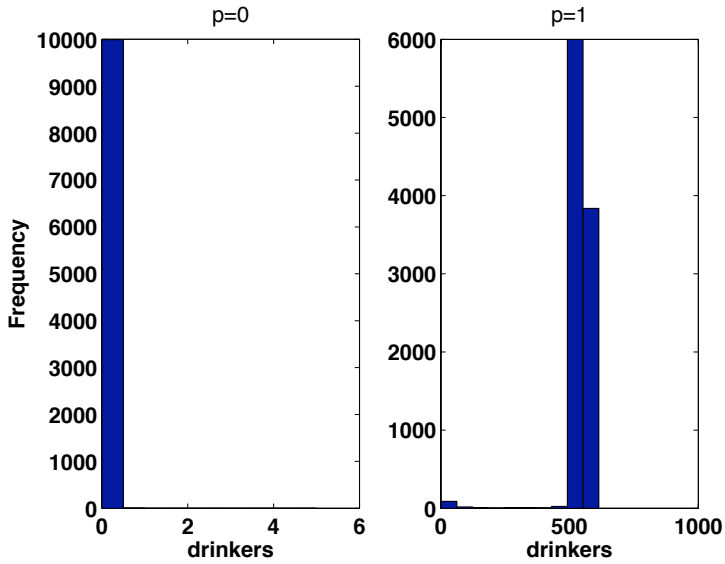

Figure 9.6: Histograms of the "problem" drinking population for two values of p when $\rho = 0.4$, $\phi = 0.8$, $\beta = 0.03$ and $\mu = 0.0000548$.

9.5 Methods

We describe the dynamics of drinking within the context of the classic SIR epidemiological framework [6]. The population in question is divided into the following drinking classes: occasional and moderate drinkers (S); problem drinkers or "infectious (D); and temporarily recovered (R). It is assumed that the population size remains constant, that is, that the time scale of interest is such that the total population size does not change significantly over the length of the study. New recruits join the population as occasional and moderate drinkers (S) and mix at random (i.e., homogeneous mixing) with the rest of the members of the population.

The rate of conversion from the susceptible state (occasional drinker) to the regular drinking state is assumed to be proportional to the size of the susceptible population, the likelihood of interacting with a randomly selected drinking partner

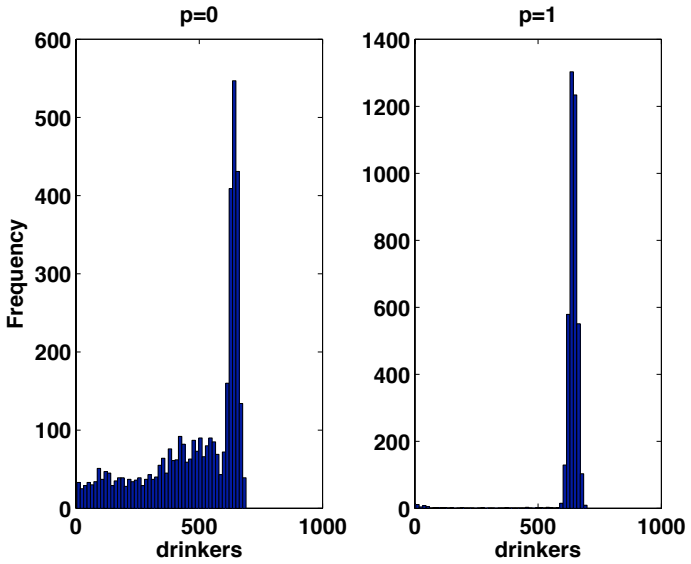

Figure 9.7: Histograms of the "problem" drinking population for two values of p when $\rho = 3$, $\phi = 0.8$, $\beta = 0.03$ and $\mu = 0.0000548$.

and the magnitude and intensity of contacts. The rate of relapse is the result of similar forces that involve contacts between R and D individuals.

Here, we looked at the SDR model using a stochastic Markov chain model.

Setup. We divide the model into events that can occur and assign rates to these events. These events are placed in a vector (*[birth S-dead S-D D-dead D-R R-dead R-D]*). There vector *state* contains the random variables t, S, D and R that will contain all the simulation data. All parameters and initial conditions are fixed and the number of realizations is established. Here, we carry out 100 realizations.

Model transitions. Individuals can be in one of three states: susceptible (S), drinkers (S) and recovered (R). A susceptible individual in contact with a drinker (D) may become a drinker at the rate $\beta SD/N$ where β is the transmission rate. Drinkers can "recover" at the rate ϕD where $\frac{1}{\phi}$ is the average time spent in the drinking class. After recovery, former drinkers (R) can relapse into the drinking

Table 9.1: SDR drinking network model. $\mathcal{D}_i$ denotes the number of *"problem" drinker* neighbors of node i.

transition	probability of transition
node i changes from *susceptible* into *"problem" drinker*	$1 - \exp(-\beta \mathcal{D}_i)$
node i changes from *"problem" drinker* into *"temporarily" recovered*	$1 - \exp(-\phi)$
node i changes from *"temporarily" recovered* into *"problem" drinker*	$1 - \exp(-\rho \mathcal{D}_i)$

class at the rate $\rho RD/N$. Note that these rates become conditional probabilities after the vector that contains them is divided by the sum of all the rates.

Procedure. The process starts once all the probabilities for each event are determined and the parameters and initial conditions are set. The stochastic process runs until the pre-determined time or when there are no more drinkers (D) or recovered (R).

9.6 Numerical simulations

We explore and compare the mean of the distribution from a Markov chain model built from the same rates used to construct the deterministic version of the SDR model. The dynamics of the simple deterministic model "match" the mean dynamics of the stochastic model. However, there are differences. When $\mathcal{R}_\phi < 1$ a number of the stochastic realizations go to zero while others generate drinking communities (endemic states) over a fixed time horizon.

In the deterministic case for specific parameter ranges and when $\mathcal{R}_\phi < 1$ we can have an endemic state (backward bifurcation effect).

The SDR model supports multiple steady states when $\mathcal{R}_{critical} < \mathcal{R}_\phi < 1$ [31].

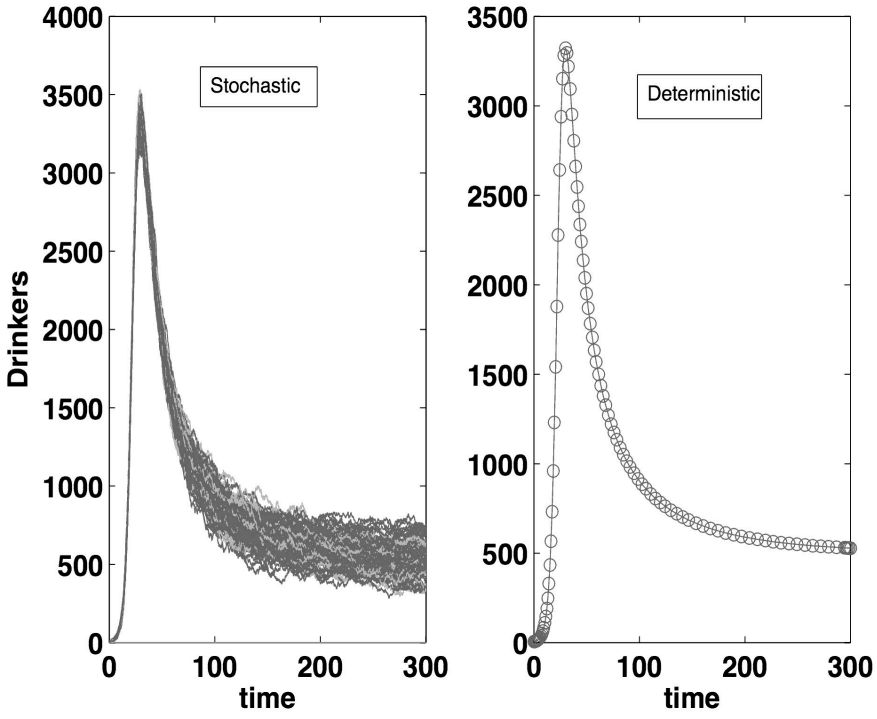

Figure 9.8: *Left.* Stochastic version of SDR model (100 realizations). *Mean*= 507. *Right.* Deterministic version of SDR model. For these simulations the parameters used were: $\beta = 0.5$, $\rho = 0.21$, $\phi = 0.1$ and $\mu = 0.0000548$ with $\mathcal{R}_\phi = 5$. We started with five drinkers ($D_0 = 5$). *Mean*= 528.

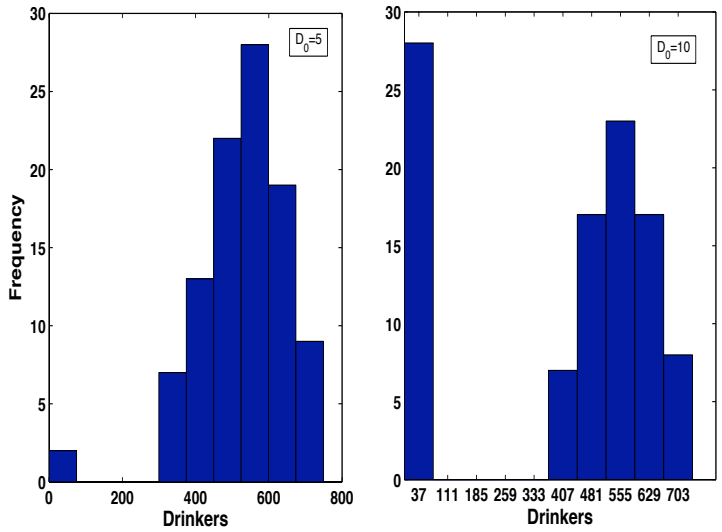

Figure 9.9: From the stochastic simulations we computed a histogram of the final size of the drinking population at a stoppage time $T = 300$. *Initial conditions: left:* $d_0 = 5$, *right*: $d_0 = 10$. $\mathcal{R}_\phi > 1$.

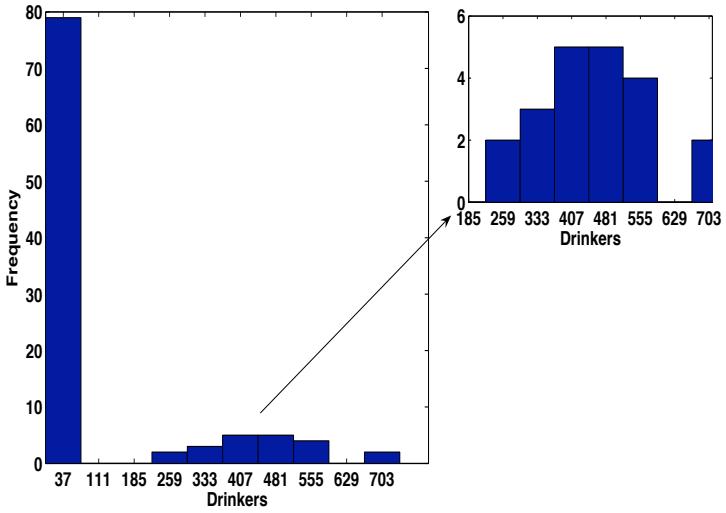

Figure 9.10: From the stochastic simulations we computed a histogram of the final size of the drinking population at a stoppage time $T = 2000$. To the right is a zoom of the histogram without the zeros. In this case $\mathcal{R}_\phi < 1$.

9.7 Conclusions

Drinking is easily established in different communities by the presence of restaurants, clubs, social gatherings, bars, etc. We explored a simple network model that takes into account a heterogeneous contact structure. We look at the effect of short and long distance connections between individuals and how they help establish or diminish drinking communities.

In the case when we have a backward bifurcation (multiple prevalent states) we find that once drinking communities are established it is difficult to eradicate them if there are enough problem drinker in the population.

A stochastic model was built to determine the validity of the simple deterministic model using its counterpart stochastic version and allowing for perturbations (stochasticity). Two cases were studied, $\mathcal{R}_\phi > 1$ and $\mathcal{R}_\phi < 1$, albeit the relevant one is when $\mathcal{R}_\phi > 1$.

From the simulations (preliminary results) we were able to match the deterministic model to the stochastic. We computed final size histograms for specific stoppage times.

This is the beginning part of this study and further cases are being sought and simulations are being conducted. Preliminary simulations show that varying the relapse rate (ρ) affects the prevalence of the drinking community which is agrees with our previous results in Section 8.4 and 8.8.

This model can be used to create generic datasets and use them in the simple deterministic model. Also, note that these simulations are computationally expensive.

Chapter 10

Effects of local and global alcohol consumption networks on drinking dynamics

Drinking is often tied into socially adaptive environmental conditions [20, 19, 21]. Environments can facilitate drinking behaviors. How frequently do individuals find themselves as temporary residents of these environments? and What is the impact of visits to these environments on their long-term drinking behavior? These are some of the questions that fit within the overall theoretical framework presented here. We hope that this framework can shed some additional insights that facilitate our understanding of these issues. Here, we explored the impact of "local" and "global" environments on drinking behavior, frequency and intensity and longevity. These questions are explored through the construction of a population level mathematical framework that assumes drinking is promoted via "contacts" in "local" and "global" environments.

10.1 Mean field example

In order to illustrate our approaches, we introduce a "mean" field model for the dynamics of the "spread" of drinking. The introduction of the setting uses specific assumptions and a selected level of complexity but from the process it should be clear that a great number of possible scenarios can be using a similar modeling approach. We look at drinking as an environmental and population driven process.

Here, our model divides the population into four "drinking" classes: abstainers, occasional, moderate and heavy drinkers. The definitions use to characterize these states are:

a) Abstainer (very low-risk drinker) - fewer than 12 drinks in a year, no more than 2 per day.

b) Occasional drinker (low-risk drinker) - 1 to 13 drinks per month and no more than 2 per day.

c) Moderate drinker (medium-risk drinker) - 4 to 14 drinks per week and no more than 2 at once.

d) Heavy drinker (high-risk) - drinks more than 2 drinks per day.

Moderate drinking is the "universal" threshold associated with "safe drinking". A drink is defined as $10cc$ of alcohol (12oz. regular beer, 5oz. glass of wine, or shot 1.5oz. 80-proof distilled spirits [13]).

The model includes drinking interactions at multiple levels. The identification of what these levels are depends on the question. For example, it may include local (bars and social activities, where non-drinkers and drinkers are assumed to interact in their own "neighborhood") and global activities (interactions outside own "neighborhood" like downtown bars) where individuals from all neighborhoods place themselves in drinking environments (nightclubs, discotheques, sport events, etc.). Here, the term "neighborhood" is define as the "space" reserved for local interactions. Additional possible interpretations are easily concocted. The population is divided into n neighborhoods. For simplicity, each neighborhood is assumed to be composed of two types of individuals "homebody" and "social". Homebody individuals are those individuals who mostly interact in local drinking

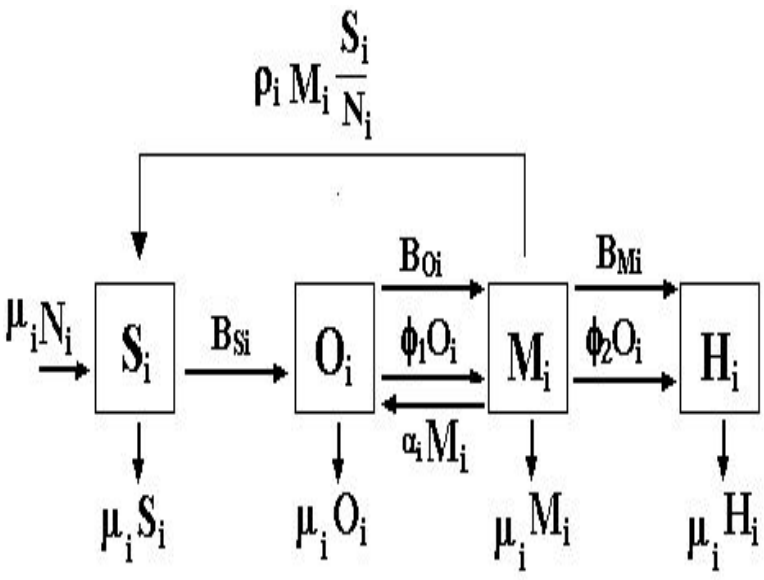

Figure 10.1: Caricature of the model.

environments. Social individuals have no boundaries. Individuals become part of drinking environments when they spend a "regular" amount of time in "local" or "global" activities that involve drinking. *Heterogeneity* in participation is modeled via average "neighborhood" activity (drinking) levels. Individuals are assumed to "budget" their social contacts (scaling parameter) in direct proportion to the time that they spend in drinking environments, etc. Individuals are assumed to "progress" towards higher levels of drinking via two routes: "promoting" social interactions (modeled by contacts between individuals of the various "drinking" classes) or through longevity in each drinking class (like aging). In other words, it is assumed that individuals may "influence" others in their social environments. The relative influence scale used here assumes that abstainers and occasional drinkers may be influenced only by moderate drinkers while moderate drinkers are only influenced by heavy drinkers. Heavy drinkers are assumed not to be influenced by anyone. It is assumed that low-risk drinkers (abstainers and occasional drinkers)

do not interact with others outside their local drinking neighborhood while moderate drinkers can be influenced by moderate drinkers and heavy drinkers from all neighborhoods. In other words, we implicitly assume that the proportion of abstainers and occasional drinkers who visit a "pure" drinking environment is negligible. All the above assumptions reduces model complexity and the limits of their validity can be tested, at least, numerically.

The introduction of this "simple" model immediately raises many challenges. How do we define an *effective contact* (average number of contacts per unit of time required for promotion into the next level)? Here, rather than explicitly defining the concept of contact, we will tend to think of such a parameter as a "fitting" parameter. Hence, the average contact rate of a particular group will be a measure of how much more or how much less active is this group in relation to all other groups. Variability in behaviors (time spent in local is global drinking environments) will be modeled not only by differential average group contact rates but also by differential resident times in each environment. The time a moderate or heavy drinker spends on its neighborhood or in a "pure" drinking place are given by $\omega_i = \tau_i/(\tau_i + \sigma_i)$ and $\psi_i = \sigma_i/(\sigma_i + \tau_i)$ respectively. Parameters and parameter descriptions are given in Table 10.2.

Table 10.1: Sub population and classes. i is the neighborhood index.

State Variables	Description
N_i	total population of neighborhood i
S_i	abstainers or non-drinkers from neighborhood i
O_i	occasional drinkers from neighborhood i
M_i	moderate drinkers from neighborhood i
H_i	heavy drinkers from neighborhood i

Table 10.2: Parameters. i is referred to the index of a neighborhood.

Parameters	Description
μ	natural mortality rate
β_i	transmission rate per contact (S_i and O_i)
λ_i	transmission rate per contact (M_i)
a_i	average number of social contacts of low-risk drinkers per unit time
b_i	average number of social contacts of high-risk drinkers per unit time
τ_i	rate at which a drinker goes to a "pure" drinking place
σ_i	rate at which a drinker leaves a "pure" drinking place
ϕ_1	rate at which an occasional drinker is predisposed to drinking and becomes a moderate drinker
ϕ_2	rate at which a moderate drinker is predisposed to drinking and becomes a heavy drinker
ρ_i	recovery into the abstainer class S_i
α_i	recovery into the low-risk class O_i
$\frac{\tau_i}{\tau_i+\sigma_i}$	fraction of time a drinker spends on a "pure" drinking place
$\frac{\sigma_i}{\sigma_i+\tau_i}$	fraction of time a drinker spends on neighborhood i

The highest modeling difficulty comes from our attempts to model the interactions between individuals of the same and different neighborhoods. Mathematical and theoretical epidemiologists have spent considerable amount of time addressing this problem [4, 7, 9]. Here, it is assumed that contacts are "frequency" dependent with weights provided by the average-activity group levels and appropriate residence times. There are two types of individuals in each neighborhood "social", that is, those who interact with everybody and everywhere and "homebody", that is, those who interact with social and homebody locally. These are some complications since the population is divided into low-risk drinkers and high-risk drinkers and high risk drinkers are the only ones who interact with drinkers from other neighborhoods. The mixing probabilities are:

1) $P_{b_i,a_i} = \tilde{P}_{a_i} = \frac{a_i(S_i+O_i)}{b_i\omega_i(M_i+H_i)+a_i(S_i+O_i)}\omega_i \rightarrow$ mixing probability between social and homebody individuals from neighborhood i in neighborhood i.

2) $P_{b_i,b_i} = \tilde{P}_{b_i} = \frac{b_i\omega_i(M_i+H_i)}{a_i(S_i+O_i)+b_i\omega_i(M_i+H_i)}\omega_i \rightarrow$ mixing probability between social individuals from neighborhood i in neighborhood i.

3) $P_{b_i,b_j} = P^*_{b_j} = \frac{b_j\tau_j(M_j+H_j)}{\sum_{l=1}^{n} b_l\tau_l(M_l+H_l)}\tau_i \rightarrow$ mixing probability between social individuals from neighborhood i and j in the commonground place.

4) $P_{a_i,a_j} = 0 \rightarrow$ homebody individuals from neighborhoods i and j do not interact.

5) $P_{a_i,b_j} = 0 \rightarrow$ a homebody individual from neighborhood i and a social individual from neighborhood j do not interact assuming $i \neq j$.

Naturally, for each neighborhood the following "conditional probabilities" identities hold:

$$\tilde{P}_{b_i,a_i} + \tilde{P}_{b_i,b_i} + \sum_{j\neq i}^{n} P_{b_i,b_j} = \omega_i + \tau_i = 1.$$

The nonlinear environmental transition progression rate are:

$$\begin{aligned}
B_{S_i}(t) &= \beta_i a_i S_i\Big[\frac{M_i\omega_i}{(S_i+O_i)+\omega_i(M_i+H_i)}\Big],\\
B_{O_i}(t) &= \beta_i a_i O_i\Big[\frac{M_i\omega_i}{(S_i+O_i)+\omega_i(M_i+H_i)}\Big],\\
B_{M_i}(t) &= \lambda_i b_i M_i\Big[\tilde{P}_{a_i}\frac{H_i}{(S_i+O_i)+\omega_i(M_i+H_i)} + \tilde{P}_{b_i}\frac{\omega_i H_i}{(S_i+O_i)+\omega_i(M_i+H_i)} +\\
&\qquad \sum_{j=1}^{n} P^*_{b_j}\frac{H_j}{(M_j+H_j)}\Big].
\end{aligned}$$

Putting all the definitions and assumptions together lead to the "mean field" model given by the following system of nonlinear differential Equations:

$$\begin{aligned}
\frac{dS_i}{dt} &= \mu N_i - B_{S_i}(t) + \rho_i M_i - \mu S_i,\\
\frac{dO_i}{dt} &= B_{S_i}(t) - B_{O_i}(t) + \alpha_i M_i - (\mu+\phi_1)O_i,\\
\frac{dM_i}{dt} &= B_{O_i}(t) + \phi_1 O_i - B_{M_i}(t) - (\rho_i+\alpha_i+\mu+\phi_2)M_i,\\
\frac{dH_i}{dt} &= B_{M_i}(t) + \phi_2 M_i - \mu H_i,
\end{aligned}$$

where $i = 1, ..., n$ and $N_i = S_i + O_i + M_i + H_i$.

For simplicity purposes we now use the following re-scaling variables: $s_i = \frac{S_i}{N_i}$, $o_i = \frac{O_i}{N_i}$, $m_i = \frac{M_i}{N_i}$ and $h_i = \frac{H_i}{N_i}$ which lead to the system below.

1) $P_{b_i,a_i} = \tilde{P}_{a_i} = \frac{a_i(s_i+o_i)}{b_i\omega_i(m_i+h_i)+a_i(s_i+o_i)}\omega_i \rightarrow$ mixing probability between social and homebody individuals from neighborhood i in neighborhood i.

2) $P_{b_i,b_i} = \tilde{P}_{b_i} = \frac{b_i\omega_i(m_i+h_i)}{a_i(s_i+o_i)+b_i\omega_i(m_i+h_i)}\omega_i \rightarrow$ mixing probability between social individuals from neighborhood i in neighborhood i.

3) $P_{b_i,b_j} = P^*_{b_j} = \frac{b_j\tau_j(m_j+h_j)}{\sum_{l=1}^{n} b_l\tau_l(m_l+h_l)}\tau_i \rightarrow$ mixing probability between social individuals from neighborhood i and j in the commonground place.

4) $P_{a_i,a_j} = 0 \rightarrow$ homebody individuals from neighborhoods i and j do not interact.

5) $P_{a_i,b_j} = 0 \rightarrow$ a homebody individual from neighborhood i and a social individual from neighborhood j do not interact assuming $i \neq j$.

$$
\begin{aligned}
B_{s_i}(t) &= \beta_i a_i s_i\Big[\frac{m_i\omega_i}{(s_i+o_i)+\omega_i(m_i+h_i)}\Big],\\
B_{o_i}(t) &= \beta_i a_i o_i\Big[\frac{m_i\omega_i}{(s_i+o_i)+\omega_i(m_i+h_i)}\Big],\\
B_{m_i}(t) &= \lambda_i b_i m_i\Big[\tilde{P}_{a_i}\frac{h_i}{(s_i+o_i)+\omega_i(m_i+h_i)} + \tilde{P}_{b_i}\frac{\omega_i h_i}{(s_i+o_i)+\omega_i(m_i+h_i)} + \\
&\qquad \sum_{j=1}^{n} P^*_{b_j}\frac{H_j}{(M_j+H_j)}\Big].
\end{aligned}
$$

$$
\begin{aligned}
\tfrac{ds_i}{dt} &= \mu - B_{s_i}(t) + \rho_i m_i - \mu s_i,\\
\tfrac{do_i}{dt} &= B_{s_i}(t) - B_{o_i}(t) + \alpha_i m_i - (\mu+\phi_1)o_i,\\
\tfrac{dm_i}{dt} &= B_{o_i}(t) + \phi_1 o_i - B_{m_i}(t) - (\rho_i+\alpha_i+\mu+\phi_2)m_i,\\
\tfrac{dh_i}{dt} &= B_{m_i}(t) + \phi_2 m_i - \mu h_i,
\end{aligned}
\tag{10.1}
$$

where $i = 1, ..., n$ and $s_i + o_i + m_i + h_i = 1$.

10.2 Threshold quantities and simulations

In mathematical epidemiology it is traditional to compute non-dimensional quantities that determine the nature of dynamic transitions.

The basic reproductive number $\mathcal{R}_0$ is defined as: *the average number of secondary cases produced by a "typical" infected (assumed infectious) individual during*

his/her entire life as infectious (infectious period) when introduced in a population of susceptibles.

Let us now outline the role of $\mathcal{R}_0$ on the study of stability of equilibria. Most reasonable epidemic models have at least two equilibria, namely, a disease-free equilibrium and a positive (endemic) equilibrium. Typically one can show that the disease-free equilibrium is locally asymptotically stable (*l.a.s*) if $\mathcal{R}_0 < 1$ and unstable whenever $\mathcal{R}_0 > 1$. In addition, there are extensive examples which show that in fact $\mathcal{R}_0 > 1$ implies the existence of a unique (l.a.s.) endemic equilibrium. It turns out that for many models a transcritical bifurcation occurs when $\mathcal{R}_0$ crosses the threshold $\mathcal{R}_0 = 1$. This is to say, asymptotic local stability is transferred from the infectious-free state to the new (emerging) endemic (positive) equilibrium. Notice that this transfer of asymptotic stability may be sensitive to the choice of initial conditions when there are multiple equilibria.

Let $\mathcal{R}_0^1$ and $\mathcal{R}_0^2$ denote the basic reproductive numbers for neighborhood 1 and 2, respectively. Our method to compute $\mathcal{R}_0^1$ and $\mathcal{R}_0^2$ is oulined in the appendix. We thus obtain,

$$\begin{aligned} \mathcal{R}_0^1 &= \frac{\phi_1\beta_1 a_1\omega_1}{(\mu+\phi_1)\left[(\lambda_1 b_1\tau_1+\phi_2)+(\mu+\rho_1+\frac{\mu\alpha_1}{\mu+\phi_1})\right]} \\ \mathcal{R}_0^2 &= \frac{\phi_1\beta_2 a_2\omega_2}{(\mu+\phi_1)\left[(\lambda_2 b_2\tau_2+\phi_2)+(\mu+\rho_2+\frac{\mu\alpha_2}{\mu+\phi_1})\right]} \end{aligned} \tag{10.2}$$

Now, let us address an interpretation of $\mathcal{R}_0^1$, the interpretation of $\mathcal{R}_0^2$ will be analogous. Consider,

$$\mathcal{R}_0^1 = \frac{\phi_1}{(\mu+\phi_1)}\beta_1 a_1\omega_1 \frac{1}{\left[(\lambda_1 b_1\tau_1+\phi_2)+(\mu+\rho_1+\frac{\mu\alpha_1}{\mu+\phi_1})\right]}$$

The ratio $\frac{\phi_1}{\mu+\phi_1}$ denotes the "system-departure"-adjusted fraction of occasional drinkers that become moderate drinkers without any type of influence from other

drinkers.

Next, $\beta_1 a_1 \omega_1$ denotes the total number of adequate contacts (sufficient contacts to progress to a higher drinking level).

The term $(\lambda_1 b_1 \tau_1 + \phi_2)$ is the contribution to escalate into the the heavy drinking state. On the other hand, we claim that $(\mu + \phi_1 + \frac{\mu\alpha_1}{\mu+\phi_1})$ is an indirect anti-contribution to reach the heavy drinking state. Since, $(\mu + \phi_1)$ is an outflow from the occasional drinking class, which is added to $\frac{\mu\alpha_1}{\mu+\phi_1}$, the fraction that leaves the system from the moderate drinking state passing through the occassional drinking state. In Figure 10.2 we illustrate the case when we have two neighborhoods. We illustrate how reducing the pool of moderate drinkers reduces the *basic reproductive ratio*. In the upper-left corner we have $\lambda_1 = 1/20$, $\lambda_2 = 1/50$. In this case individuals from neighborhood two have a higher transmission ("convincing") rate and the number of moderate drinkers decreases. In this case $\mathcal{R}_0^1 = 6.9$ and $\mathcal{R}_0^2 = 9$ for neighborhood one and two as noted. In the upper-right corner the number of personal contacts moderate drinkers from neighborhood one have. The result is similar, the number of moderate drinkers decreases and the resulting $\mathcal{R}_0^1 = 4.96$ and $\mathcal{R}_0^2 = 9$. In the bottom-left corner the time moderate drinkers spend on outside their own neighborhood is increased, that is, this reduces the possibility of "infecting" local individuals. The resulting $\mathcal{R}_0^1 = 5.37$ and $\mathcal{R}_0^2 = 9$. In the bottom-right corner we increased the time moderate drinkers from neighborhood one spend outside their own neighborhood and the number of personal contacts. In this case $\mathcal{R}_0^1 = 4.2$ and $\mathcal{R}_0^2 = 9$.

Uncertainty Analysis for $\mathcal{R}_0^i$ for $i = 1, 2$. We used a Monte Carlo procedure (simple random sampling) to assess the variability in the reproductive ratios due to the uncertainty in estimating model parameters [32]. We assigned distributions

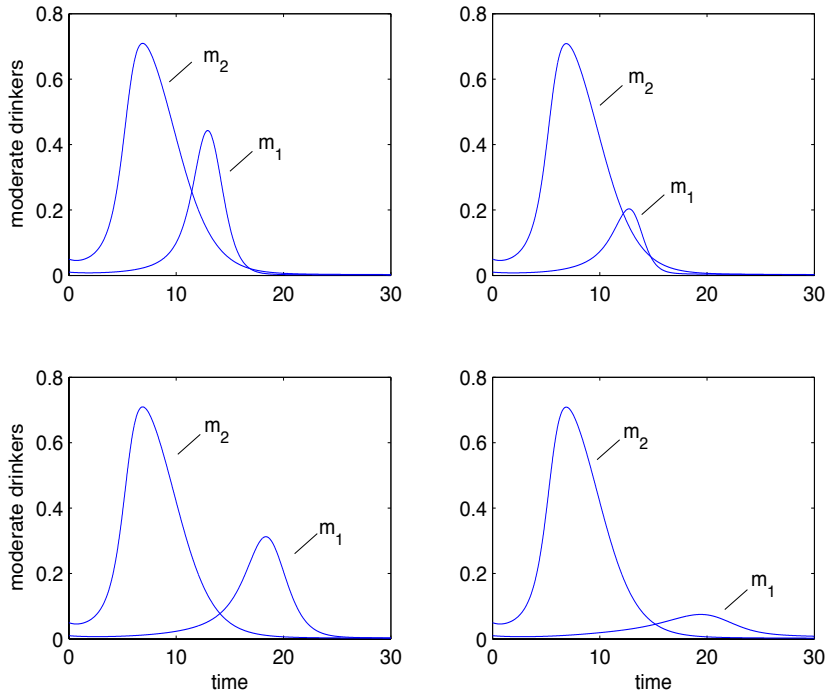

Figure 10.2: Two neighborhoods. *Parameter values:* $\mu = 0.0000548$, $\phi_1 = \phi_2 = 1/30$, $\beta_1 = \beta_2 = 1/5$, $a_1 = a_2 = 15$, $b_2 = 30$, $\tau_1 = \tau_2 = 0.1$, $\rho_1 = 1/5$, $\alpha_1 = 1/30$. *Initial conditions:* $s_0^1 = 0.99$, $o_0^1 = 0$, $m_0^1 = 0.01$, $h_0^1 = 0$, $s_0^2 = 0.95$, $o_0^2 = 0$, $m_0^2 = 0.05$, $h_0^2 = 0$.

to each of the parameters in Table 10.5. The sample size was 10^6. It is assumed that $a_1 > a_2$, $\omega_1 > \omega_2$. Figures 10.3 and 10.4 show the resulting histograms of $\mathcal{R}_0^1$ and $\mathcal{R}_0^2$.

Table 10.3: Estimates of $\mathcal{R}_0^1$ from 10 Monte Carlo simulations.

Realization	Mean ($\mathcal{R}_0^1$)	Median ($\mathcal{R}_0^1$)	IQR ($\mathcal{R}_0^1$)	Pr($\mathcal{R}_0^1 > 1$)
1	49.9	12.7	37	0.913
2	49.8	12.7	36.8	0.913
3	49.6	12.7	36.9	0.913
4	50	12.8	37	0.914
5	49.8	12.7	37	0.913
6	49.6	12.7	36.8	0.913
7	49.9	12.7	37	0.913
8	50.3	12.8	37	0.914
9	49.9	12.7	37	0.913
10	49.8	12.7	36.9	0.913
Mean	49.86	12.72	36.96	0.9134
SE	0.06501	0.009145	0.02109	8.163×10^{-5}
CV	0.004124	0.002273	0.001805	0.000283

Table 10.4: Estimates of $\mathcal{R}_0^2$ from 10 Monte Carlo simulations.

Realization	Mean ($\mathcal{R}_0^2$)	Median ($\mathcal{R}_0^2$)	IQR ($\mathcal{R}_0^2$)	Pr($\mathcal{R}_0^2 > 1$)
1	1.25	0.244	0.835	0.913
2	1.25	0.244	0.833	0.913
3	1.25	0.244	0.835	0.913
4	1.24	0.245	0.836	0.914
5	1.25	0.245	0.833	0.913
6	1.25	0.245	0.834	0.913
7	1.24	0.244	0.835	0.913
8	1.25	0.244	0.836	0.914
9	1.25	0.244	0.835	0.913
10	1.25	0.245	0.838	0.913
Mean	1.248	12.72	0.835	0.2315
SE	0.001578	0.0001226	0.000481	7.316×10^{-5}
CV	0.003998	0.001587	0.001822	0.0009995

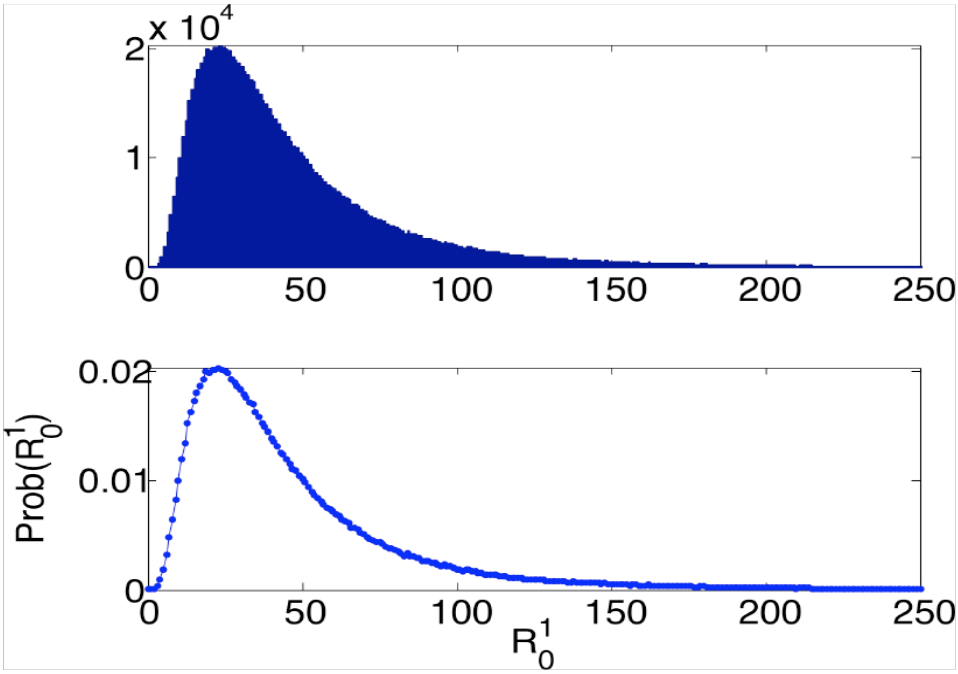

Figure 10.3: Distribution for $\mathcal{R}_0^1$.

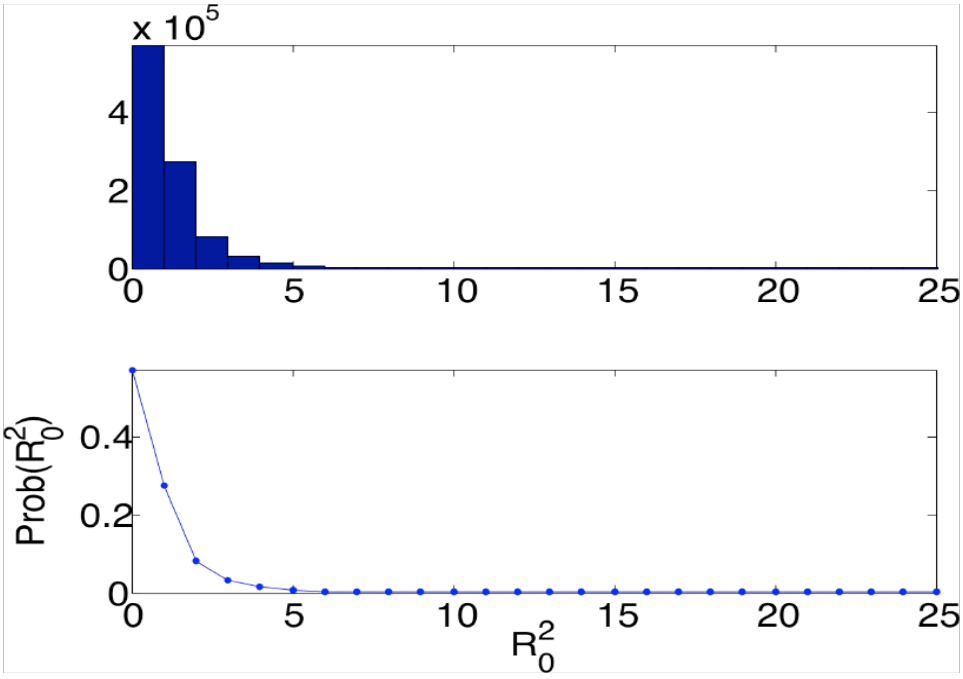

Figure 10.4: Distribution for $\mathcal{R}_0^2$.

Table 10.5: Parameter distributions.

Parameter	Distribution	Parameter	Distribution
a_1	$Poisson(200)$	μ	$Beta(4 \times 10^{-5})$
a_2	$Poisson(15)$	ω_1	$Uniform[0.5, 1]$
α_1	$Uniform[0, 0.5]$	ω_2	$Uniform[0, 0.5]$
α_2	$Uniform[0, 0.5]$	ϕ_1	$UnifDiscrete[0, 28]$
b_1	$Poisson(5)$	ϕ_2	$UnifDiscrete[0, 28]$
b_2	$Poisson(5)$	ρ_1	$Uniform[0, 1]$
β_1	$Exponential(30)$	ρ_2	$Uniform[0, 1]$
β_2	$Exponential(30)$	τ_1	$Gamma[3, 6]$
λ_1	$Exponential(4.6)$	τ_2	$Gamma[3, 6]$
λ_2	$Exponential(4.6)$		

Potential Control Strategies. As we have explained above, $\mathcal{R}_0^1$ and $\mathcal{R}_0^2$ are used as threshold quantities that somehow control the transfer of stability of the "disease-free" into the "endemic" equilibria. In order to keep a population free of alcohol abusive comsuption (heavy drinkers go extinct) we need to favor substantial decreases in $\mathcal{R}_0^1$ and $\mathcal{R}_0^2$. Recall, that if $\mathcal{R}_0^1 < 1$ and $\mathcal{R}_0^2 < 1$ then the disease-free equilibria for both neighborhoods are locally asymptotically stable.

Again, let us focus into $\mathcal{R}_0^1$ since the following results apply analogously to $\mathcal{R}_0^2$. We write,

$$\mathcal{R}_0^1 \frac{\phi_1}{(\mu+\phi_1)} \beta_1 a_1 \omega_1 \frac{1}{\left[(\lambda_1 b_1 \tau_1 + \phi_2) + (\mu + \rho_1 + \frac{\mu\alpha_1}{\mu+\phi_1})\right]}$$

It is clear, that a decrease in $\frac{\phi_1}{(\mu+\phi_1)}$- fraction of occasional drinkers that become moderate drinkers- implies a decrease in $\mathcal{R}_0^1$. Similarly, a decrease in $\beta_1 a_1 \omega_1$- the total number of adequate contacts- will induce a decrease in $\mathcal{R}_0^1$.

Now, let ϕ_1 and α_1 be fixed. Define,

$$F(\mu) = \mu + \phi_1 + \frac{\mu\alpha_1}{\mu+\phi_1}$$

It follows that $F'(\mu) = 1 + \frac{\phi_1\alpha_1}{(\mu+\phi_1)^2} > 0$, which in turn implies that F is an increasing function of μ. Now, fix all other parameters and let μ increase, then $\frac{1}{\left[(\lambda_1 b_1 \tau_1 + \phi_2) + (\mu + \phi_1 + \frac{\mu\alpha_1}{\mu+\phi_1})\right]}$ decreases, which implies that $\mathcal{R}_0^1$ decreases as well.

Let us fix μ, and ϕ_1. Define,

$$G(\alpha_1) = \mu + \phi_1 + \frac{\mu\alpha_1}{\mu+\phi_1}$$

Then, $G'(\alpha_1) = \frac{\mu}{\mu+\phi_1} > 0$, that is, G is an increasing function of α_1. Hence, if one fixes all the other parameters and let α_1 increase, then $\mathcal{R}_0^1$ decreases.

10.3 Conclusions

We have developed a mathematical drinking model that describes the interactions between the classes of drinkers. Our results suggest that the number of personal contacts and the time that a high-risk drinker spends on its own neighborhood have the biggest impact on the reproductive ratio, $\mathcal{R}_0^i$.

The global structure of the model is governed by individuals that meet at other places. In our model only moderate and heavy drinkers leave their neighborhood to interact in the drinking environment outside their neighborhood. The resulting interaction is crucial in determining the number of individuals at risk of becoming a burden to society or to others (family, friends, etc.). If the number of heavy drinkers increases due to this interaction we would have to consider a model that incorporates treatment and its effectiveness.

The local structure of the model plays an important role in the spread of social contagion (drinking behavior). The number of contacts of 'low-risk' drinkers and the time 'high-risk' drinkers spend on their neighborhood is crucial to the growth of the drinking culture.

Our model suggests that the key transition to have an endemic drinking culture is from occasional drinker to moderate drinker. Furthermore, it is seen in the basic reproductive ratio that reducing the progression into the heavy drinking class contributes to the growth of the drinking culture. As a control strategy in our model the focus should be on moderate drinkers.

We observe that reducing the number of low-risk contacts (a_i) can reduce the growth in the drinking communities. Also, individuals at borderline of becoming problem drinkers play a crucial role in spreading the sentiment that drinking is acceptable. However, these drinkers are typically not considered a problem.

BIBLIOGRAPHY

[1] National institute on alcohol abuse and alcoholism (niaaa) of the national institutes of health. http://www.niaaa.nih.gov/.

[2] L. Allen and P. van den Driessche. Stochastic epidemic models with a backward bifurcation. *Mathematical Biosciences and Engineering*, 3(3):445–458, July 2006.

[3] T. Banks and C. Castillo-Chávez, editors. *Bioterrorism*. SIAM Frontiers in Applied Mathematics, 2003.

[4] S. Blythe, S. Busenberg, and C. Castillo-Chávez. Affinity and paired-event probability. *Mathematical Biosciences*, 128:265–284, 1995.

[5] B. Bollobas. Random graphs. *Academic, London*, 1985.

[6] F. Brauer and C. Castillo-Chávez. *Mathematical Models in Population Biology and Epidemiology*, volume 40 of *Texts in Applied Mathematics*. Springer-Verlag, 2001.

[7] S. Busenberg and C. Castillo-Chávez. A general solution of the problem of mixing subpopulations, and, its application to risk and age-structured epidemic models. *IMA J. Math. Appl. Med. Biol.*, 8:1–29, 1991.

[8] C. Castillo-Chávez and Z. Feng. Global stabiliy of an age-structure model for tb and its applications to optimal vaccination strategies. *Mathematical Biosciences*, 151(2):135–154, August 1998.

[9] C. Castillo-Chávez and B. Song. An epidemic model with virtual mass transportation: The case of smallpox in a large city. *In: Bioterrorism*, SIAM Frontiers in Applied Mathematics, 2003.

[10] G. Chowell, C. Castillo-Chávez, P. Fenimore, C. Kribs-Zalet, L. Arriola, and J. Hyman. Model parameters and outbreak control for sars. *Emerging Infectious Diseases*, 10:1258–1263, 2004.

[11] G. Chowell, P. Fenimore, M. Castillo-Garsow, and C. Castillo-Chávez. Sars outbreaks in ontario, hong kong and singapore: the role of diagnosis and isolation as a control mechanism. *Journal of Theoretical Biology*, 224:1–8, 2003.

[12] G. Chowell, N. Hengartner, C. Castillo-Chávez, P. Fenimore, and J. Hyman. The basic reproductive number of ebola and the effects of public health measures: the cases of congo and uganda. *Journal of Theoretical Biology*, 229:119–126, 2004.

[13] M. Dufour. What is moderate drinking? *Alcohol Research & Health*, 23(1), 1999.

[14] J. Epstein. *A theoretical perspective on the spread of drugs*. Westview Press, 1997.

[15] Z. Feng, C. Castillo-Chávez, and A. Capurro. A model for tuberculosis with exogenous reinfection. *Theoretical Population Biology*, 57:235–247, 2000.

[16] B. González, E. Huerta-Sánchez, A. Ortiz-Nieves, T. Vázquez-Alvarez, and C. Kribs-Zalet. Am i too fat? bulimia as an epidemic. *Journal of Mathematical Psychology*, 47:515–526, 2003.

[17] D. Gorman. The failure of drug education. *Public Interest*, 1997.

[18] D. Gorman. *Developmental processes*, volume International Handbook of Alcohol Dependence and Problems. Wiley, 2001.

[19] D. Gorman, P. Gruenewald, P. Hanlon, I. Mezi, L. Waller, C. Castillo-Chávez, E. Bradley, and J. Mezic. Implications of systems dynamic models and control theory for environmental approaches to the prevention of alcohol - and other drug-related problems. *Alcohol Abuse*, 2003.

[20] D. Gorman, P. Speer, P. Gruenewald, and E. Labouvie. Spatial dynamics of alcohol availability, neighborhood structure and violent crime. *Journal of Alcohol Studies*, 62:628–636, 2001.

[21] P. Gruenewald, L. Remer, and R. Lipton. Evaluating the alcohol enviornment: Community geography and alcohol problems. *Alcohol Research & Health*, 26(1), 2002.

[22] P. McEvoy, W. Stritzke, D. French, A. Lang, and R. Ketterman. Comparison of three models of alcohol craving in young adults: a cross-validation. *Addiction*, 99:482–497, 2003.

[23] W. Miller, S. Walters, and M. Bennett. How effective is alcoholism treatment in the united states? *Journal of Studies on Alcohol*, 62:211–220, 2001.

[24] M. Newman. Mixing patterns in networks. *Physical Review E*, 67, 2003.

[25] M. Newman. The structure and function of complex networks. *SIAM Review*, 45(2):167–256, 2003.

[26] M. Nuño, Z. Feng, M. Martcheva, and C. Castillo-Chávez. Dynamics of two-strain influenza with isolation and cross-protection. *SIAM Journal of Applied Mathematics*, 65(3):964–982, 2005.

[27] S. Patten and J. Arboleada-Florez. Epidemic theory and group violence. *Social Psychiatry and Psychiatric Epidemiology*, 39:853–856, 2004.

[28] J. Rehm, G. Gmel, C. Sempos, and M. Trevisan. Alcohol-related morbidity and mortality. *Alcohol Research & Health*, 27(1), 2002.

[29] R. Ross. *The Prevention of Malaria*. London, 2nd edition, 1911.

[30] C. Rydell, J. Caulkins, and S. Everingham. Enforcement of treatment? modeling the relative efficacy of alternatives for controlling cocaine. *Operations Research*, 44:687–695, 1996.

[31] F. Sanchez, X. Wang, C. Castillo-Chávez, P. Gruenewald, and D. Gorman. *Drinking as an epidemic – a simple mathematical model with recovery and relapse*. Evidence Based Relapse Prevention. 2006.

[32] M. Sanchez and S. Blower. Uncertainty and sensitivity analysis of the basic reproductive rate; tuberculosis as an example. *American Journal of Epidemiology*, 145(12), 1997.

[33] B. Song, C. Castillo-Chávez, and J. Aparicio. Tuberculosis models with fast and slow dynamics: the role of close and casual contacts. *Mathematical Biosciences*, 180:187–205, 2002.

[34] B. Song, M. Castillo-Garsow, C. Castillo-Chávez, K. Ríos-Soto, M. Mejran, and L. Henso. Raves, clubs, and ecstasy: the impact of peer pressure. *Mathematical Biosciences and Engineering*, 3(1):249–266, January 2006.

[35] T. Stockwell and P. Gruenewald. *Controls on the physical availability of alcohol*. Wiley, 2001.

[36] T. Stockwell, P. Gruenewald, J. Toumbourou, and W. Loxley. *Prevention of Harmful Substance Use: The Evidence Base for Policy and Practice*. Wiley, 2005.

[37] A. Treno and H. Holder. *Prevention at the local level*, volume International Handbook of Alcohol Dependence and Problems. Wiley, 2001.

[38] D. Watts and S. Strogatz. Collective dynamics of 'small-world' networks. *Nature*, 383:440–442, 1998.